The Gamma To Alpha Alumina Phase Transformation And Synergetic Pressure-sintering Of High Density Polycrystalline Alumina.

THE GAMMA TO ALPHA ALUMINA PHASE TRANSFORMATION AND SYNERGETIC PRESSURE-SINTERING OF HIGH DENSITY POLYCRYSTALLINE ALUMINA

by

Charles J-P. Steiner

A DISSERTATION

Presented to the Graduate Committee

of Lehigh University

in candidacy for the Degree of

Doctor of Philosophy

in

Metallurgy and Materials Science

Lehigh University

1971

CERTIFICATE OF APPROVAL

Approved and recommended for acceptance as a dissertation in partial fulfillment of the requirements for the degree of Doctor of Philosophy.

DEC 14 1971
(date)

R M Spriggs
Professor in Charge

Accepted

DEC 14 1971
(date)

Special committee directing
the doctoral work of
Mr. Charles J-P. Steiner

R M Spriggs
Chairman

D F Hasselman
Chairman

H C Hahn, Jr.

Henry P. Kirchner

ACKNOWLEDGMENTS

The author wishes to express his deepest gratitude to Dr. R. M. Spriggs and Dr. D. P. H. Hasselman for their advice, encouragements and patience, during a very trying period, as well as for their numerous technical suggestions.

I am also grateful to the remaining members of my committee, Dr. W. C. Hahn, Dr. G. Krauss, Dr. F. Feigl and Dr. H. P. Kirchner for their many beneficial discussions.

The help of Mr. R. Korastinsky and Mr. G. Kozma is also greatly appreciated.

I also wish to thank Dr. R. B. Runk from Western Electric and Mr. K. Gruver of the Electron Microscope Laboratory of the Bethlehem Steel's Research Laboratory and Dr. H. Stanley from C. Pfizer for their outside help.

Last but not least I wish to dedicate this thesis to Drs. A. J-P. Steiner and M. Steiner, my beloved parents, my brother Mr. J-F. Steiner and my sister Mrs. C. Rocquet and their respective spouses for their kind help during this period.

Finally, the financial assistance of the U.S. Army Research Office, Durham in the form of contract number DA-ARO-D31-124-61106 is acknowledged with gratitude.

TABLE OF CONTENTS

LIST OF FIGURES

LIST OF TABLES

THE GAMMA TO ALPHA ALUMINA PHASE TRANSFORMATION AND SYNERGETIC PRESSURE-SINTERING OF HIGH DENSITY POLYCRYSTALLINE ALUMINA

by Charles J-P. Steiner

ABSTRACT

The reaction kinetics of the γ-to-α-Al_2O_3 phase transformation were investigated in order to determine the feasibility of using the phase transformation to obtain a beneficial synergetic effect in the pressure-sintering of alumina for the production of high density ceramic articles.

Rate constants for the formation of α-Al_2O_3 from a commercial γ-Al_2O_3 of high purity containing substantial amounts of θ-Al_2O_3 were determined by x-ray techniques over the temperature range extending from 1025°C to 1200°C by measuring the relative amount of α-Al_2O_3 formed. It was established that the transformation was a thermally activated process following zero order kinetics. An activation energy of 116 ± 5 kcals/mole was obtained, suggesting the transformation was of reconstructive nature. The discrepancy

between this value and those advanced by other workers was attributed to the greater purity for the material in the present work. Scanning electron microscopy showed a fragmentation of the γ-Al_2O_3 grains into smaller α-Al_2O_3 particles. A Time-Temperature-Transformation diagram was then constructed showing the respective stability of γ-Al_2O_3 and α-Al_2O_3.

The results were analyzed with Avrami's approach to isothermal transformations, which suggested that the phase transformation was nucleated on grain boundary sites and that the parent phase was "site saturated" at the onset of the transformation. Experimental results were further analyzed according to the theory developed by Cahn for discontinuous processes, then compared with expected values calculated from Christian's relationship for interface controlled processes, and found to be larger by an order of 10^4. These results together with those obtained from the Avrami analysis for the distribution of the nuclei suggest that each γ-Al_2O_3 particle is composed of approximately 10^4 subparticles, the boundaries of which act as α-Al_2O_3 nuclei.

The results for the kinetics of the phase transformation suggested that in synergetic pressure-sintering, advantage of the phase change could be attained only if high heating rates were employed. Experiments where γ-Al_2O_3 was

used as the starting material in combination with heating rates of the order of 150°C per minute produced higher final relative densities in markedly shorter times than when α-Al_2O_3 was used. A trend towards higher strength values, of the order of 100,000 psi and a reduction in scatter of the strength results.

Preface

Recent technological advances in high temperature applications call for a new class of engineering materials. As almost all possibilities in metallic systems have reached their limits, scientists have recently turned to non-metallic inorganic materials, mostly ceramic.

Ceramic components can be fabricated by various methods. Among them vacuum hot pressing is currently used for articles of simple shapes. This technique is unfortunately a slow batch process and often uneconomical. This situation could be altered if the densification kinetics could be accelerated by a phase change or decomposition reaction and mechanical energy; but this view is not agreed on unanimously.

Since alumina is widely used as an engineering material it was decided to verify if the phase change from metastable to alpha alumina could be used to increase the economic efficiency of the hot pressing operation.

The kinetics of formation of the stable alpha form from the metastable gamma in ordinary atmospheric conditions were first investigated. When the stability of each phase relative to the other was determined, the information thus obtained was then utilized to determine experimentally if any benefit resulted when metastable alumina was used as a starting material.

I. INTRODUCTION

A. Polymorphism

General definition. Many crystalline substances can exist in more than one crystallographic modification (1). This phenomenon is referred to as polymorphism by ceramists and crystallographers and allotropism by metallurgists and chemists.

Polymorphism is encountered in a great variety of solids. It exists in many metals such as: iron, manganese, tin, uranium (2); ceramic materials: silica, zirconia, silicates, barium titanate, alumina (1); and even in polymers (3), e.g., glassy and crystalline modifications of the same polymer.

A polymorph is thermodynamically stable over a given temperature range if it has lower free energy than other polymorphs in that range. The free energy of each phase is governed by the well-known relationship:

$$G = E + PV - TS \qquad (1)$$

where E is the internal energy, P the pressure, V the volume, T the absolute temperature, and S the entropy. The product PV is very small in polymorphic transformations and is usually neglected. The TS term is a measure of the

amount of departure of the crystal from perfect order. Such disorder can arise from departure of atoms from their equilibrium position due to heat motion, or by impurities in solid solutions, or various local defects such as dislocations, vacancies, etc. (4). As the temperature increases, so does the TS term and a point will be reached where the possibility of a larger entropy in an alternative structural arrangement can lead to an over-all free energy decrease. The temperature where this occurs is referred to as the transformation temperature; at that point the free energy of each phase is equal. This is illustrated in Fig. 1.

If E_1 is the internal energy of phase I and E_2 that of phase II, the quantity $E_2 - E_1$ is identified as the latent heat of transformation. As heat is supplied in the direction of increasing temperatures, the quantity $E_2 - E_1$ is always positive in the case of a low temperature equilibrium form transforming into a high temperature modification. In addition, the entropy of the high temperature form must be larger than that of the low temperature one. The increased structural energy and entropy of the high form is often physically replaced by a more open structure.

Polymorphic relationships between stable and metastable phases.

Polymorphism may involve relationships between stable as well as metastable forms. Metastable systems exist in

Fig. 1

Relationship Between Internal Energy E and Free Energy G of Polymorphic Forms:

$E_2 > E_1$ and $S_2 > S_1$

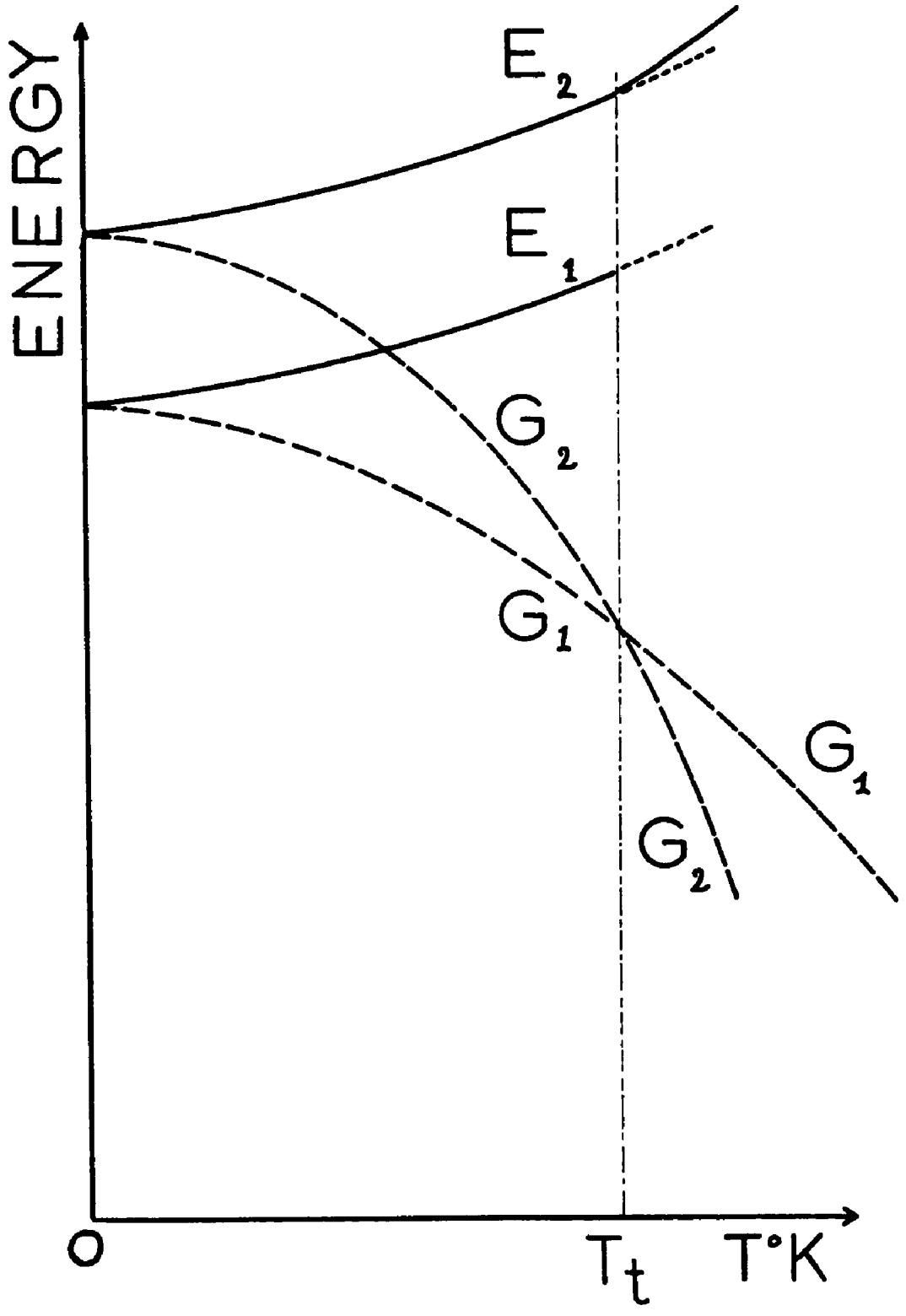
ENERGY
E2
E1
G2
G1
G1
G2
O
Tt
T°K

modifications of higher internal energy than normally allowed for a given crystal structure, and are very common in ceramic materials. One of the most notable departures from equilibrium is the ease with which many silicates are cooled from the liquid state to form non-crystalline solids such as glasses. Another common source of non-equilibrium phases in ceramics is uncompleted reactions during the time allowed for firing, resulting from the formations of a layer of reaction products. A third example is provided by the existence of stranded phases, which occur when a high temperature form fails to transform into its equilibrium low temperature modification and therefore persists below its range of stability (5). A fourth common type of non-equilibrium behavior is the formation of a metastable phase with a lower energy than the parent phase but not the lowest possible energy equilibrium phase, for instance, silica glass producing cristoballite instead of the more stable form tridymite on devitrification of silica glass (1).

When metastable systems are supplied enough thermal energy to overcome the energy barriers responsible for their existence, they will try to achieve thermodynamic equilibrium. Furthermore, the process taking place will be irreversible. The various heat treatments of steels and the transformation of transition aluminas into corundum are the best examples. In such cases, there is no definite trans-

formation temperature. Such reactions are found to be exothermic because the reaction towards equilibrium will cause the loss of the extra internal energy responsible for the metastable condition. Changes among equilibrium phases are usually rapid and take place at definite temperatures. They can, however, be extremely sluggish if metastable forms are involved. In both cases the role of impurities can be very significant in promoting or hindering the transformation (1, 6).

Solid state transformations in crystalline solids. Solid state transformations in crystalline solids are broadly divided into two categories:

i) Those where material transport occurs by diffusion, precipitation being the most notable.

ii) Those where it takes place by shear (simultaneous cooperative movement of a large number of atoms). They are referred to as diffusionless transformations.

This division is, however, not clear cut for there are several examples of phase changes exhibiting some characteristics of both categories.

Christian (7) has therefore proposed a more refined classification for metals and alloys. He considered most transformations to be heterogeneously nucleated and classi-

fied them by growth process into three over-all groups:

1) Those with athermal growth, i.e., where the amount of the new phase is a function of temperature only. Most martensitic reactions fall in this category.

2) Those where the rate of growth of the new phase is a function of both time and temperature; these are referred to as thermally activated. These fall into two subgroups:

   a) Interface controlled processes in which the new phase has the same mean composition as the parent one and forms by diffusion through a thin interface. Such changes include polymorphic transformations, recrystallization and order-disorder changes.

   b) Processes involving long-range transport by diffusion for the interface migration.

A transformation is designated as continuous if the mean composition of the respective phases changes gradually towards an equilibrium value. If, however, the parent phase remains unchanged until swept over by the interface, it is said to be "discontinuous" and to be diffusion as well as interface controlled.

Diffusionless transformations are found in ceramic

as well as metallic systems. In the former they are represented by the displacive mode, while in metallic systems martensitic transformations are the most notable examples. Diffusionless transformations are often observed after cooling below a critical temperature (the iron-based martensites are the best known examples), but some are known to occur on heating: monoclinic to tetragonal ZrO_2 (8), α to β quartz (1). There is no agreement as yet whether they nucleate on existing defects (9).

The main characteristics of diffusionless reactions are summarized below:

1) They are generally time independent. At a constant temperature, a fraction of the original phase transforms very rapidly, after which there is usually no further change, isothermal martensite being an exception.
2) The fraction of material transformed is characteristic of temperature if all other variables are held constant.
3) They are thermodynamically very reversible in the sense that an initial atomic configuration can be repeatedly obtained. Exceptions, where reversibility is not observed, are attributed to interfering secondary effects.
4) Plastic deformation can increase the rate of

transformation by several orders of magnitude.

5) In diffusionless transformations each crystal transforms to new crystals of the same chemical composition.

6) There is always a definite relation between the orientation of the original structure and that of the new phase.

Thermally activated heterogeneous transformations include almost all other classical phase changes encountered in materials and involve nucleation and growth. The general characteristics of these reactions may be summarized as follows:

1) They are time as well as temperature dependent.

2) They display the well-known C curve behavior.

3) These transformations are thermodynamically irreversible. If phase I is converted into a new structure II, the crystals of phase I formed on reverting of phase II will be crystallographically unrelated to those that were initially present.

4) Nucleation can be assisted by mechanical energy, in a lesser degree than for diffusionless transformation.

5) The composition of the reaction products may or

may not be related in any way to the original phase. The same statement holds for the crystallographic orientation of the two lattices.

The changes discussed so far apply to all inorganic crystalline solids. Since most ceramic materials are, like metals and alloys, crystalline substances, basically similar solid state transformations are to be expected. Complications, however, will arise from the fact that ceramics are ionic materials with the requirement that electrical charge be maintained. In addition there are additional transformations specific to ceramics arising from the fact that many ceramic substances are not in a state of thermodynamic equilibrium. Many are not even crystalline but amorphous, that is, with only short range crystallinity (glass for instance). Should enough thermal energy be supplied, such thermodynamically metastable structures would strive toward thermodynamic equilibrium (10).

Polymorphic transformations in ceramics. Polymorphic transformations in ceramic materials are usually divided in two main groups. In one, the transformation occurs at a high rate without breaking bonds or changing the number of nearest neighbors and is called "displacive." In contrast, other transformations will require that bonds be broken and reformed with a different coordination number; this process,

called "reconstructive," will require more energy and cause the transformation to be sluggish (1).

The speed of a polymorphic transformation depends on the magnitude of energy barrier opposing the process, i.e., an activation energy must be supplied for the transformation to proceed. The transformation rate will therefore be a thermally activated process of the form exp(-E/kt), where E is the activation energy.

The activation energy E for a given transformation may be indicative of the particular mechanism involved. For instance an activation energy of the order of 110-150 kcals/mole is consistent with diffusion in alumina. It would hence be conceivable that in a solid state transformation involving pure alumina a diffusion mechanism might occur if an activation energy of that order was measured. The enthalpy change ΔH is the difference between the parent and the product phase and relates to a change in bonding in the atoms of the structure.

The activation energy and enthalpy change are illustrated on Fig. 2 for a transformation where the parent phase lies in the energy trough A and the product phase in B.

The enthalpy change ΔH, during a transformation, will correspond to a change in bonding of the atoms in the structure. This change in bonding can come about by either:

a) A complete change in the amount of bonding, or

Fig. 2

Schematic Variation of the Free Energy

for an Exothermic Reaction

A → B Across the AB Energy Barrier

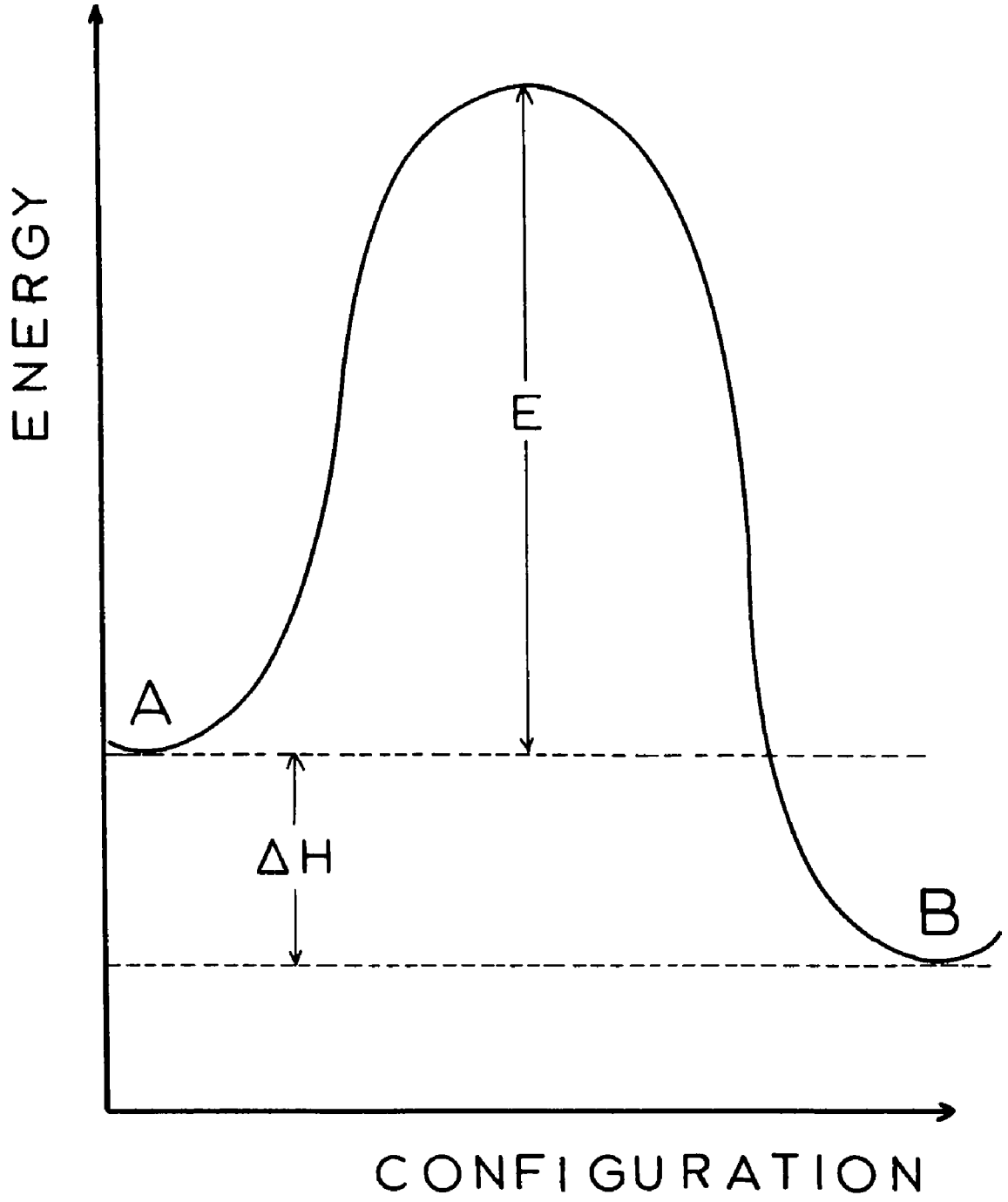
ENERGY
E
A
ΔH
B
CONFIGURATION

b) A complete change in the bonding type.

From a structural point of view, a change in the bonding can imply a change in the interaction between neighboring atoms which include the nearest as well as the more distant neighbors. Buerger (11) has therefore proposed a more detailed classification of polymorphic transformations based on the change in bonding involved and has divided them into clear-cut groups with respect to transformation speeds, as follows:

I - Transformations of secondary coordination	
Displacive	rapid
Reconstructive	sluggish
II - Transformations of disorder	
Rotational	rapid
Substitutional	sluggish
III - Transformations of first coordination	
Dilatational	rapid
Reconstructive	sluggish
IV - Transformations of bond type:	usually sluggish

Transformations involving no change in the first coordination are among the least drastic in non-metallic inorganic crystals. In such instances, the energy change is accounted for by a change in the coordination of non-nearest neighbors.

In a displacive change (Fig. 3), the structure be-

Fig. 3

Schematic Representation of a

Displacive Transformation

Fig. 4

Schematic Representation of a

Reconstructive Transformation

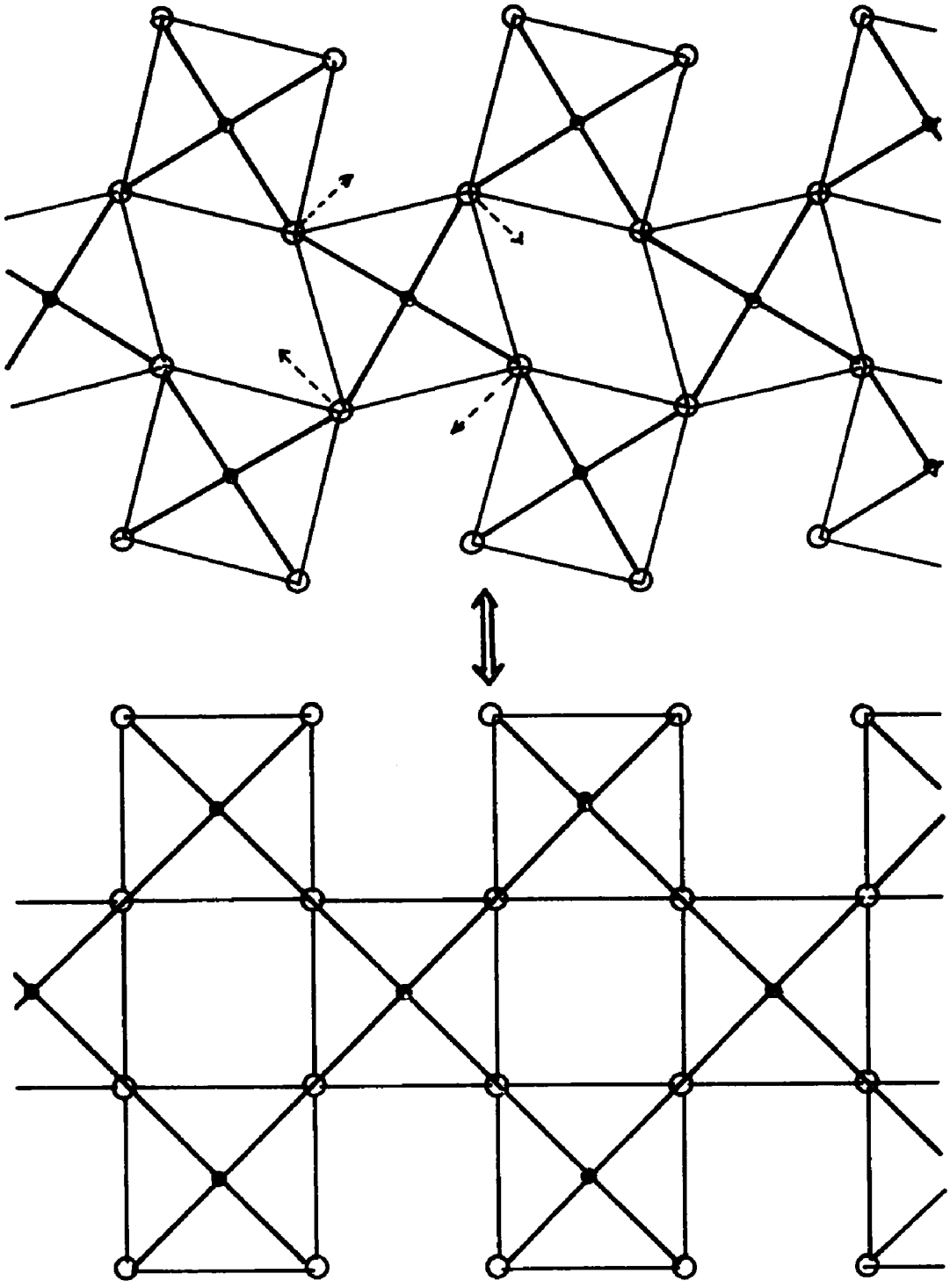

DISPLACIVE
TRANSFORMATION

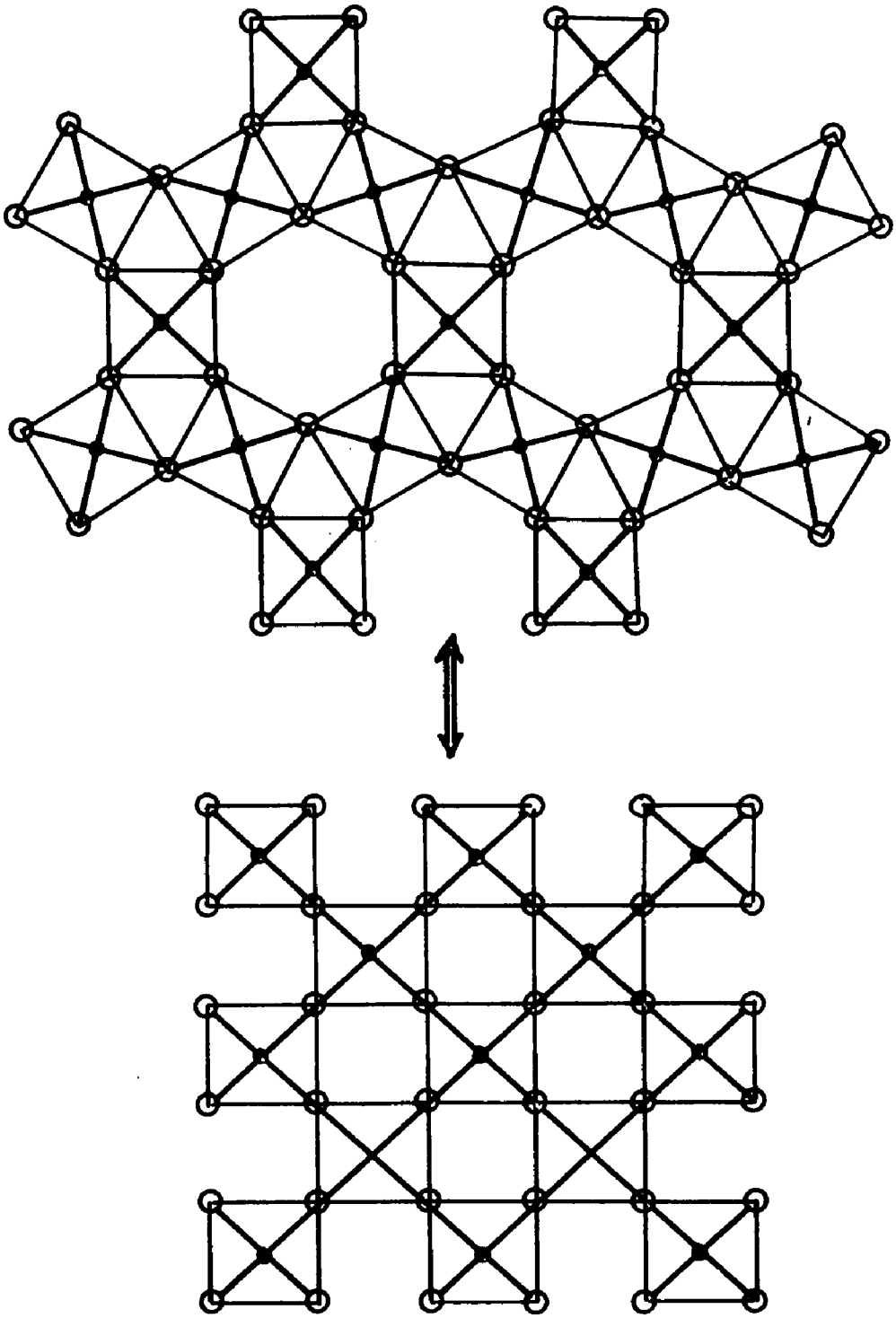

RECONSTRUCTIVE
TRANSFORMATION

comes distorted so that non-contacting atoms are displaced with respect to one another. Such a transformation is opposed only by a low energy barrier and should therefore proceed at high speed.

In a reconstructive change (Fig. 4), it is also possible to keep the first and alter the second coordination contacts. The primary bonds will have to be temporarily broken and reformed in a new structure. This represents a high energy barrier.

Class II has characteristics of displacive transformations, but the speed can vary from very rapid to sluggish; in this respect, they resemble the reconstructive transformations. They occur in structures where atoms of X are bonded to atoms of Y by bonds of different strength. Thermal fluctuations will then destroy the weakest bonds and leave the strong ones intact. The tightly bonded groups may separate and constitute free domains. When this happens, the change is called rotational (12).

Substitutional changes are encountered when under thermal influence atoms of Y rearrange themselves on new sites to become statistically equivalent. Such changes are reported in silicates (13).

Class III involves changes in the first coordination. They depend on the fact that the coordination of two atoms is related to their stoichiometric ratio. Consequently, if

there is a coordination change in a crystal, there must be a coordination change in at least two kinds of atoms. Again, a rapid and a sluggish variety can be recognized. The former occurs rapidly because the first coordination change is due to mere dilatation. Accordingly, Buerger called it a dilatation transformation. The CsCl transformation may be a typical example (11). Below the transition temperature, both ions have a coordination of 8. At the transition temperature, they suddenly assume a coordination of 6 by simple expansion of a [100] axis and contraction at right angle to it. There is no obvious barrier to such changes which accounts for their rapidity.

In some cases an intermediate coordination will be assumed, which interposes an important barrier to the transformation, which proceeds essentially the same way as the reconstructive transformation discussed in Class I. The change from aragonite to calcite ($CaCo_3$) is believed to be an example of such a transformation (14).

Class IV involves a complete change in bond nature among polymorphs, the graphite-diamond and the white-gray tin phase changes being the most notable. Such changes are as yet not fully understood.

Polymorphs connected by displacive transformations are also referred to as "high-low" polymorphs and display the following characteristics (14):

i) The high temperature form is usually the open form and therefore has the larger specific volume.

ii) The high temperature form has the largest entropy.

iii) The high temperature form has the highest symmetry.

iv) As a consequence of iii) the low temperature form is a derivative structure of the high temperature form and on cooling the transformation from the high to the low temperature modification frequently results in twins.

v) The transformation occurs at a definite temperature.

The following general characteristics can be observed for polymorphs connected by reconstructive changes:

i) They tend to show nucleation and growth characteristics.

ii) They require a large activation energy for their formation, which is frequently sluggish as a result.

iii) They can occur in several ways: diffusion in the solid, or transport via a gaseous or liquid phase.

iv) The transformation can be speeded up by mechanical energy.

v) There is no necessary symmetry relation between the original and the transformed modification.

B. Reaction order and Activation Energy

Classical reaction kinetics are primarily concerned with homogeneous reactions and should not be applied literally to many phenomena occurring in solid materials. Analogy to reaction orders in homogeneous systems can, however, be used to predict the evolution of a particular heterogeneous reaction.

Many important solid state reactions in ceramics have been best represented by first-order kinetics (15). In a first-order process the rate of change of the concentration of the untransformed product c as a function of time t varies according to the relation:

$$\frac{dc}{dt} = -kc \tag{2}$$

which gives, on integration,

$$\ln \frac{c}{c_0} = -k(t - t_0) \tag{3}$$

where k is the rate or velocity constant for this particular process and c_0 the initial concentration at time $t = t_0$.

A reaction process will be regarded as following zero-order kinetics if the rate of concentration change with time is constant, i.e.:

$$\frac{dc}{dt} = k \tag{4}$$

Integrating will yield:

$$c = kt + A \tag{5}$$

Zero-order processes are few in homogeneous systems but often found in the solid state because of its heterogeneous character produced by large numbers of defects always present. Not unexpectedly, they are very important in surface mechanisms and catalysis (16).

According to Gomes (17), the definition of a rate constant for a solid state reaction gives rise to some difficulty, the primary problem being that it cannot be defined in the same way as for a homogeneous reaction. For the same reason, the activation energy of a solid state reaction does not have the significance that it has in a homogeneous process, for it is usually dependent on complex diffusional phenomena.

The rate constant for any chemical change can be markedly increased by raising the temperature because it is related to the activation energy and the temperature by the following equation:

$$\frac{d \ln k}{dT} = \frac{E}{RT^2} \tag{6}$$

which on integration yields

$$\ln k = -\frac{E}{RT} + B \qquad (7)$$

or

$$k = Be^{\frac{-E}{RT}} \qquad (8)$$

A plot of ln k vs. reciprocal temperature will give a straight line, the slope of which will be a quantitative measure of the activation energy E for the process.

C. Polymorphism in Alumina

Alumina is used in large quantities in both the stable α and metastable γ modifications. In the former, it is used for high temperature and strength applications, while in the latter for chemical and catalytic use because of its very porous surface which, combined with a fine particle size gives it a large specific area. However, surprisingly little is known about the transformation from γ- into α-Al_2O_3, and its kinetics. It is therefore desirable to cite what is known so far about the different modifications of alumina.

The Engineering Properties of Selected Ceramic Materials Handbook (18) lists the physical properties of aluminum oxide in two broadly divided categories: α-Al_2O_3 reported belonging to the trigonal system and γ-Al_2O_3 which is considered to be cubic.

However, this classification is only to be looked upon as a general division of alumina into its stable α and metastable γ forms; γ denoting, in reality, an ensemble of closely related structures as evidenced by the extreme similarity of their x-ray diffraction patterns (13).

According to Ryschkewitch (20), only α-Al_2O_3 has a well established crystal structure. The other modifications are considered to be cubic or quasi-cubic. He also claims that the combination of the forms of what he calls "gamma" alumina represents the structure called "eta" by other workers.

All investigations conclude that the formation of α-Al_2O_3 or corundum is the end product of the dehydration of hydrargillite or hydrated aluminum oxide of composition $Al_2O_3 \cdot 3H_2O$.

Saalfeld (21), in an exhaustive survey, has summarized the findings of many workers on the nature of hydrated aluminum oxide, the intermediate "gamma" modifications, their transformation into α-Al_2O_3, as well as the intermediate transformations.

Besides α-Al_2O_3, seven intermediate modifications have been reported (22), but the existence of some of them is not universally accepted, nor are all the proposed structures (21). According to de Boer (23), there are a great number of possible modifications ranging from a completely

random distribution of aluminum ions to a more or less ordered distribution over the tetrahedral or octahedral sites in the oxygen lattice.

Since only α-Al_2O_3 has a well established crystal structure, we shall therefore describe it first. It can be best described as an hexagonal close packing arrangement of oxygen ions inside of which the smaller aluminum ions are enclosed. It has a density of 3.98 ± 0.02 gr/cm^3 (21) and a c/a ratio of 1.366. It is the only thermodynamically stable modification of alumina at all temperatures. It possesses the highest degree of crystallinity of all alumina polymorphs, as the transition aluminas all show more or less pronounced amorphous characters. It is insoluble in strong mineral acids and, as expected, has the lowest internal energy.

Its crystallographic structure was first determined by Pauling and Hendricks (24). They proposed an arrangement whereby each aluminum ion was surrounded by six oxygen ions which were not exactly at the corners of a regular octahedron. This distortion arises from the fact that one-third of all possible aluminum sites are vacant (to keep electrical neutrality in Al_2O_3). Each oxygen ion is surrounded by four aluminum ions, two of which are nearer than the other two for the same reason. They found the following atomic distances:

Smallest 0-0 distance: 2.495 Å

Smallest Al-0 distance: 1.845 Å

Largest Al-0 distance: 1.990 Å

The unit structure was found to be a rhombohedron with $a = 5.12$ Å and $\alpha = 55°17'$ and the unit cell to contain two Al_2O_3 elementary units.

These results were later found to be essentially correct by Newnham and de Haan (25) using more refined techniques.

As for γ-Al_2O_3, it was first thought to possess an FCC lattice with a lattice constant of $a = 7.90$ Å and to consist of only one form which transformed irreversibly into α-Al_2O_3 when a suitable temperature was reached (26). It was only later found that "gamma" alumina in reality consisted of at least six forms of closely related structures which undergo on heating a succession of irreversible transformations leading to α-Al_2O_3 as an end point (27).

Saalfeld (21) gives a good description of all stages occurring in the dehydration of hydrated aluminum oxide (hydrargillite) down to its final stage, the formation of corundum, as well as the best description so far of alumina's transitional phases. His work was based on following by x-ray diffraction the dehydration of hydrargillite single crystals heated through increasing temperatures.

He observed that the dehydration sequence could fol-

low two possible paths, but that they always produced α-Al_2O_3 as the end product. The first sequence took place when hydrargillite was heated in a hydrothermal atmosphere, while in the second one it was dehydrated in air.

In hydrargillite, the oxygen ions form a non-close packed hexagonal structure. They are arranged in double layers directly one above the other with an ABAB sequence while the aluminum ions are hexagonally arranged in the octahedral holes of the oxygen lattice, with one-third of those holes remaining unoccupied. The over-all structure of hydrargillite is monoclinic.

Considering first the hydrothermal series, the first step in the dehydration is the formation of boehmite (of chemical composition $Al_2O_3 \cdot H\ O$)which starts to form at appreciable rates between 200 and 300°C. There is as yet much uncertainty about its formation mechanism. It appears that several boehmites of different degrees of crystallinity exist and that the original hydrargillite's characteristics play an important part (28) in determining which boehmite will be formed. Different boehmites will behave differently in the formation of the further decomposition products. The structure of boehmite is believed to be orthorhombic with a cubic layer sequence (21).

If boehmite is heated about 450°C, γ-Al_2O_3 forms. This is the original gamma modification. The crystals ob-

tained were found to be tetragonal with the following lattice constants: $a = b = 7.94$ Å, $C = 7.79$ Å. As one can see, the degree of tetragonality is slight, with only a 2% difference between the a, b and c parameters. In the same reference, Saalfeld (21) reported it had a perturbed spinel lattice attributable to the constitutional aluminum ions' vacant sites. Jagodzinsky and Saalfeld (29) also found that the aluminum ions as well as the aluminum vacant sites were in the octahedral holes of a face centered cubic oxygen lattice. A distorted as well as unstable lattice was evidenced by the few and diffuse lines observed from powder diffraction patterns.

Cowley (30) also observed on oxidized aluminum foils that γ-Al_2O_3 had a cubic spinel-type structure. He observed good single crystal electron diffraction patterns that showed extra lines which he attributed to faults occurring in the close packed oxygen sequence. He found there were two possible configurations for the aluminum ions. In one configuration they would be in the octahedral holes with one-third of them missing, while in the other configuration two-thirds of all aluminum ions are in the tetrahedral sites.

Jellinek and Fankuchen (31) showed that on heating lattice distortions anneal out in γ-Al_2O_3 and the crystallites' size increased. They also noticed the presence of

new peaks which did not correspond exactly to the spinel structure, but were found to belong to the θ-Al_2O_3 modification.

Recent surface studies by Frisch and Kruger (32) of the transition aluminas by adsorption techniques have shown that their surface is very porous, containing narrow cylindrical pores and crevasses of various sizes; this was particularly pronounced for γ-Al_2O_3. The perturbed nature of the surface is responsible for the latter's large specific area and its ensuing catalytic properties.

Stumpf et al. (27) observed a form which they called η-Al_2O_3, that had almost identical x-ray diffraction peaks as γ-Al_2O_3. Those two forms would thus only be differentiable by some small variations in certain peaks' intensity. The existence of this form is widely doubted and omitted by most recent workers.

Tetragonal γ-Al_2O_3 is stable up to about 900°C. Heating for several hours at 900°C or shorter times at higher temperatures will bring the transformation $\gamma \rightarrow \theta$-$Al_2O_3$. Some diffuse γ-peaks are observed to get sharper and sharper while others shift by a small angle. Tertian (33) claimed it was merely an improved ordering arrangement of γ-Al_2O_3 rather than a new phase and proposed a model whereby the oxygen ions have an FCC arrangement while the aluminum's is the same as in α-Al_2O_3, i.e., a structure

halfway between γ- and α-Al_2O_3.

Saalfeld reported otherwise (21). He found strong evidence of lattice correspondence between γ and Θ-Al_2O_3 and from isomorphic relationship with β-Ga_2O_3 derived the following characteristics for Θ-Al_2O_3:

i) The oxygen sequence is ABCABC but with a monoclinic strain in the unit cell.

ii) The aluminum ions are predominantly on well determined tetrahedral locations and show no evidence of any hexagonal arrangement as reported by Tertian.

iii) There are 12 ions per unit cell.

iv) The average O-Al distance is between 1.93 and 2 Å. It corresponds to the Al-O distance one finds in the spinel structure.

v) It has a perturbed spinel lattice derived from γ-Al_2O_3.

On further heating Θ-Al_2O_3 will transform irreversibly into α-Al_2O_3 at measurable rates, at temperatures upwards of 1000°C.

Some workers (27, 33) have reported the existence of a modification very close in structure to Θ-Al_2O_3, it is referred to as δ-Al_2O_3. Recent x-ray studies have shown that the difference between them is negligible (34).

All of the modifications mentioned so far involve

initial dehydration of hydrargillite in hydrothermal conditions. If dehydration is performed in anhydrous conditions, the resulting products will be different.

The first form appearing then is χ-Al_2O_3. Both Saalfeld (21) and Brindley (35) report its structure to be hexagonal. Brindley found in addition that it retained a large amount of water and that its degree of crystallinity was very low, causing it to be often referred to as amorphous alumina.

From 800° to 1000°C Saalfeld (21) reports the gradual formation of a new polymorph called κ-Al_2O_3. This form was independently discovered by Stumpf (27) and Jellinek (31). Its hexagonal structure has been confirmed by Saalfeld (24) and calls for a comparison with corundum's. Lattice constant measurements showed the a and b axis in κ-Al_2O_3 to be twice those of corundum. He proposed an HCP arrangement for both forms but with different packing sequences in the c direction. He also found κ-Al_2O_3's crystallinity was improved with respect to χ-Al_2O_3.

Finally, upwards of 1200°C, κ-Al_2O_3 peaks gradually disappear and are replaced by corundum's. The transformation rate becomes high above 1300°C.

It appears from this work that hydrargillite's layer structure is gradually destroyed on heating through higher temperatures, decomposing according to two different sequences

depending on whether hydrothermal or dry conditions prevail.

In the first case, the cubic oxygen packing is retained right up to the θ-phase and changes in a discontinuous manner to hexagonal at the onset of α-Al_2O_3.

In the second case, the hexagonal packing sequence occurs immediately after hydrargillite and by-passes the boehmite stage. Theoretically, it should be easier to obtain the hexagonal corundum. However, because of κ-Al_2O_3's greater stability, the final transformation occurs about 300°C higher.

D. Previous Work on Polymorphic Changes in Alumina

Qualitative work. While a large amount of work has been done on the various forms of "gamma" alumina in conjunction with its catalytic properties, little attention has been paid to the transformation into α-Al_2O_3.

It was first investigated in a purely qualitative manner by Biltz and Lemke (26), who found that the cubic modification of alumina converted into the stable α-modification at observable rates around 1000°C.

Later, Stumpf et al (27), working with calcined alumina hydrates found corundum appeared between 1150°C and 1250°C depending on the particular hydrate used as starting material and the prevailing experimental conditions. They,

however, concentrated their efforts on the changes occurring in the transition aluminas rather than on their transformation into α-Al_2O_3 and proposed the following sequence:

$$Al_2O_3 \cdot 3H_2O \xrightarrow{200^\circ C} Al_2O_3 \cdot H_2O \xrightarrow{400^\circ C} \eta/\gamma\ Al_2O_3 \xrightarrow{1000^\circ C} \Theta\text{-}Al_2O_3 \xrightarrow{1200^\circ C} \alpha\text{-}Al_2O_3.$$

Rooksby (35) working independently found the series of transformations were as follows:

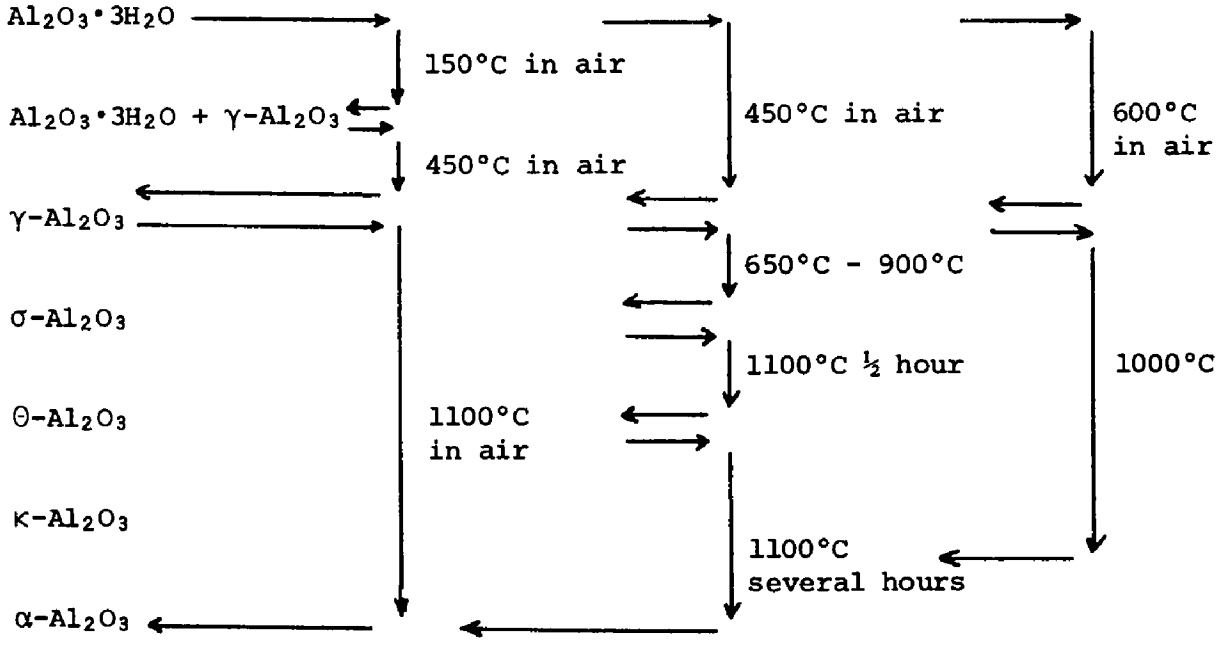

Day and Hill (36) suggested the following changes:

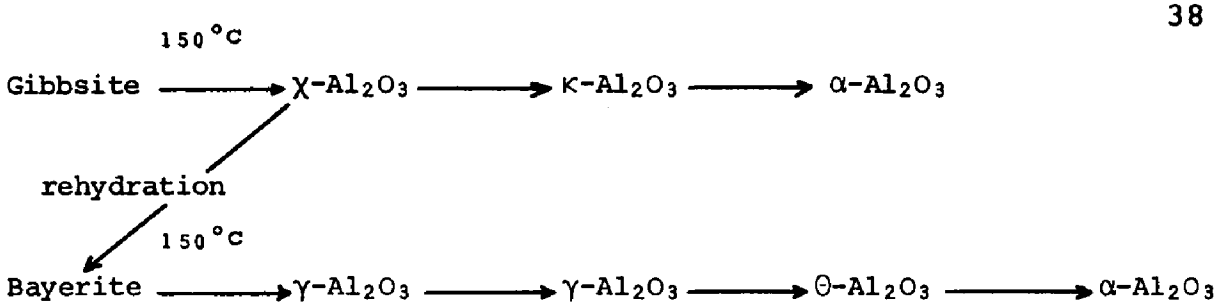

They indicated a lack of certainty as to when the transitions take place.

The most comprehensive study is that of Saalfeld (21), who showed that a crystallographic relationship persisted from hydrargillite up to θ-Al_2O_3 in the hydrothermal decomposition sequence, indicating a possible succession of displacive changes. However, the relationship was destroyed when α-Al_2O_3 formed, suggesting at that point evidence of a reconstructive nature. The paths he proposed are illustrated below:

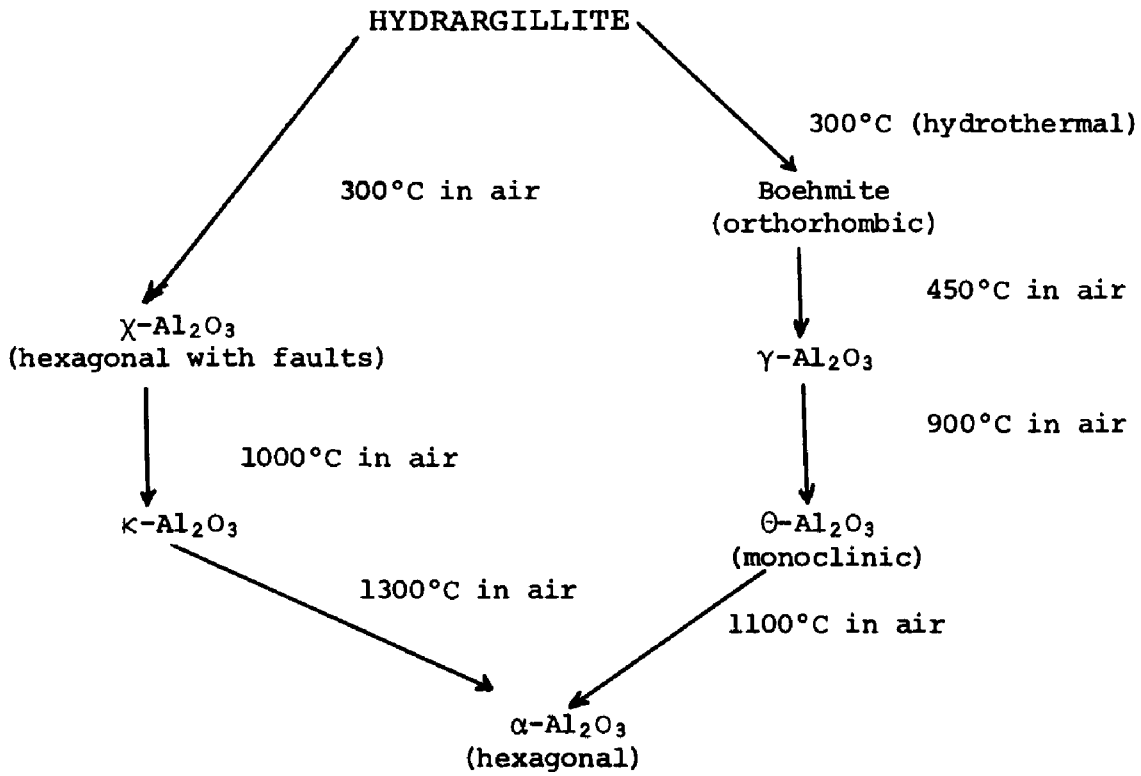

Gitzen (37), summarizing the results of all workers, found the path followed was essentially controlled by the morphology of the starting material in terms of particle size and the chemical conditions prevailing during its thermal decomposition with respect to moisure and alkalinity.

Kalinina (38) looked at the intermediate forms of alumina not only as discrete phases but as transition stages from a finely dispersed to a more orderly state, as well as possible transitions from one modification to another. She also found the formation of different polymorphs greatly depended on the initial material.

Stirland and his co-workers (39), looking at alumina's transformation from a morphology standpoint, found that the final phase change to α-Al_2O_3 started between 1000° and 1100°C and was accompanied by considerable changes in the specimen's appearance. Such morphological changes had been noticed earlier but at considerably higher temperatures (40).

Stirland suggested that material transport took place by a process akin to the first stage of sintering which could be made possible by atomic rearrangements occurring during the phase change to α-Al_2O_3. Coble has defined the first stage of sintering as limited geometrical changes due to neck growth between particles (41). The

shrinkage resulting would be due to vacancy diffusion.

Iler (42), starting with fibrillar boehmite, observed the formation of γ-Al_2O_3 between 500° and 700°C and found that two very closely related forms followed around 1000°C. He identified them as Θ and δ-Al_2O_3 (but the latter's existence is still widely disputed), both transforming irreversibly to corundum between 1000° and 1100°C. He also shared Kalinina's views (38) that θ was merely a better ordered form of the same basic crystal structure as γ-Al_2O_3 and claimed that Θ-Al_2O_3 consisted of finely divided particles while α-Al_2O_3 was much coarser. At no time did he observe any crystal of either Θ or α-Al_2O_3 of intermediate size.

He then proposed the formation of an amorphous transitory phase connecting the diminishing Θ crystals to the increasing α through which both the aluminum and the oxygen ions would diffuse during the transformation. A similar amorphous phase has been reported during the quartz to cristobalite transition (43).

In a recent investigation, the transformation of noncrystalline Al_2O_3 into α-Al_2O_3 was followed by x-ray powder patterns (44). It merely showed qualitatively that amorphous alumina prepared by a solid state reaction transforms into corundum by way of only one intermediate transition alumina in the course of heating, thus confirming Saalfeld's

findings that χ-Al_2O_3 can be considered as amorphous on account of its low degree of crystallinity.

Quantitative investigations. The first and most significant study of the kinetics of transformation of γ to α-Al_2O_3 was conducted by Clark and White (45). They prepared γ-Al_2O_3 by calcining hydrated alumina at 840°C and followed the transformation isothermally by comparing density measurement of densifying green compacts made initially from γ and α-Al_2O_3 respectively, as a function of time for selected temperatures between 1195° and 1500°C. The curves of fraction transformed against time that they obtained are shown on Fig. 5, while Fig. 6 shows the plots of the log of the fraction untransformed vs. time. For all temperatures the initial portions of Fig. 6's plots were considered straight, suggesting the reaction obeys first-order kinetics. Clark and White indicated that the slope for each curve at time t = 0 was a quantitative measure of the initial rate constant (i.e. at the beginning of the transformation). They obtained the activation energy by plotting the rate constants at all investigated temperatures vs. reciprocal temperature and obtained a value of 79 kcal/mole but did not attempt to propose a phenomenological explanation for this value.

More recently, a group of Chinese workers investigat-

Fig. 5

Fraction α-Al_2O_3 Formed Against Time,

After Clark and White

Fig. 6

Semilog Plot of the Fraction of Untransformed

γ-Al_2O_3 Against Time Showing

First-order Kinetics, After Clark and White

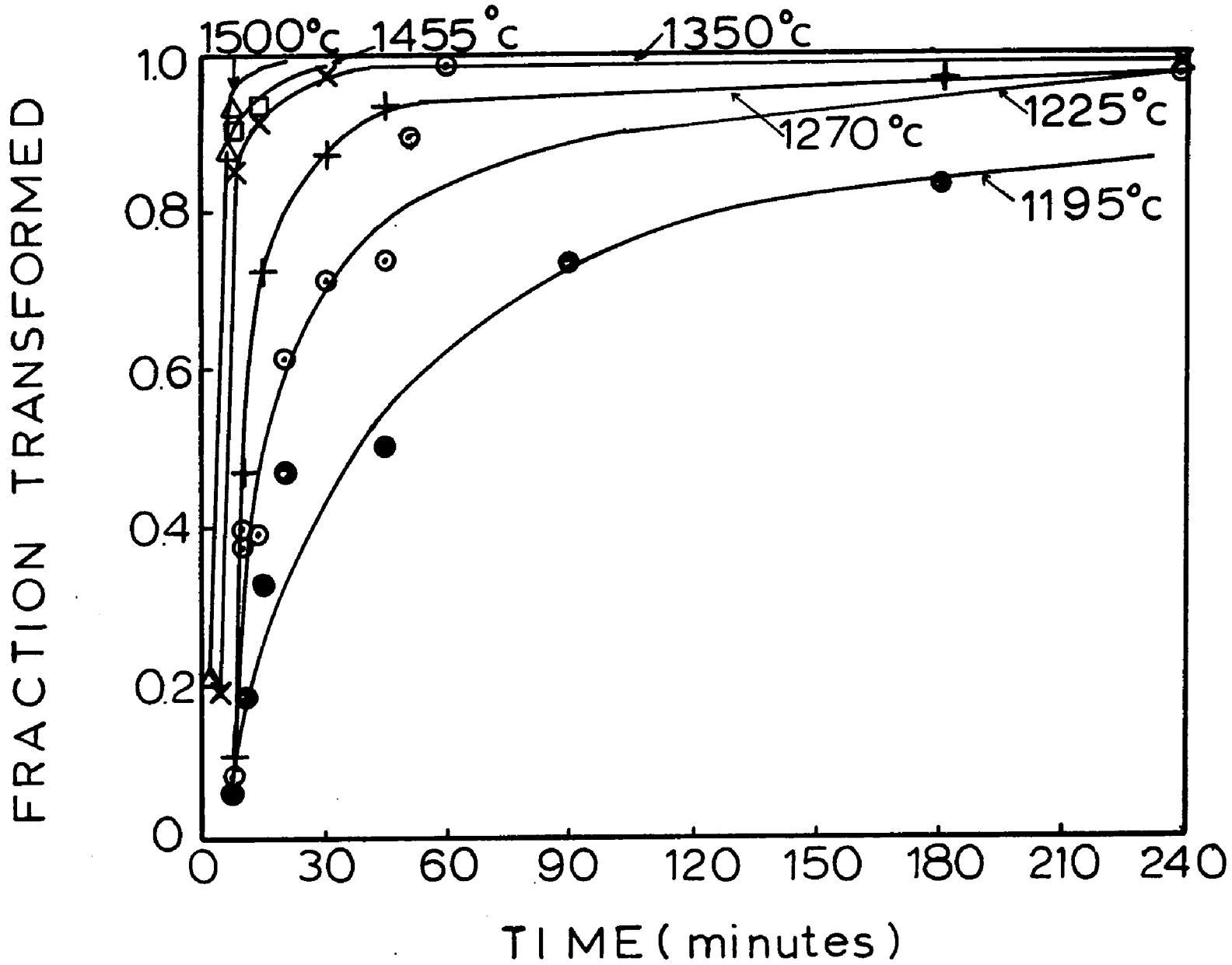
1500°c
1455°c
1350°c
1270°c
1225°c
1195°c
FRACTION TRANSFORMED
1.0
0.8
0.6
0.4
0.2
0
0
30
60
90
120
150
180
210
240
TIME (minutes)

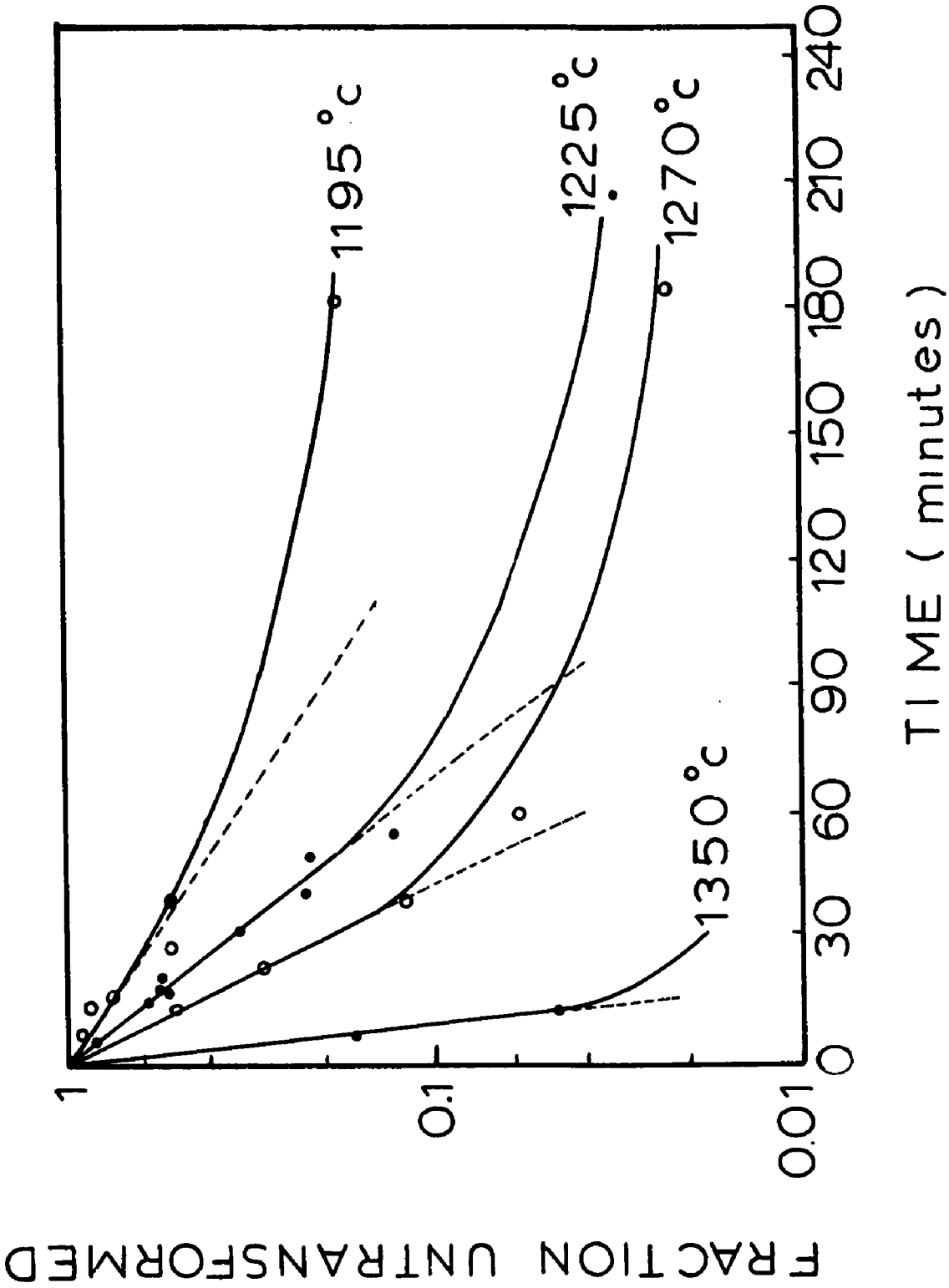
1195 °c
1225 °c
1270 °c
1350 °c
1
0.1
0.01
0
30
60
90
120
150
180
210
240
TIME (minutes)
FRACTION UNTRANSFORMED

ed the kinetics of transformation of some metastable alumina's transition into corundum (46). They prepared their material by melting some α-Al_2O_3 followed by very rapid cooling and followed the transformation by density measurements. It unfortunately contained substantial amounts of impurities which could considerably modify the transformation kinetics (40, 47). They obtained a very high value: 153 kcal/mole. They attributed their discrepancy with Clark and White's results to the extremely large particle size of their material (of the order of 30 microns), which is an order of magnitude larger. They also proposed a first-order kinetics mechanism.

Yanagida and Yamaguchi (48) investigated both the transformation of θ and γ-Al_2O_3 into corundum by x-ray diffraction technique. They found activation energies respectively of 101.6 and 144 kcal/mole and showed that the role of water vapor could be important in accelerating the transformation. High atmospheric moisture content was also found to decrease the activation energy; they also made no attempt to explain these observations.

Kleppa and Yokokawa (49) made some indirect measurements by calorimetry of the enthalpies of transformation of γ-Al_2O_3, δ-Al_2O_3 and κ-Al_2O_3, respectively, and reported exothermic values of -5.3, -3.6 and -2.7 kcals/mole. It is probable the form they called δ was in reality θ-Al_2O_3.

These are small values, as we can see, indicating a small internal energy difference between parent and product phase. Because the conversions are sluggish, the heats of transformation were obtained indirectly by comparing the heats of solution of the transition aluminas with that of α-Al_2O_3 in a lead borate melt at 705°C.

It appears from this survey that the kinetics of the transformation of metastable alumina to α-Al_2O_3 are strongly dependent upon the characteristics of the material investigated. The activation energies are reported to vary between 79 and 153 kcal/mole. This difference can be caused by many factors besides purity, for instance particle size and distribution, heat-treatment atmosphere, etc.

It was therefore decided to take a fresh look at the transformation and to investigate the kinetics of formation of α-Al_2O_3 from a commercially available high purity "gamma" alumina of fine particle size.

II. EXPERIMENTAL PROCEDURE

Powder characterization. Several commercially available "gamma" aluminas were considered, but most were found unsuitable because they contained sizeable amounts of α-Al_2O_3 in the as received powders. A high purity material, supplied by Cerrac Inc., was finally selected because of its availability and total measurable absence of α-Al_2O_3. The alumina content was reported to be 99.95% + with the following cationic impurities:

Si: 0.005 - 0.05%

Fe: 0.001%

Ag: 0.0001%

Cu: 0.0001%

Mg: 0.0001 - 0.001%

These quantities were determined by flame spectroscopy. The apparent partical size, measured by sedimentation was reported to be in the 0.2 - 0.5μ range. This quantity should not be confused with the average individual crystallite size, for each particle is probably made up of several agglomerated crystallites.

A particle size distribution analysis was performed by Dr. R. B. Runk of the Western Electric Corporation by a sedimentation technique. It revealed that over 80% of the

cumulative mass of the particles was smaller than equivalent spheres of 2 microns in diameter and 25% was smaller than spheres 1 micron in diameter. This is compatible with the electron and scanning electron microscope observations.

Two independent BET measurements yielded respectively a specific area of 58.7 and 63.1 m^2/g.

An electron micrograph of the powder is shown on Fig. 7. Individual particles have a cube shape with rounded corners varying in dimensions from about 0.05 to 1μ in edge length. The pictures were taken with an RCA EMU-3 electron microscope using a 100kv beam and a magnification of 5900x.

Fig. 8 shows a scanning electron micrograph of the same material and confirms the morphology observed on the micrograph of Fig. 7.

Moisture content was determined by heating a known quantity of powder at 900°C for several hours and comparing the weight before and after the treatment. A moisture content of 3.26% was found. It was comparable with two independent measurements at the Bethlehem Steel Corporation Homer Research Laboratories which yielded 2.90 and 3.18% respectively.

The powder's density was measured with a pycnometer. Three measurements yielded respectively 3.344, 3.402 and 3.333 gr/cm^3 or an average of 3.36 gr/cm^3 including a 3.26% moisture content.

Fig. 7

Electron Micrograph of the

As-received γ-Al_2O_3 (x5920)

Fig. 8

Scanning Electron Micrograph of the

As-received γ-Al_2O_3 (10,000x)

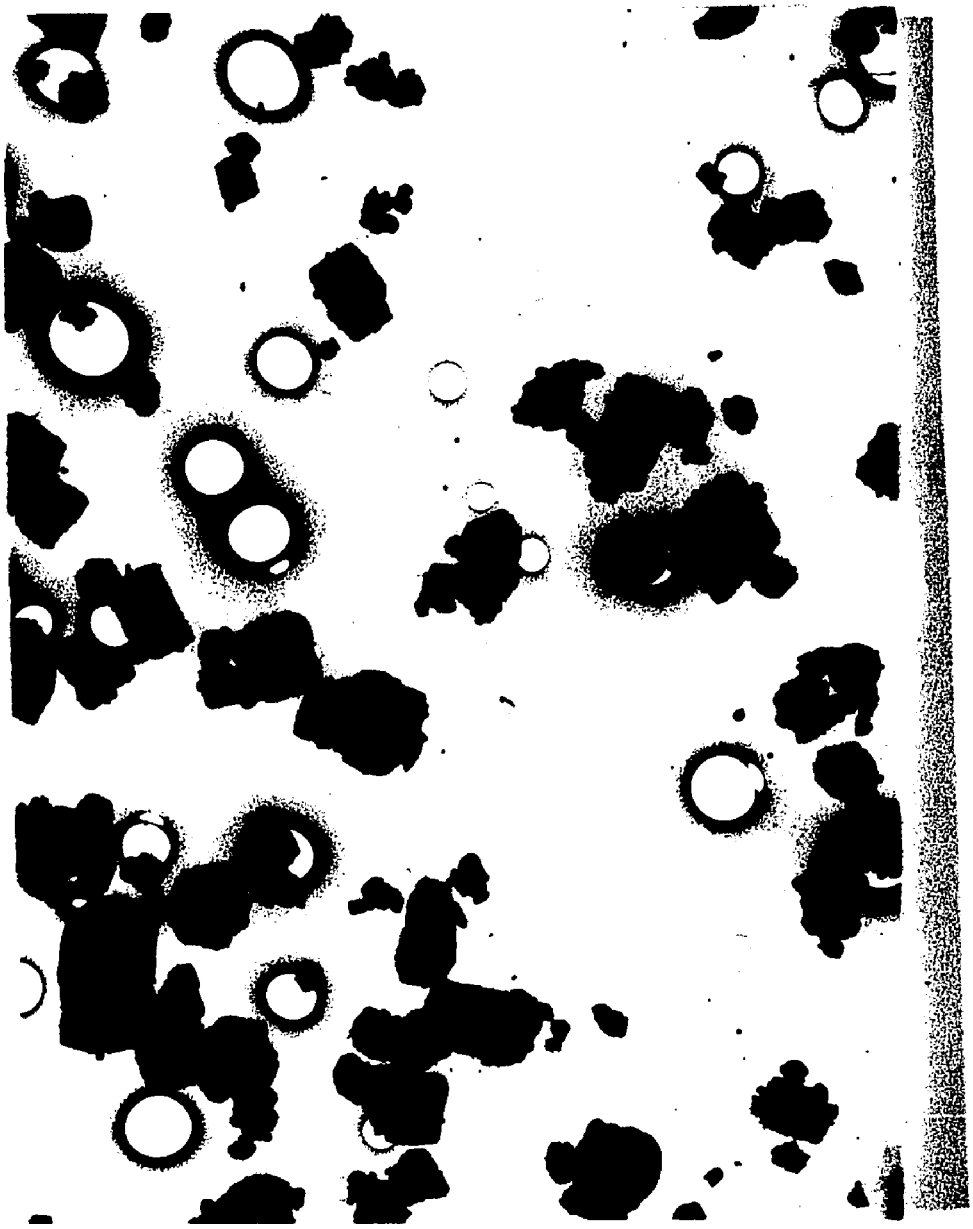

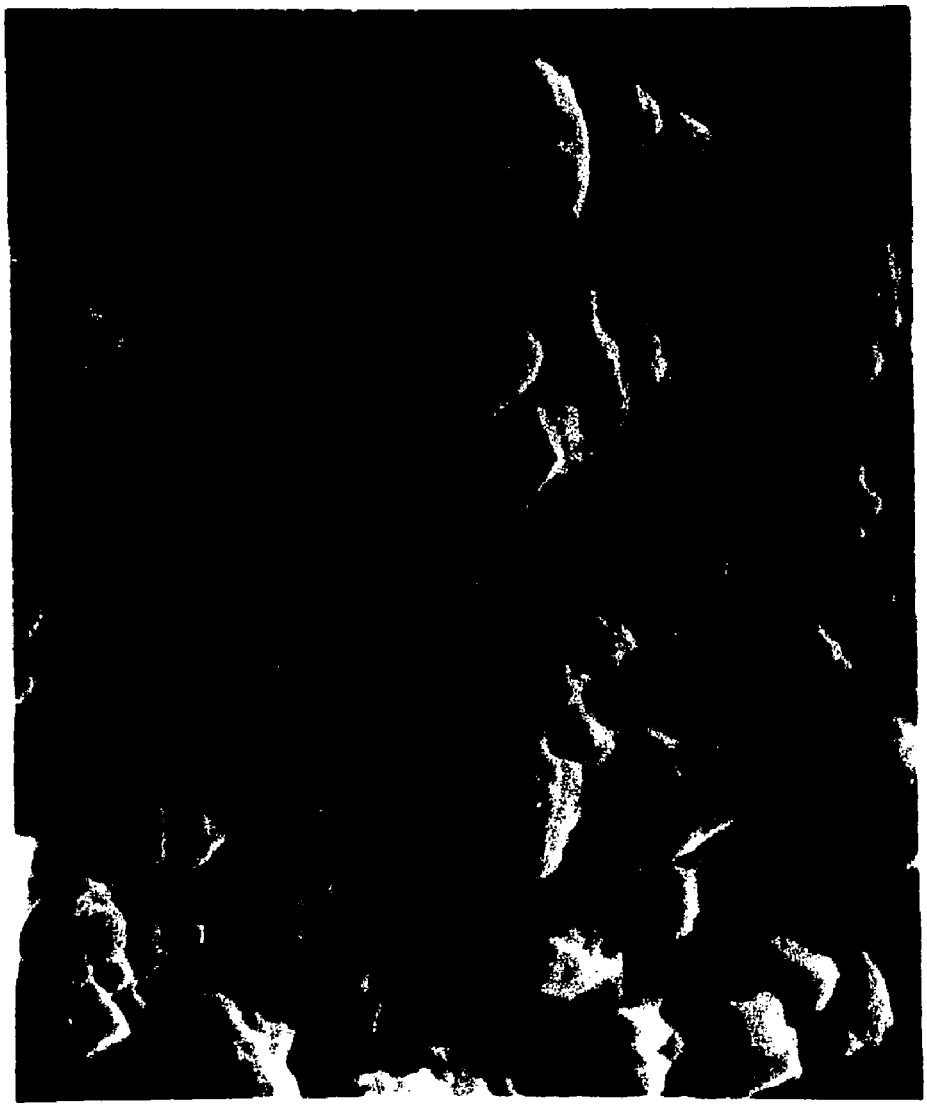

Measurement of α-Al_2O_3 concentration. X-ray diffractometry appeared to be the most suitable analytical method to determine the amount of transformed γ-Al_2O_3, or alternately, the amount of α-Al_2O_3 formed.

The technique is based on the fact that when the x-ray absorbing power of the substance measured in a binary mixture is the same as that of the entire mixture, as in mixtures of various polymorphic forms of a substance, the intensity of a diffracted peak is directly proportional to the concentration of that phase producing this peak (50).

The reason for this phenomenon is shown in the equation below relating the concentration x_1 of a phase I, its mass absorption coefficient μ_1^* and the mass absorption coefficient of the matrix μ^*. If I_1 is the intensity of x-ray diffracted by some selected plane:

$$I_1 = \frac{k_1 x_1}{\rho_1 \left[x_1 \left(\mu_1^* - \mu_M^*\right) + \mu_M^*\right]} \qquad (9)$$

k_1 is a constant depending upon the nature of component 1 and the geometry of the apparatus. However $\mu_1^* = \mu_M^*$ in polymorphic binary mixtures, thus equation (9) reduces to

$$I_1 = \frac{k_1}{\rho_1 \mu_M^*} x_1 \simeq k x_1 \qquad (10)$$

The validity of equation (10) has been demonstrated by Klug and Alexander (54) with binary quartz and cristobalite mix-

tures.

It was decided to verify whether this procedure could be used for the present experiment. Known mixtures of the as-received material and α-Al_2O_3 produced by isothermally transforming a batch of as received powder for 3 hours at 1400°C, were prepared and the latter's concentration was measured as a function of its most intense peak (the 11.3)'s relative intensity.

The standard mixtures were prepared by mixing known quantities of dried as-received alumina and α-Al_2O_3 with isopropyl alcohol, agitated for 15 minutes in a Spex mixer. At the end of that period, the jar was removed and powder particles were washed away from the walls back into the suspension. The alcohol was then evaporated over a steam-bath.

In this manner seven standard mixtures of known α-Al_2O_3 concentrations were prepared containing respectively 10, 22, 33, 50, 67, 80 and 90% by weight of α-Al_2O_3.

The powdered samples were then mounted for x-ray examination in a hollow plastic holder and the intensity of the (11.3) peak measured for each mixture and compared to that for a 100% α-Al_2O_3 sample.

CuK_α radiation with nickel filter was used. Counting was done by a proportional counter and the intensity was recorded as a function of the angle of incidence between the

beam and the specimen by a strip chart recorder. The specimen was allowed to rotate by ¼ of a degree per minute and the chart speed was fixed at 2 inches per minute to give an easily measurable peak.

The relative intensity of the peak was obtained by comparing its intensity to that obtained for the fully transformed sample. Six readings were taken for each concentration. Peak height measurements gave reasonable evidence of linearity between the relative intensity of (11.3)α and the α-Al_2O_3 concentration as shown on Fig. 9. However, substantially better results were obtained when integrated intensities were used, i.e., the total area under the peak corrected for background radiation as shown on Fig. 10. These results persuaded us to use integrated intensities for later work.

Determination of the transformation rate

Samples consisting of two grams of the as-received powder in covered platinum crucibles that were held for various periods of time in a SiC resistance heated oven. The crucibles were cooled in a dessicator, emptied in an agate mortar and pestle and the aggregate crushed to ensure good mixing between α-Al_2O_3 and the untransformed material. The mortar was then emptied into a glass jar, isopropyl alcohol added and the same procedure employed as in the

Fig. 9

Peak Height - Concentration Curve for Standard Mixtures of γ-Al_2O_3 and α-Al_2O_3

Fig. 10

Integrated Intensity - Concentration Curve for Standard Mixtures of γ- and α-Al_2O_3

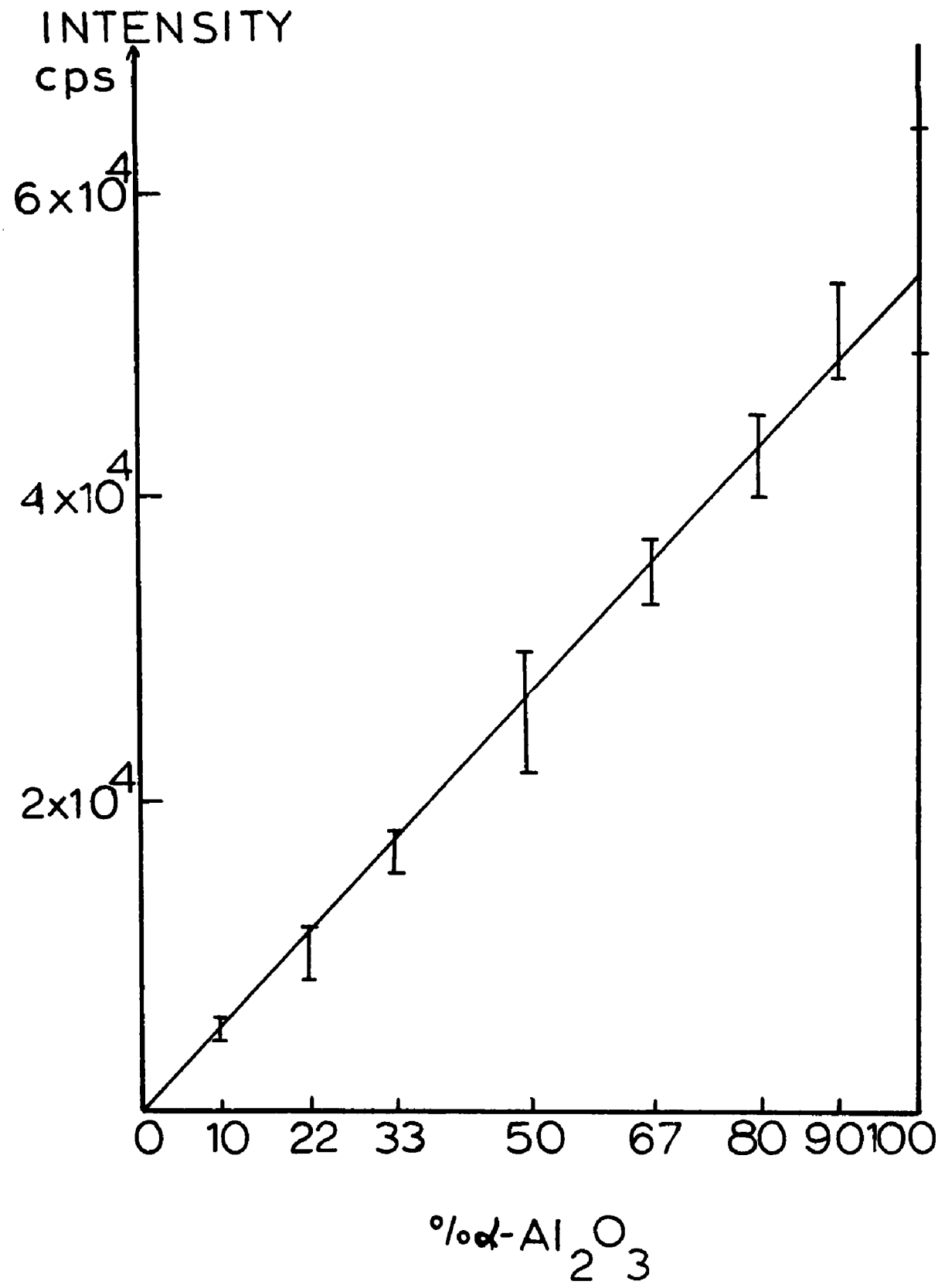
INTENSITY
cps
6x10^4
4x10^4
2x10^4
0
10
22
33
50
67
80
90
100
%α-Al2O3

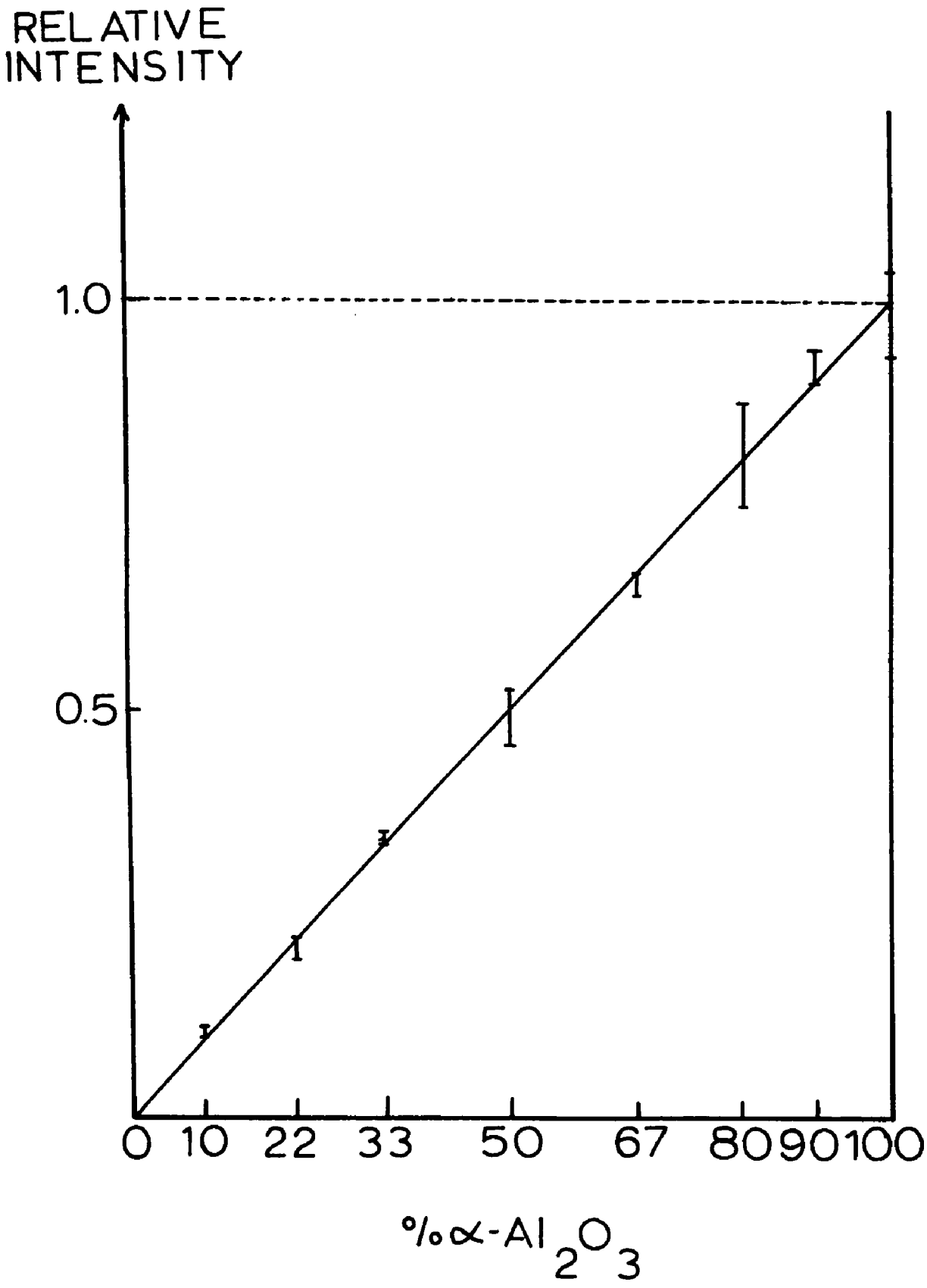
RELATIVE
INTENSITY
1.0
0.5
0 10 22 33 50 67 80 90 100
% α-Al2O3

preparation of homogeneous standard mixtures.

The amount of α-Al_2O_3 formed for each given condition of time and temperature was then measured by comparing for a given set of specimens the integrated intensity of the (11.3)α peak with the intensity measured in a fully transformed sample in identical conditions. The ratio of the two areas then gave the relative amount of α-Al_2O_3 formed. The operating variables, beam aperture, receiving slit width, pulse height, window width, sensitivity scale and statistical errors were chosen so as to give an optimum peak over background ratio.

Measurements were made every 25°C between 1025° and 1100°C, every 20°C between 1100° and 1140°C and every 10°C between 1140° and 1200°C. The number of specimens for each temperature varied from 4 to 11.

A statistical analysis of the results obtained was done by a CDC 6400 computer at Lehigh University using a standard program held in that center's library.

At the higher temperatures where the transformation occurs in shorter times, care was taken to consider the time necessary to heat up the crucible and its content to the desired temperature. It was determined by connecting a thermocouple so arranged that its hot junction was immersed in the powder to a recorder and found to be of the order of 100 seconds.

III. RESULTS

Qualitative aspects of the transformation. Certain peaks were found to have shifted on partially transformed materials. This led us to examine our material more closely. Samples of the as-received powder were annealed at 220° and 550°C for 24 hours and at 800°C and 900°C for 12 hours.

The scan on the 220° probe as shown by Fig. 11 revealed all peaks belonged to γ, Θ and δ-Al_2O_3 (the existence of which is widely doubted). Because those structures are very closely related, the peaks are impossible to separate and they merely undergo a slight shift or change in intensity when one of the transitions occurs. Our "gamma" material appeared to contain substantial amounts of Θ-Al_2O_3 in the as-received condition. The specimen annealed at 550°C showed little change. The one annealed at 800°C showed a decline of typical γ peaks such as (222), (331) and (400) and a sharpening of Θ peaks such as (200), (111). The scan of the 900° anneal sample showed an enhancement of that trend (Fig. 12). γ-Al_2O_3's most intense peak (440) had split into two peaks belonging to the Θ structure and had shifted by about a quarter of a degree.

A slight lattice change then occurred around 900°C

Fig. 11

30° - 50° X-ray Scan of As-Received γ-Al_2O_3

Fig. 12

30° - 50° X-ray Scan of Material

Annealed 12 Hours at 900°C

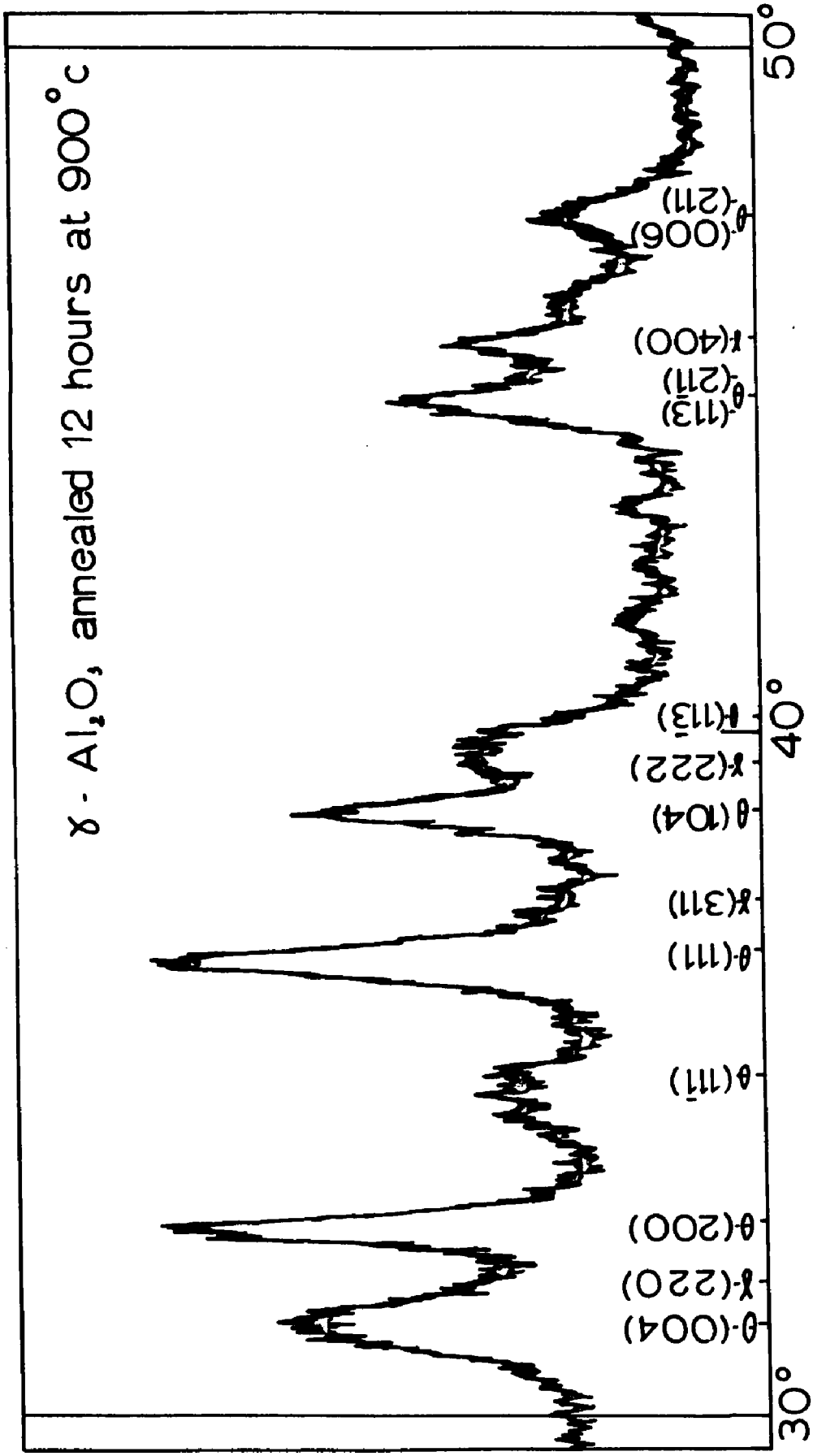
γ - Al2O3 annealed 12 hours at 900°c
30°
40°
50°
θ-(004)
γ-(220)
θ-(200)
θ(11$\bar{1}$)
θ-(111)
γ(311)
θ(10$\bar{4}$)
γ-(222)
θ(11$\bar{3}$)
θ-(11$\bar{3}$)
θ-(21$\bar{1}$)
γ-(400)
θ-(006)
θ-(211)

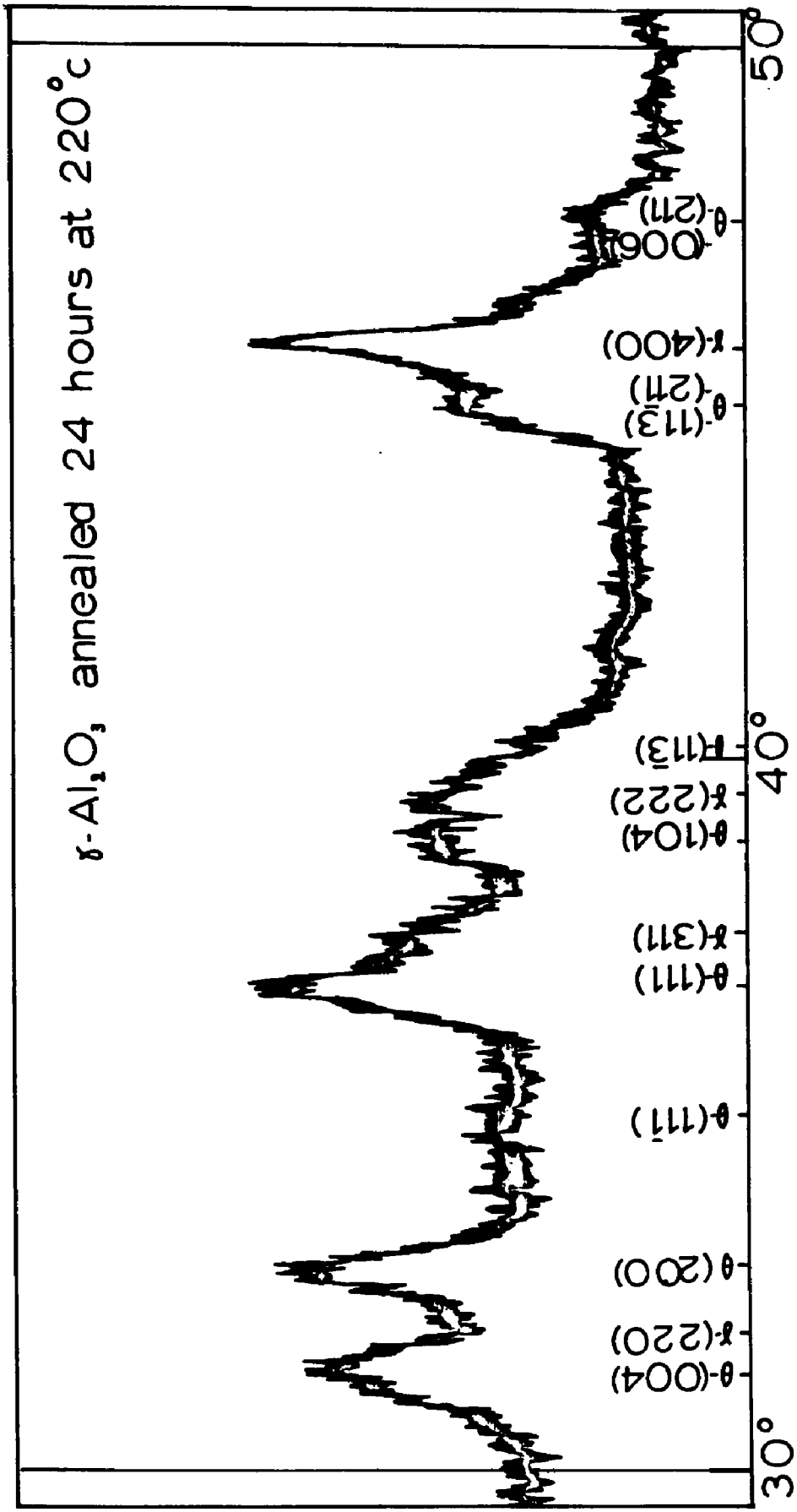
γ-Al₂O₃ annealed 24 hours at 220°c
30°
40°
50°
θ-(004)
γ-(220)
θ (200)
θ-(111̄)
θ-(111)
γ-(311)
θ-(104)
γ-(222)
Γ(113̄)
θ-(113̄)
θ-(211)
γ-(400)
θ-(006)
θ-(211)

before corundum started forming. This is consistent with many workers' observations (21, 33, 39). We also have reason to suspect that our material consisted largely of Θ-Al_2O_3 and that the transformation to α-Al_2O_3 is that of Θ rather than of γ-Al_2O_3.

Density measurements were made of the 900°C anneal sample and yielded a density of 3.57 gr/cm which is consistent with the reported figure for Θ-Al_2O_3 (21).

Quantitative observations of the transformation. The fraction of α-Al_2O_3 formed appeared to vary linearly with time. In other words, the transformation in the powder specimen can be considered to follow zero-order kinetics: $dc/dt = k$. Unlike in Clark and White's experiment, a plot of the log of the amount of untransformed product of the present material vs. time for the present data showed definite non-linearity (Fig. 13). This would preclude the possibility of the transformation's following first-order kinetics for the present material.

The fraction of α-Al_2O_3 obtained for each temperature as a function of time is listed in Table I and plotted in Fig. 14 to Fig. 19.

For each concentration vs. time plot, the best slope forced through the origin (since it appeared there was no incubation period at any of the temperatures investigated) was obtained by a least square regression analysis to a

Fig. 13

Semilog Plot of the Fraction of Untransformed γ-Al_2O_3 Against Time Showing Nonlinearity

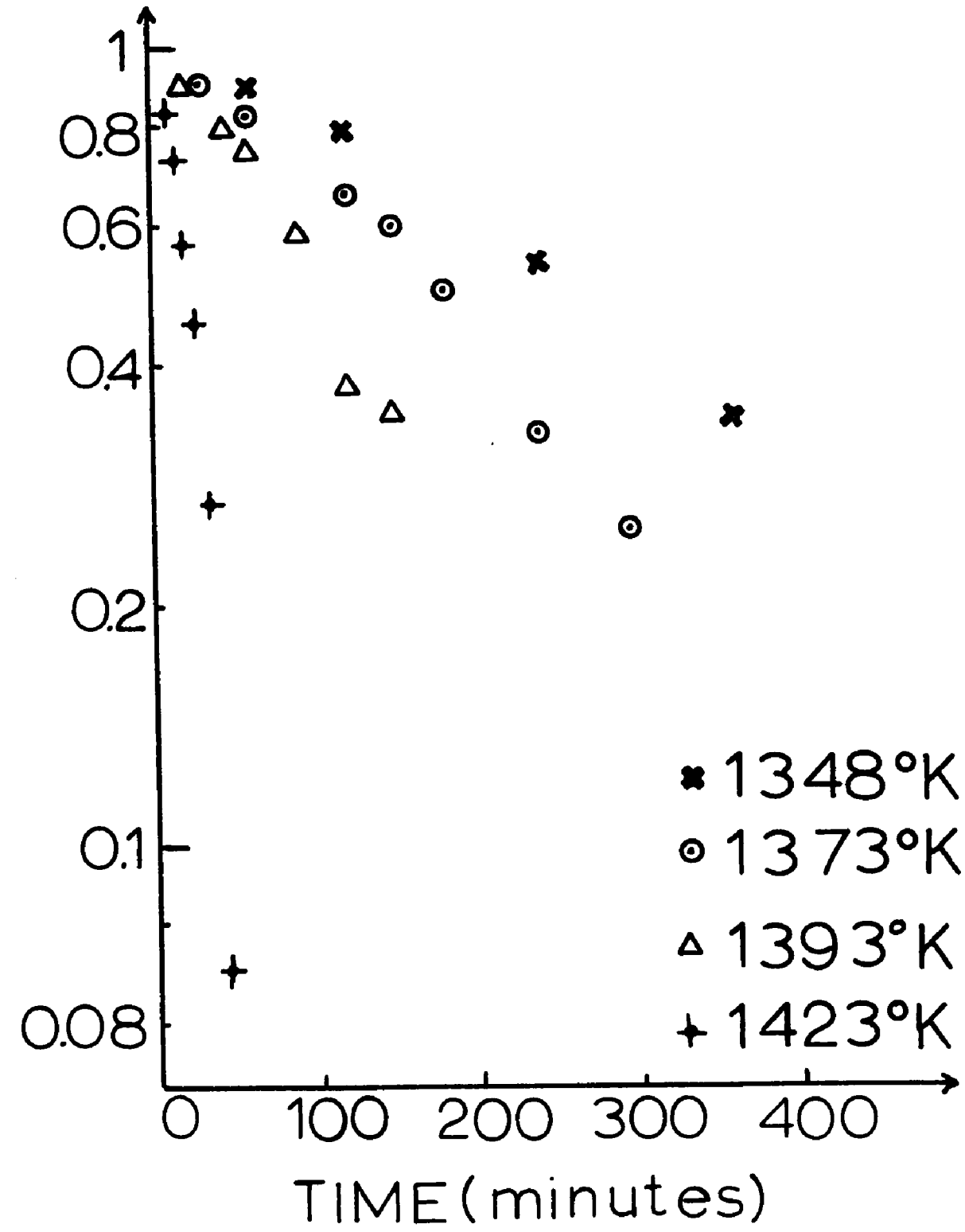
FRACTION
UNTRANSFORMED
1
0.8
0.6
0.4
0.2
0.1
0.08
0
100
200
300
400
TIME (minutes)
1348°K
1373°K
1393°K
1423°K

TABLE I

Fraction α Transformed vs. Time and Temperature.

T°C	T°k	time (min)	% α- Al_2O_3
1025°	1298°	180	6.06
		360	13.22
		540	22.20
		720	28.21
		900	34.06
		1200	40.90
		1440	48.49
		1800	55.86
		2160	76.22
		2400	81.35
1050°	1323°	60	6.33
		120	9.65
		150	10.85
		240	14.78
		300	17.60
		360	25.35
		600	36.50
		720	55.55
		960	86.55
1075°	1348°	30	6.50
		60	10.95
		120	19.41
		240	46.15
		360	65.00
		600	90.55

TABLE I (Cont.)

T°c	T°k	time (min)	% α-Al_2O_3
1100°	1373°	30	8.37
		60	16.80
		120	34.22
		150	38.45
		180	50.37
		240	64.67
		300	74.10
1120°	1393°	20	9.71
		45	20.73
		60	23.65
		90	41.46
		120	62.30
		150	64.10
1140°	1413°	20	24.20
		40	60.25
		60	74.25
1150°	1423°	5	9.55
		10	16.10
		15	27.04
		20	43.75
		25	54.65
		35	72.95
		45	93.30

TABLE I (Cont.)

T°c	T°k	time (min)	% α-Al_2O_3
1160°	1433°	5	12.09
		10	25.28
		15	34.45
		18	50.40
		23	57.18
		27	70.85
		30	78.10
1170°	1443°	5	13.60
		10	23.05
		12	23.30
		15	28.95
		20	57.30
		24	61.26
		27	71.31
		30	76.80
		33	85.95
		40	91.80
1180°	1453°	4	10.15
		8	27.27
		12	44.55
		16	62.66
		20	69.70
		24	81.07
1190°	1463°	4	16.31
		8	39.95
		12	61.20
		16	83.00
		20	94.40

TABLE I (Cont.)

T°c	T°k	time (min)	% α-Al_2O_3
1200°	1473°	4	19.65
		8	58.93
		12	83.86
		15	92.07

Figs. 14 - 19

Fraction α-Al_2O_3 Formed Against Time

for All Investigated Temperatures

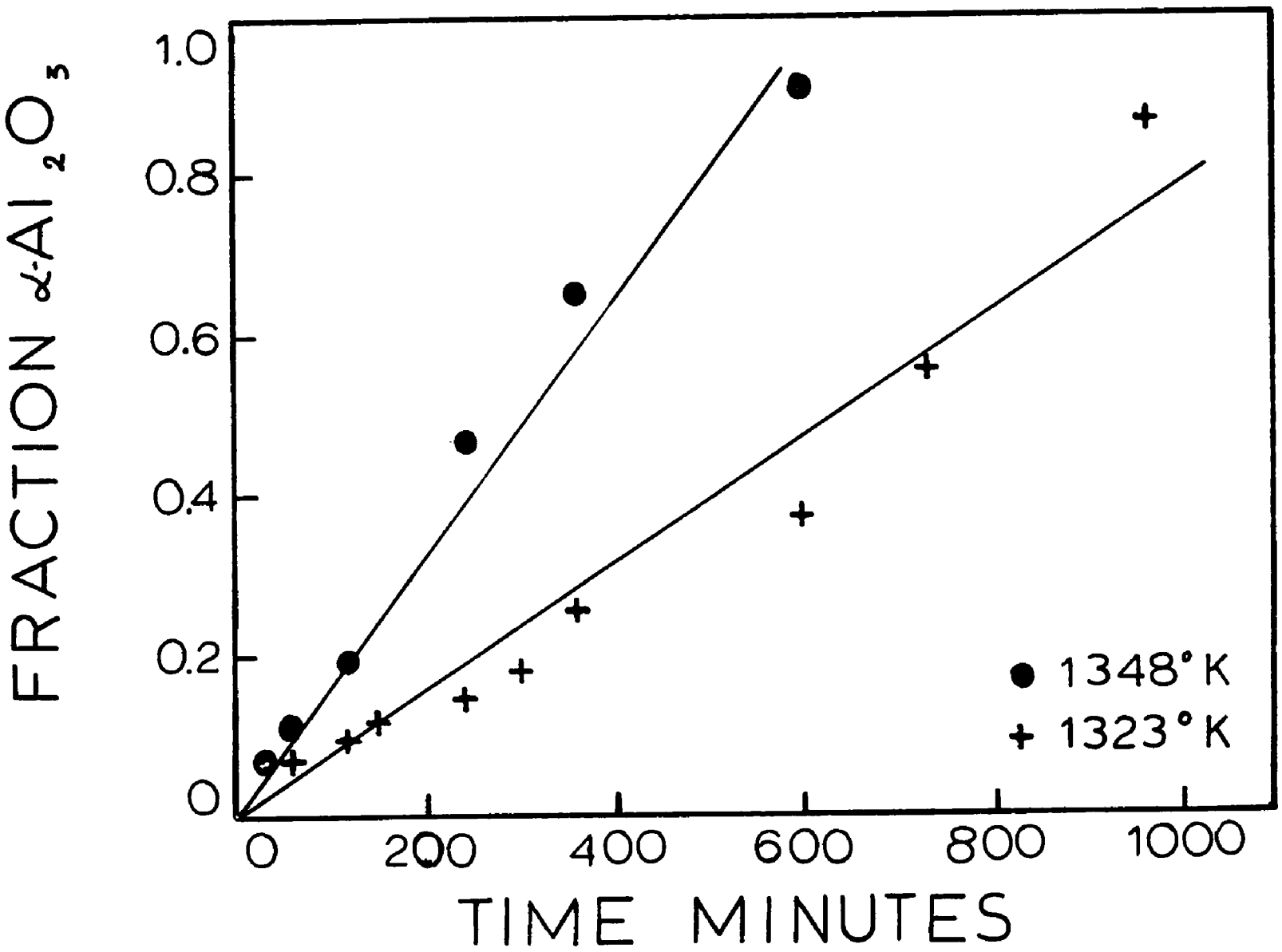
FRACTION α-Al2O3
1.0
0.8
0.6
0.4
0.2
0
0
200
400
600
800
1000
TIME MINUTES
1348° K
1323° K

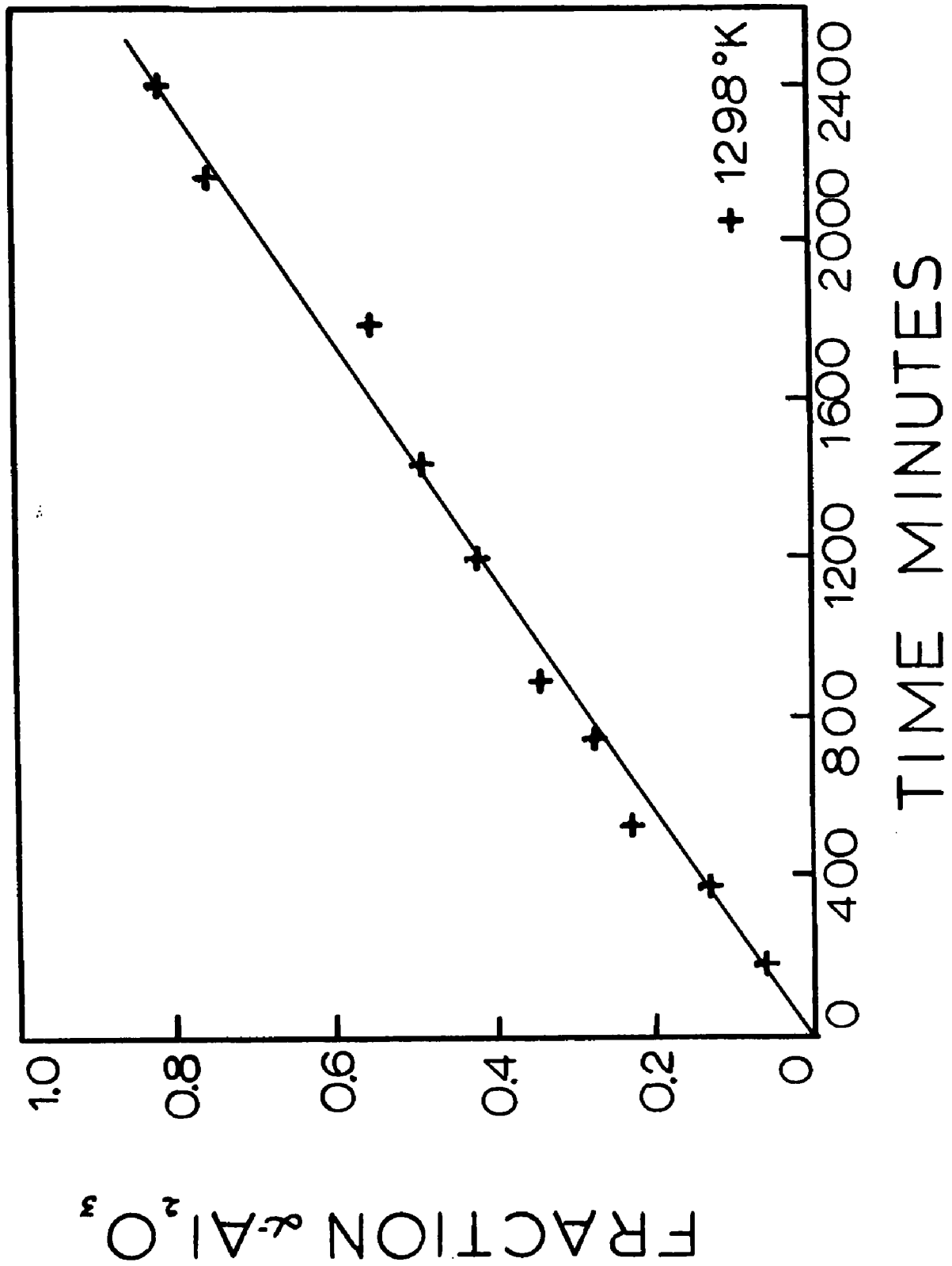
FRACTION α-Al2O3
1.0
0.8
0.6
0.4
0.2
0
0
400
800
1200
1600
2000
2400
TIME MINUTES
+ 1298°K

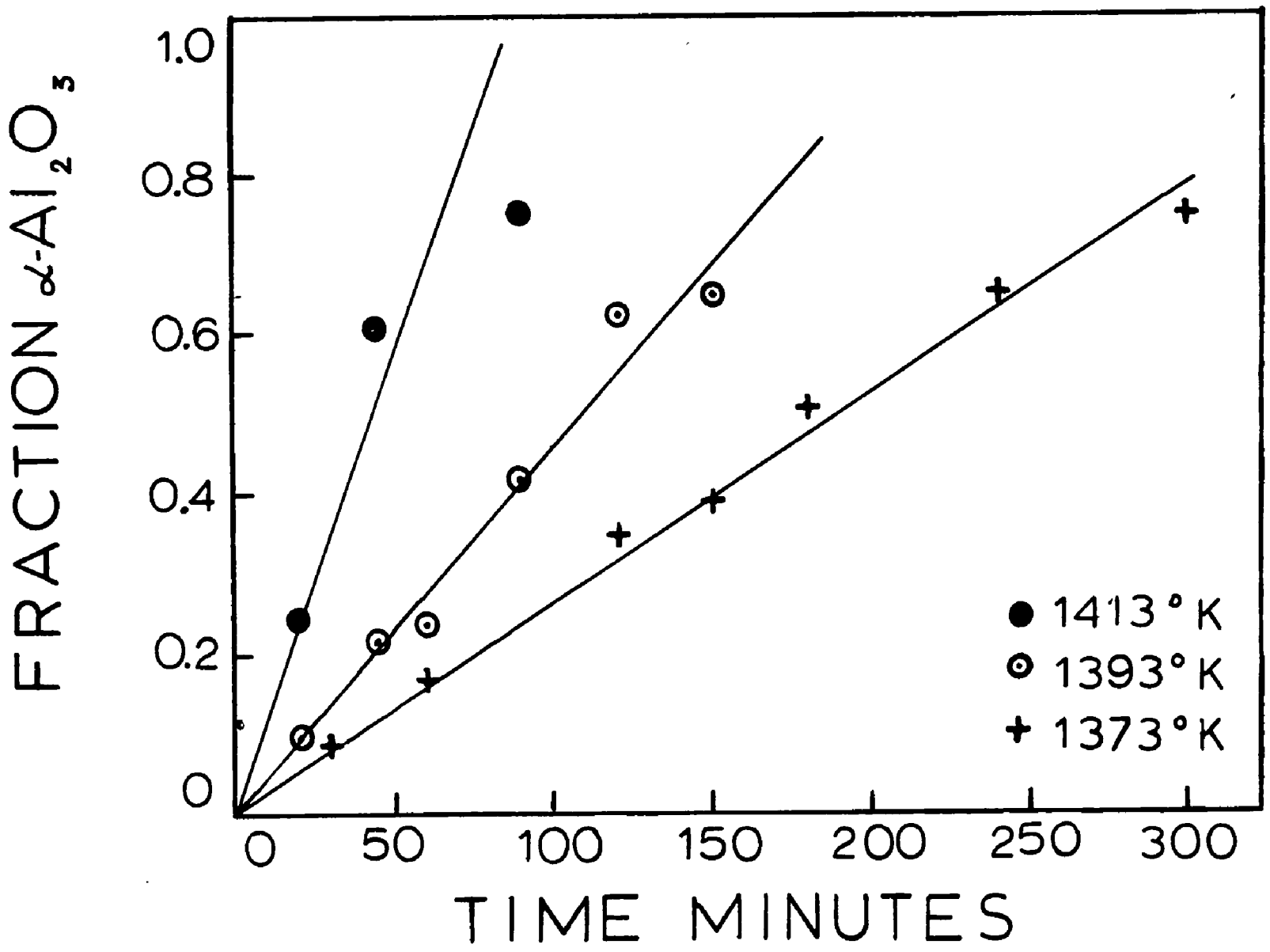
FRACTION α-Al2O3
1.0
0.8
0.6
0.4
0.2
0
0
50
100
150
200
250
300
TIME MINUTES
1413° K
1393° K
1373° K

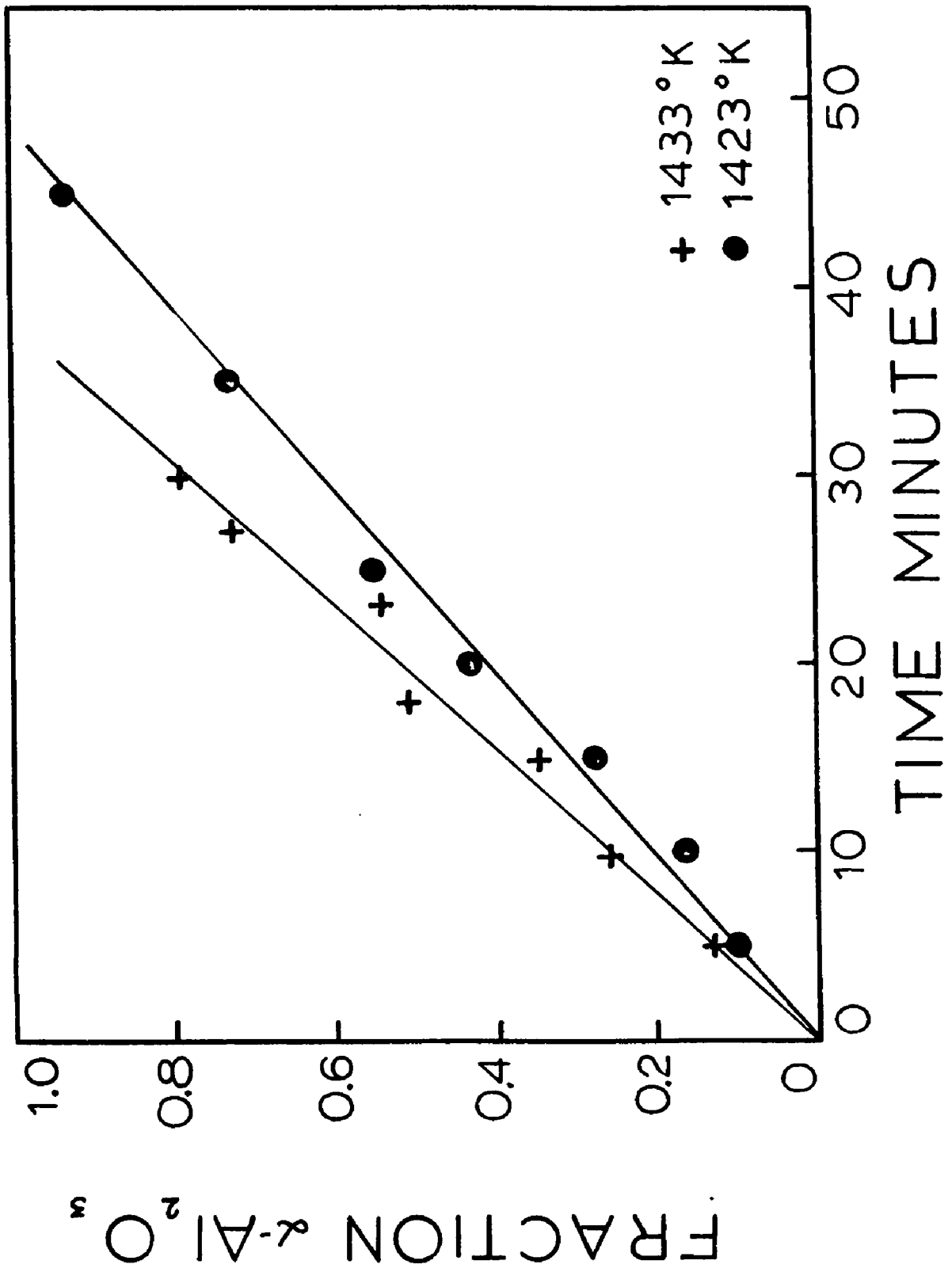
FRACTION α-Al2O3
1.0
0.8
0.6
0.4
0.2
0
0
10
20
30
40
50
TIME MINUTES
+ 1433°K
● 1423°K

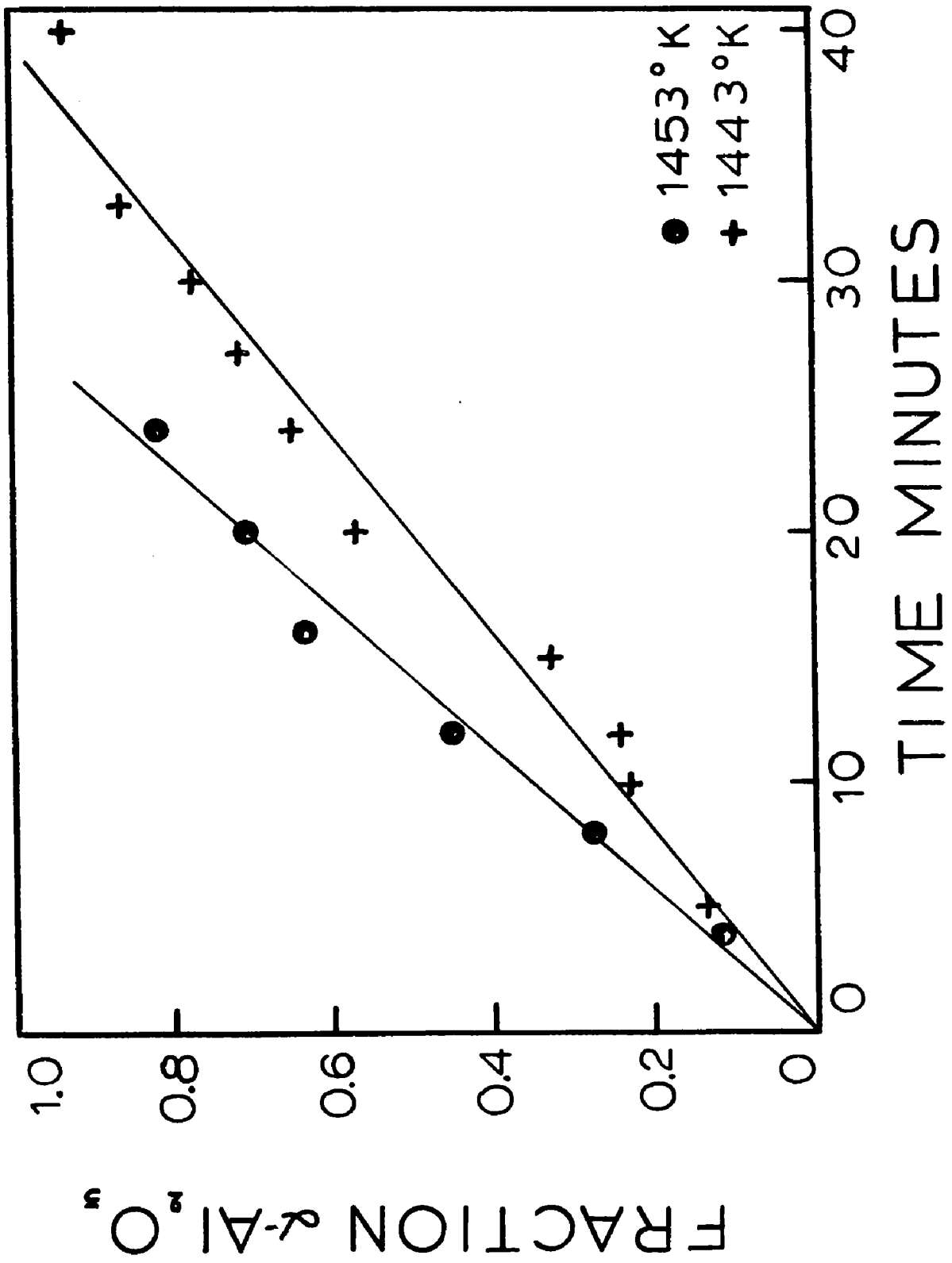
FRACTION α-Al2O3
1.0
0.8
0.6
0.4
0.2
0
0
10
20
30
40
TIME MINUTES
1453°K
1443°K

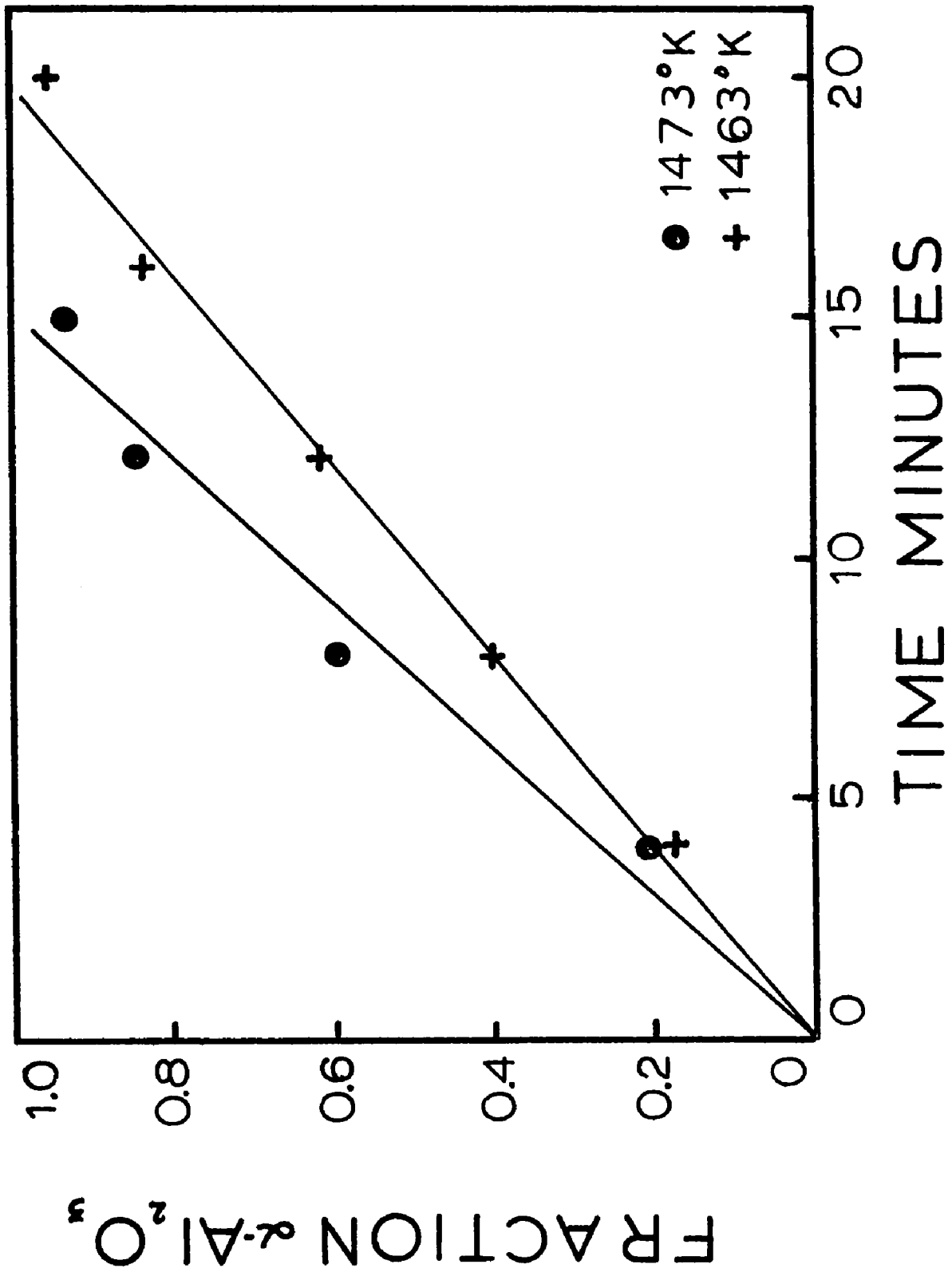
FRACTION α-Al2O3
1.0
0.8
0.6
0.4
0.2
0
0
5
10
15
20
TIME MINUTES
● 1473°K
+ 1463°K

TABLE II

Rate Constants for the Kinetics
of the γ-Al_2O_3 Phase Transformation

T°k	k [min^{-1}]
1298	$(3.149 \pm 0.146) \times 10^{-4}$
1323	$(7.843 \pm 0.920) \times 10^{-4}$
1348	$(1.620 \pm 0.152) \times 10^{-3}$
1373	$(2.617 \pm 0.130) \times 10^{-3}$
1393	$(4.581 \pm 0.440) \times 10^{-2}$
1413	$(1.318 \pm 0.297) \times 10^{-2}$
1423	$(2.077 \pm 0.098) \times 10^{-2}$
1433	$(2.580 \pm 0.112) \times 10^{-2}$
1443	$(2.495 \pm 0.160) \times 10^{-2}$
1453	$(3.527 \pm 0.236) \times 10^{-2}$
1463	$(4.926 \pm 0.298) \times 10^{-2}$
1473	$(6.542 \pm 0.923) \times 10^{-2}$

polynomial of degree one. The slope thus obtained was a measure of the rate constant of the formation of corundum at a given temperature. The values obtained are shown in Table II. The rate constants were then plotted on a semi-log paper against reciprocal temperatures to determine the activation energy (Fig. 20).

The "t" test was applied to the square root of the slope variance for each plot of fraction transformed vs. time to get the limits corresponding to a 95% confidence level. It was also performed on the plot of Fig. 20.

An activation energy of 116 ± 5 kcals/mole was found with a frequency factor of 10^{16} min^{-1}, which is of similar magnitude to that observed for first order gas reactions (51). The significance of such a value is, however, hard to understand in solid state reactions because solid state reactions are inhomogeneous and usually take place in more or less complicated sequences.

Electron microscopy. Powder samples after the transformation were examined under the electron microscope for visible evidence of any morphological changes, as suggested by Iler (42). Pictures were taken at a magnification of 6000x. Fig. 21 shows such particles on a carbon support film after a 12 hour anneal at 900°C, presumably in the θ

Fig. 20

Reaction Rate Constant k vs Reciprocal Temperature for the γ- to α-Al_2O_3 Phase Transformation

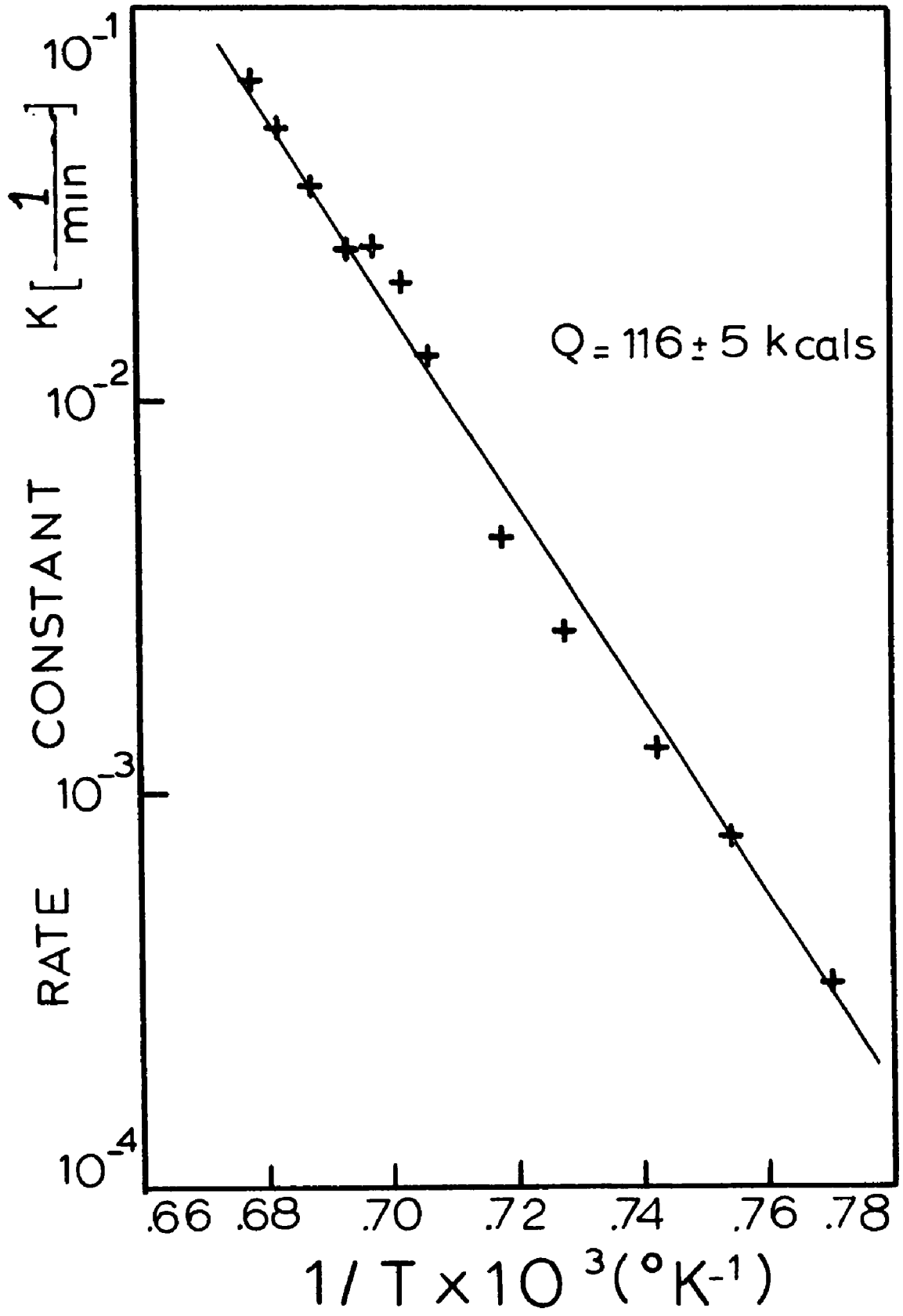
RATE CONSTANT K [1/min]
10^-1
10^-2
10^-3
10^-4
Q = 116 ± 5 k cals
.66 .68 .70 .72 .74 .76 .78
1/T x 10^3 (°K^-1)

state. It shows little difference from the as-received powder. Fig. 22 shows a supposedly fully transformed specimen, and again no difference in appearance can be noticed. It is not possible at that stage to notice whether the particles observed are single crystals or consist of an agglomeration of smaller crystallites. Fig. 23 taken from a specimen less than 10% transformed shows also no practical difference from the two previous pictures.

Scanning electron micrographs were made at the Bethlehem Steel Homer Research Laboratories on the as-received material (see characterization of initial powder), the material in the Θ-Al_2O_3 state, halfway transformed into α-Al_2O_3 and 100% α-Al_2O_3(Fig. 23 to Fig. 26). While little difference is noticed between the as-received material, that in the Θ-Al_2O_3 condition, and the 50% transformed sample, this is no longer the case with the fully transformed specimen. In the first three figures (Fig. 24 to Fig. 26), the grains appear to be monolithic blocks of presumably polycrystalline assemblies, in the 100% α-Al_2O_3, the blocks appear to be broken down in aligned strata of small corundum grains (Fig. 27). It appears that not only does the average particle size not increase as first thought by Iler (42), but in fact, the Θ-Al_2O_3 particles break down into smaller units.

Specific surface area measurements were made by Dr.

Fig. 21

Electron Micrograph of γ-Al_2O_3 After a 12 Hour Anneal at 900°C (5920x)

Fig. 22

Electron Micrograph of α-Al_2O_3 After a 24 Hour Anneal at 1050°C (5920x)

Fig. 23

Electron Micrograph of Material Containing $\sim$10% α-Al_2O_3 After a 2 Hour Anneal at 1050°C (5920x)

H. Stanley at C. Pfizer's Research Laboratories on the following four samples: as-received material, material in the θ-Al_2O_3 condition, material 50% transformed and finally fully transformed. Specific surface areas of 63, 48, 24 and 8 m^2/gram were obtained respectively. Those measurements are consistent with those obtained by other workers (32, 42, 44).

The γ/α transformation diagram. From the observed measurements of the fraction of α-Al_2O_3 at each temperature, it became possible to construct a time-temperature-transformation diagram. The lines drawn were arbitrarily chosen to represent those points where respectively 10, 50 and 90% of the original powder has transformed. The diagram is illustrated on Fig. 28.

Fig. 24

Scanning Electron Micrograph of

As-Received Material (10,000x)

Fig. 25

Scanning Electron Micrograph of Alumina in

the θ-Al_2O_3 Condition (10,000x)

Fig. 26

Scanning Electron Micrograph of Alumina

50% Transformed (10,000x)

Fig. 27

Scanning Electron Micrograph of a Fully

Transformed Sample (10,000x)

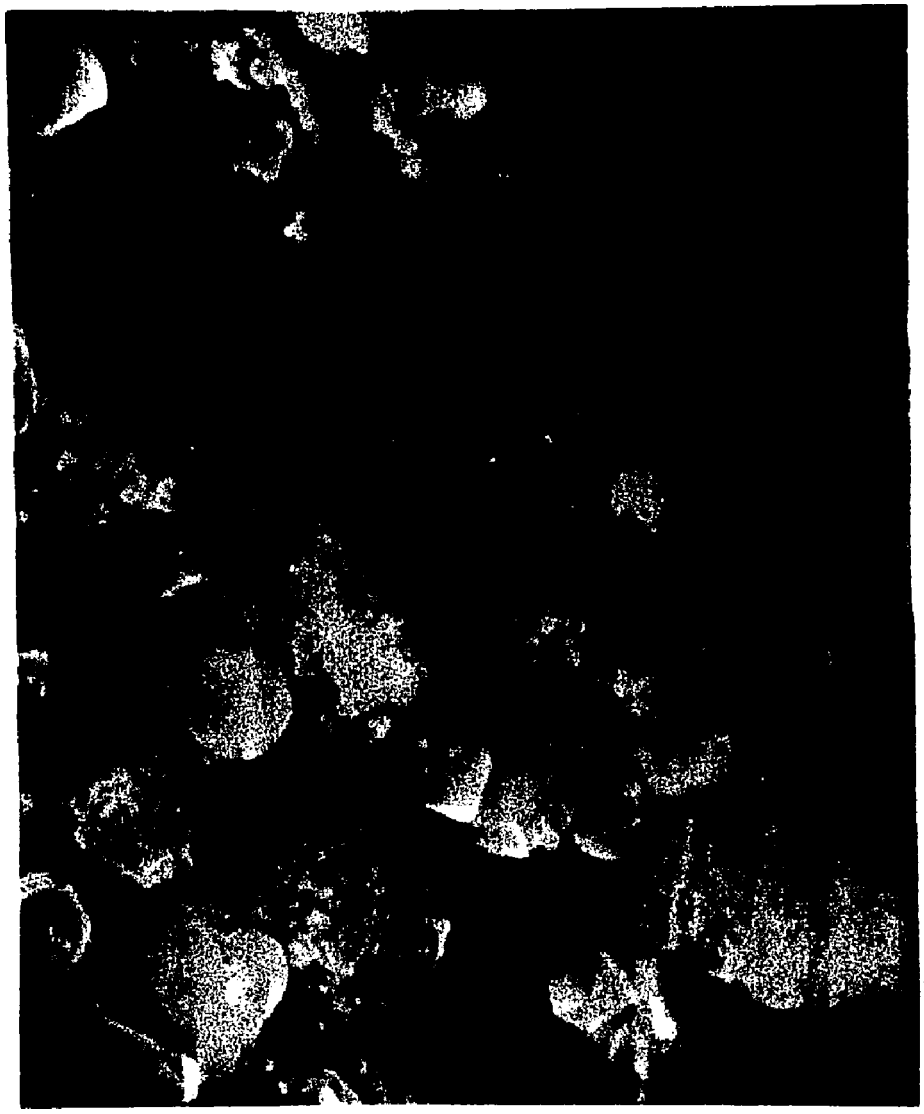

Fig. 28

The Alumina Transformation Diagram

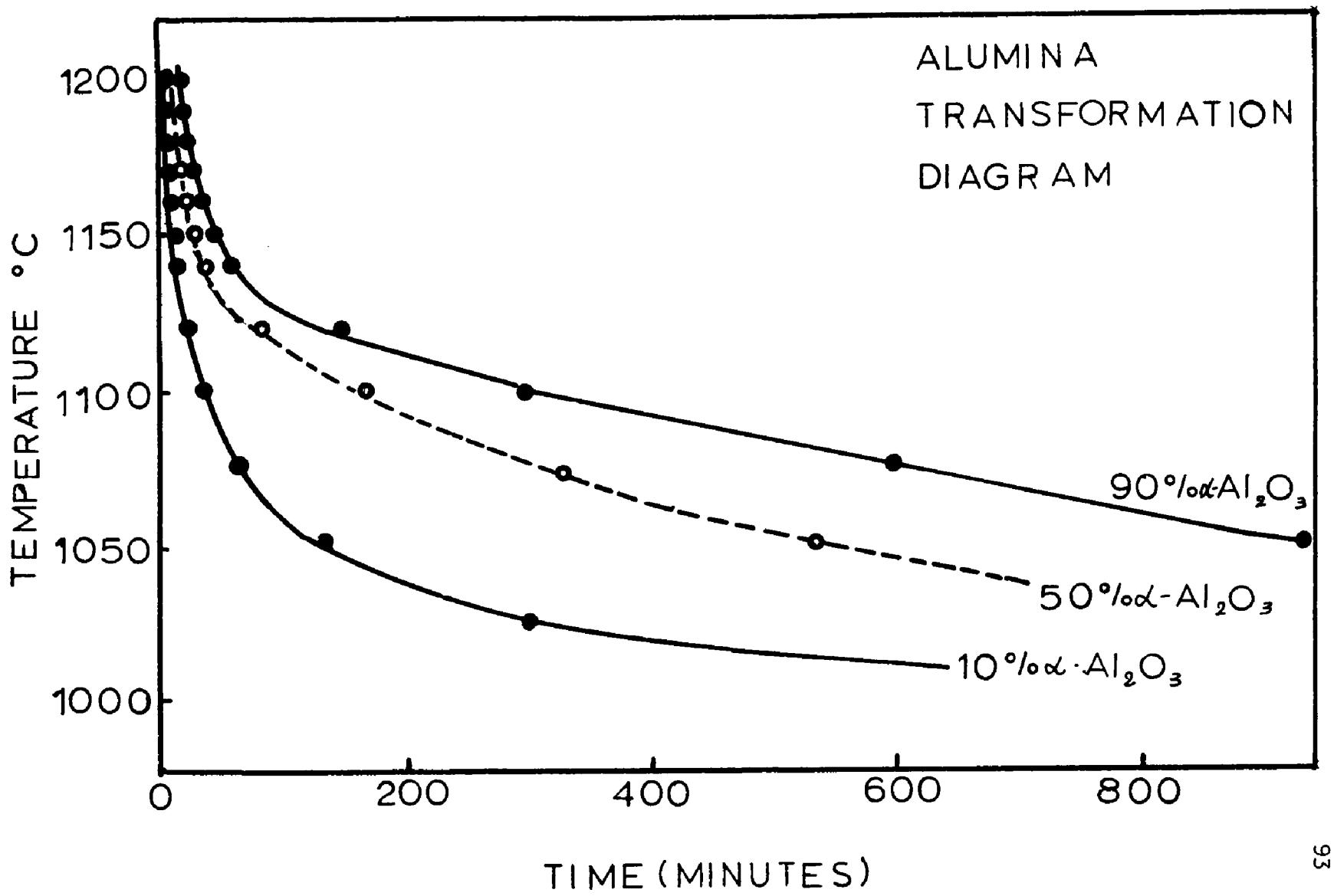
ALUMINA
TRANSFORMATION
DIAGRAM
TEMPERATURE °C
1200
1150
1100
1050
1000
0
200
400
600
800
TIME (MINUTES)
90% α-Al2O3
50% α-Al2O3
10% α-Al2O3

IV. DISCUSSION

Temperature dependence of the transformation. An interesting finding was the difference in activation energy observed by Clark and White: 79 kcals/mole, Ching and Sheng: 153 k/cals/mole, Yanagida's: 101.6 and 143 kcals/mole, and the present experiment: 116 kcals/mole.

Clark and White (65) worked between 1195° and 1500°C, Ching and Sheng (48) between 1100° and 1190°C, Yanagida et al.(48) between 1030° and 1250°C, and in the present work between 1025° and 1200°C.

Timewise, there are also several discrepancies. It took Clark and White's material 30 minutes at 1350° to be fully transformed while Ching and Sheng's transformed in a similar period of time at 1190°C. However, for some reason they did not explain, Yanagida's material never went to 100% transformation. By comparison, our material transformed fully in less than one hour at 1150°C and slightly more than 15 minutes at 1200°C.

Based on activation energy considerations alone, Clark and White's material has a lower energy barrier to overcome, but it, however, converts into α-Al_2O_3 at substantially higher temperatures. A possible explanation can be provided if their initial material consists of κ-Al_2O_3 rather

than γ or Θ-Al_2O_3 for κ-Al_2O_3 transforms into α-Al_2O_3 at temperatures 150° to 200°C above Θ-Al_2O_3 (21). Since commercially available "gamma" aluminas consist usually of several of the transition forms mixed in different proportions, widely different transformation ranges will be observed depending on the individual polymorphic make-up of a particular powder.

Clark and White's material had a higher silica content than the present material by a factor of five, and 0.07% CaO while the latter is in negligible amount in our material. It has been shown that silica tends to hinder the transformation of transition aluminas into corundum (52, 53).

The role of particle size in explaining the discrepancy between these workers' results and ours is not clear. Transformation speeds appear to be decreased by smaller particle size in displacive changes. Buerger (7) gives two possible explanations for this phenomenon:

1 - If nucleation arises in each grain of powder, the finer the powder the more nuclei have to be created.

2 - Heat is transmitted by radiation from one grain to another, which is a slower way to conduct heat than by conduction across each grain.

While it is difficult to estimate the validity of statement

2, that of statement 1 can be easily understood if nuclei have to be formed during the transformation. In such a case, more nuclei, the formation of each requiring a certain amount of work, would have to be created. This is, however, no longer true if the nuclei already exist at the onset of transformation or if a second type of nucleation site enters into the transformation process at early times, as indicated by Durdaller et al. (54), who observed that smaller particles favored the α to β transformation in tin. It is also reversed for reconstructive transformations for small crystals where the structural bits are unlinked, dispersed and reassembled. The process is also aided by a gaseous or liquid transporting medium (11).

If the formation of α-Al_2O_3 resulted from a displacive transformation, particle size would undoubtedly play an important effect, but since this transformation appears to have reconstructive characteristics, the role of impurities which control atomic transport characteristics, as well as the structural composition of the material prior to the transformation into α-Al_2O_3 plays a predominant part.

It is of interest to note that, in the anatase to rutile transformation, which is reconstructive, a large surface area appears to favor the transformation by lowering the activation energy as the surface area of the starting material increases (55). It was thus proposed that

structural imperfections acting as nucleation sites were increased as the particle size decreased. Larger particle size has also been found to favor the reconstructive quartz to cristoballite transformation (56).

Impurities not only affect transformation temperatures but also the basic mechanisms underlying a transformation (57). Their role can therefore be of greater significance than that of particle size.

Carniglia (58) showed that small amounts of impurities can have a pronounced effect on material behavior when they segregate at grain boundaries and surfaces, for instance by changing the diffusion characteristics from intrinsic to extrinsic. He also indicated that surface diffusion in oxide materials could contribute to such processes as sintering, condensation, and phase changes. If this should be true, any impurities causing acceleration of surface diffusion would cause a decrease in the activation energy and therefore allow the transformation to be observable at lower temperatures.

The importance of the surface to the transformation is evidenced by the sharp reduction in specific area per gram when θ-Al_2O_3 transforms into α-Al_2O_3, from 48 to 8 m^2/gr.

The reduction in specific area per gram seems to contradict the apparent breaking up of larger θ-Al_2O_3

crystals into smaller α-Al_2O_3. It should be remembered that a BET measurement assumes a smooth particle surface as well as a single layer of adsorbed gas and a smooth but small particle may very well display a smaller surface area per unit weight than a larger particle of irregular shape and a surface covered with pores and crevasses which have been shown to exist on the surface of transition aluminas but not on α-Al_2C_3. This is why the former but not the latter displays catalytic properties (28).

If the surface of θ-Al_2O_3 is covered with pores and many surface irregularities, one can assume the surface will have many high energy sites that will provide easy nucleation centers for the α-Al_2O_3 grains. It is also at the surface that the temperature suitable for the transformation to occur will be first reached.

Tompkins (59) has shown that nucleation is considerably easier at some point defect or some extended non-equilibrium defect such as dislocations or stacking faults which are two-dimensional defects. If nucleation starts at the surface or the grain boundaries of the θ-Al_2O_3 crystals, the new phase will grow inward at the expense of the parent phase.

There is a substantial density increase on the formation of α-Al_2O_3 from θ-Al_2O_3 (from 3.56 gr/cm^3 to 3.98 gr/cm^3) as well as a change in the oxygen packing sequence;

that will lead to a new crystallographic system. This will cause the grains to shrink and pull away from each other as result of the transformation. Such an effect can also be seen when β-Sn transforms into α-Sn of substantially different density (60). In this transformation it is also felt that nucleation occurs at the surface.

The BET results could indicate that despite the fragmentation of individual θ particles into smaller α grains a smaller specific surface area could result from the elimination of surface defects normally present in the metastable transition aluminas. The ensuing surface readjustment would then be responsible for the reduction in surface area.

Isothermal Kinetics of the Transformation

Avrami (61) proposed for a three dimensional nucleation and growth mechanism the following relationship

$$x = 1 - \exp(-bt^n) \qquad (11)$$

where x is the fraction of transformed product, b a term representing the nucleation and growth of the new phase, t the time, n an exponent the value of which is indicative of the new phase's nucleation characteristics.

Christian (7) proposed the values of n indicated in Table III for discontinuous processes (which polymorphic

TABLE III

Variation of n in Avrami's Relation

Condition	n
Increasing nucleation rate	>4
Constant nucleation rate	4
Decreasing nucleation rate	3 - 4
Zero nucleation rate (saturation of point sites)	3
Grain edge nucleation after saturation	2
Grain boundary nucleation after saturation	1

transformations are).

In three dimensional cases $3 < n < 4$ should cover all cases where the nucleation is a decreasing function of time to the limit where it is constant. Furthermore this equation remains valid for two and one dimensional growth cases except that n is reduced respectively by 2 and 1.

Rewriting Avrami's relation

$$1 - x = \exp(-bt^n)$$

$$\frac{1}{1-x} = \exp(bt^n)$$

$$\log \frac{1}{1-x} = \frac{bt^n}{2.3}$$

$$\log \log \frac{1}{1-x} = \log \frac{1}{2.3} + \log b + n \log t \qquad (12)$$

Hence a plot of log log [1/(1-x)] vs log t should ideally give us a straight line of slope n. Relation (11) has also been derived by Haberlin and Slattery (62) who proposed that n could vary between 1.5 and 3 when growth alone took part in the transformation.

A log log (1/1-x) vs. log t plot was constructed for each temperature and the slope determined by a least square regression analysis for a polynomial of degree one. The exponent of t was found to vary from 1.140 to 1.84. The results are plotted on Figs. 29 and 30 and summarized on

Figs. 29 - 30

Log log (1/1-x) Versus log Time Plots

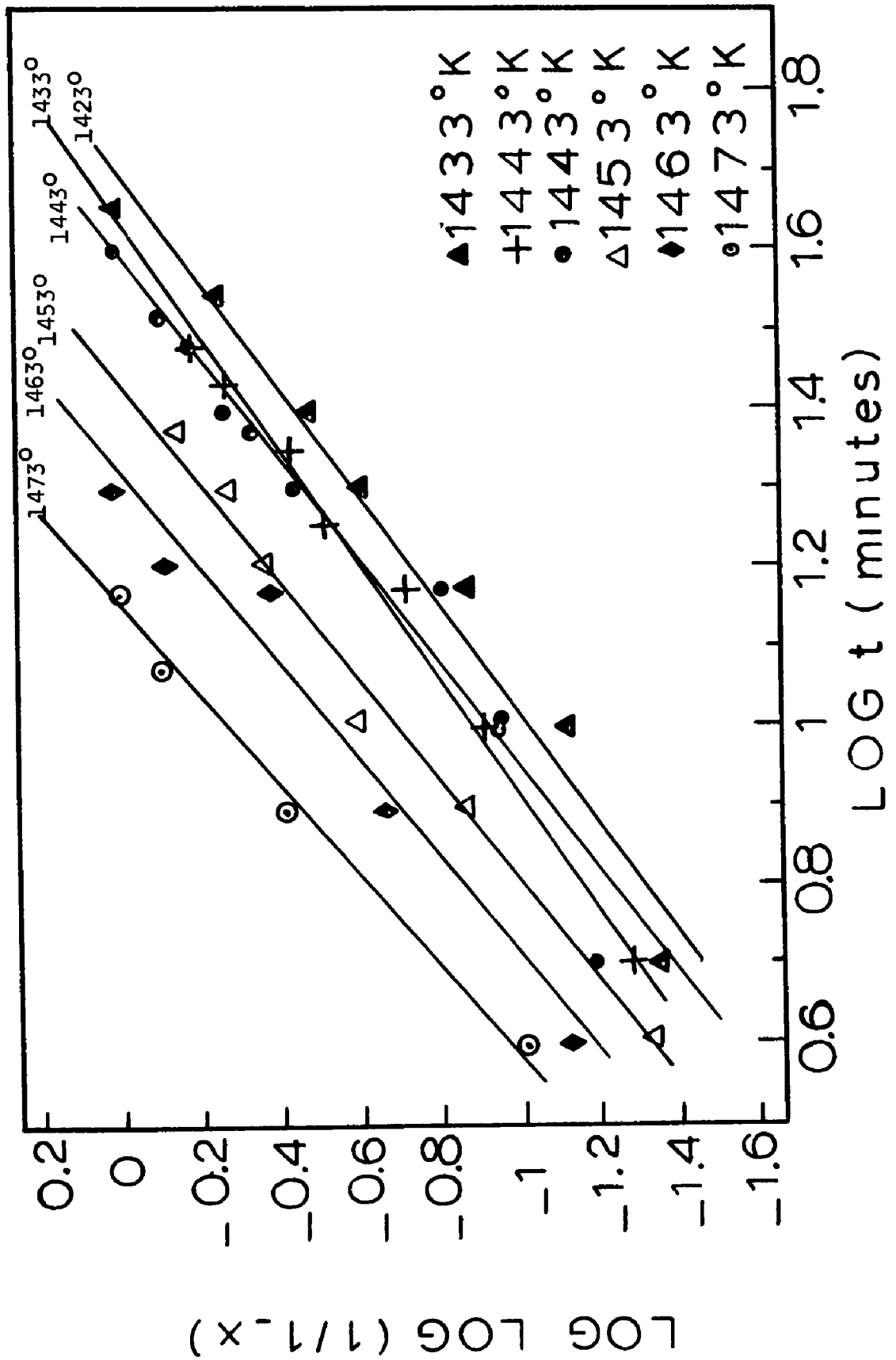
LOG LOG (1/1-x)
LOG t (minutes)
0.2
0
-0.2
-0.4
-0.6
-0.8
-1
-1.2
-1.4
-1.6
0.6
0.8
1
1.2
1.4
1.6
1.8
1423°
1433°
1443°
1453°
1463°
1473°
▲1433°K
+1443°K
●1443°K
△1453°K
◆1463°K
○1473°K

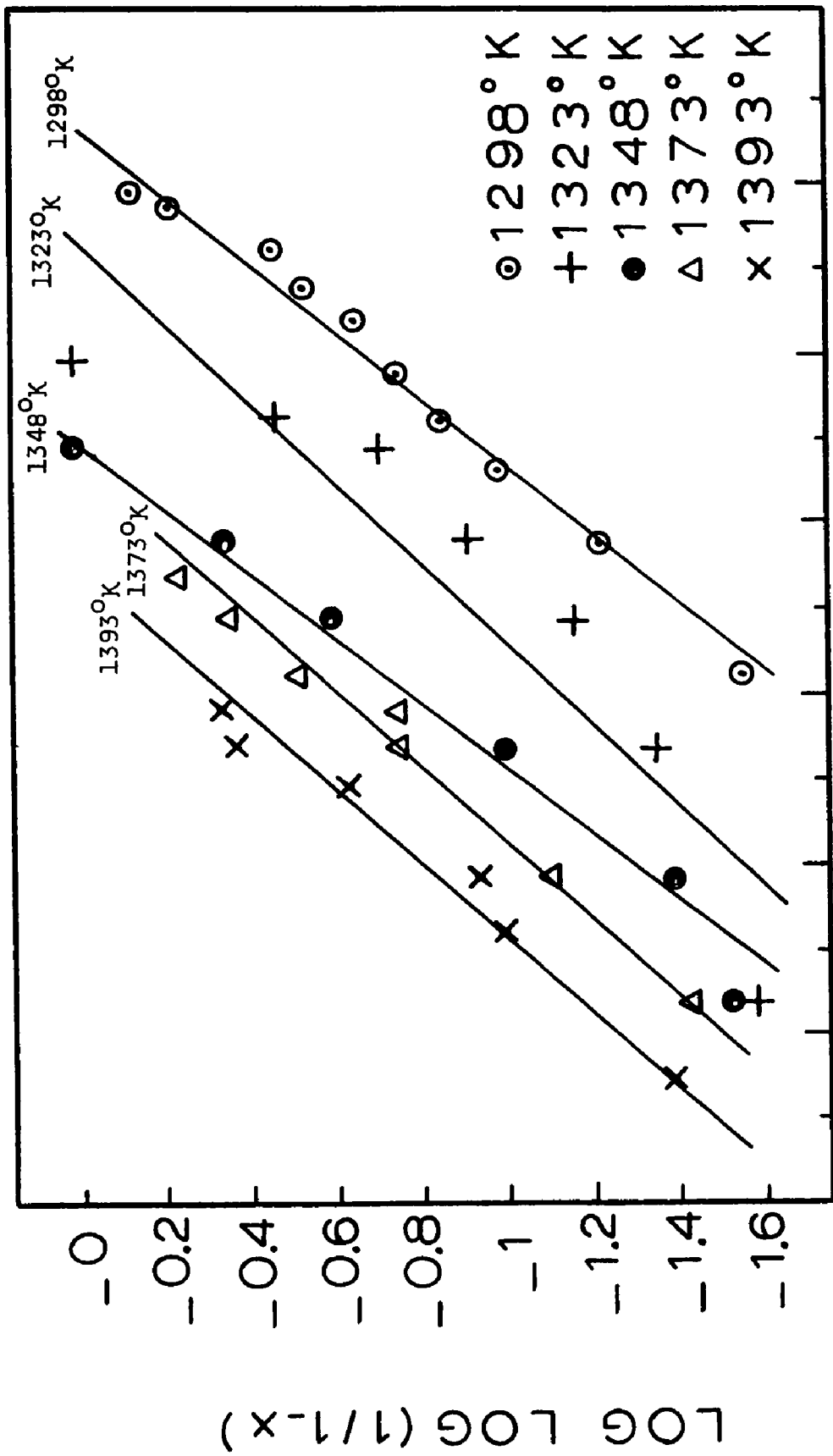
LOG LOG (1/1-x)
LOG t (minutes)
1298°K
1323°K
1348°K
1373°K
1393°K
⊙ 1298° K
+ 1323° K
● 1348° K
Δ 1373° K
x 1393° K
0
-0.2
-0.4
-0.6
-0.8
-1
-1.2
-1.4
-1.6
1
1.4
1.8
2.2
2.6
3
3.4

Table IV:

TABLE IV

Exponents from log log (1/1-x) vs. log t Plots

T°K	n
1298	1.196 ± 0.124
1323	1.140 ± 0.402
1348	1.220 ± 0.274
1373	1.180 ± 0.177
1393	1.246 ± 0.279
1423	1.402 ± 0.295
1433	1.360 ± 0.217
1443	1.485 ± 0.308
1453	1.533 ± 0.103
1963	1.700 ± 0.247
1473	1.843 ± 0.325

The n values in the table above are given for a 95% confidence level. An average n value of 1.38 results for all temperatures.

The fact that our exponent was found to vary between 1.18 and 1.84 suggests the α-Al_2O_3 crystals were nucleated

at the grain boundaries or grain edges of the θ-Al_2O_3 particles, or most probably a mixture of both. It also suggests a zero nucleation rate; in other words, the nuclei are already present at the onset of the transformation. Further evidence for the existence of preexisting nuclei is the measurable absence of any incubation period during which nuclei are normally formed. We can, therefore, assume that only growth will take part in the over-all process.

If one considers the findings of the Avrami analysis that the transformation proceeds from a nuclei saturated surface as correct, and that it is of discontinuous nature, the whole process can be viewed as particles of γ-Al_2O_3 covered with α-Al_2O_3 nuclei growing, the latter growing towards the center of the γ-Al_2O_3 grains.

Similar conclusions have been obtained by Buergers (60) on the polymorphic transformation of tin and Freiman and Herch (63) on the kinetics of cristallization of Li_2Si_2O from glasses in the Li_2O-SiO_2 system.

The above authors got large variations in n from one set of samples to another. Buergers (64) feels n can be drastically affected by the number of nuclei, the particle size of either the growing phase, or the parent crystal, and especially the purity of the material investigated.

If the surface is so important in providing sites for nuclei of α-Al_2O_3 to grow from, modification of the surface

condition could then significantly affect the possibilities of nucleation and therefore affect the kinetics of the transformation into α-Al_2O_3. Water vapor was found to facilitate the nucleation of α-Al_2O_3 from transient aluminas, by Yanagida et al (48). They suggested that water vapor could act as a mineralizer by breaking the Al-O-Al bond on the surface where chemical bonds are weaker, to from an Al-O(H)-Al bond that would lower the activation energy for the formation of a nucleus of α-Al_2O_3.

Wakao and Hibino (64) investigated the effects of additions of 1 to 10% of MgO, CuO, NiO, MnO_2 , Fe_2O_3 and TiO_2 for their effect on the temperature dependence of the $\gamma$to α transformation and found that they generally lowered the transformation temperature the larger the cationic radii and the higher the vapor pressure which usually indicate the possibility of ion transport by vapor phase in the production of nucleation sites prior to the transformation. This would be consistent with Iler's (52) hypothesis that SiO_2, which has a smaller cationic radius than Al_2O_3, retards the conversion to α-Al_2O_3 by forming a very viscous layer around the θ-Al_2O_3 grains' surface. This layer would be responsible for the stabilization of both γ and θ-Al_2O_3 by reducing very sharply the number of suitable α-Al_2O_3 nucleation sites. Fink (65) showed that V_2O_4 reacted with γ-Al_2O_3 to give $AlVO_4$ which melted incongruently to give

V_2O_5 and α-Al_2O_3. He found above 700°C 1% V_2O_5 could also greatly accelerate the kinetics of the γ to α-Al_2O_3 transformation and even bypass the formation of the intermediate θ phase. The impurities probably act as mineralizers that will help in destroying the metastable Al-O-Al bond in γ or θ-Al_2O_3 and reform it in the thermodynamically stable α-Al_2O_3 condition. Such mineralizers appear to be very effective when they involve a liquid (V_2O_4) or a vapor phase(H_2O).

It is also noteworthy that neutron irradiation has shown evidence of slowing down the kinetics of the transformation of transition into α-Al_2O_3 (66). No explanation for this observation was proposed. A possible explanation would be a destruction of probable high energy nucleation sites under the action of neutron bombardment.

All of the aforementioned observations would indicate the surface plays a considerable role in providing nucleation sites for α-Al_2O_3 and any chemical environment affecting the surface condition could affect the transformation kinetics by altering the number of possible sites provided.

Cahn (67) reexamined Avrami's analysis in discontinuous processes, and derived a relationship connecting the average grain diameter L (of a grain assumed to be a tetrakaidodecahedron), the growth rate G of the new phase and

the half-life $t_{\frac{1}{2}}$ (time at which 50% of the transformation has been completed. His relationship is only valid if saturation of the nucleation sites has taken place before the reaction starts or very early in the process.

It is formulated below:

$$t_{\frac{1}{2}} = \frac{0.1\ L}{G} \qquad (13)$$

The next step was to calculate the growth rate of the α-Al_2O_3 particles at each temperature using Cahn's relationship. L was taken to be 0.1 which is the figure obtained for the size of an average α-Al_2O_3 particle from the scanning electron micrograph of Fig. 26. $t_{\frac{1}{2}}$ was obtained from the volume of α-Al_2O_3 formed as a function of time. The calculated growth rates are presented in Table V:

TABLE V

Calculated Growth Rates Using Cahn's Relationship

T°K	$t_{\frac{1}{2}}$ (min)	$G_{cm/sec}$
1298	1400	1.18×10^{-9}
1323	630	2.65×10^{-9}
1348	330	5.00×10^{-9}
1373	183	9.08×10^{-8}
1393	95	1.75×10^{-8}
1413	38	4.40×10^{-8}
1423	24	6.92×10^{-8}
1433	20	8.33×10^{-8}
1443	20	8.33×10^{-7}
1453	15	1.11×10^{-7}
1463	10	1.66×10^{-7}
1473	7.5	2.22×10^{-7}

The transformation as an interface controlled process.

A theoretical relationship based on the reaction rate theory of atomic transfer across a reaction interface has been proposed by Christian (7) relating the velocity of the interface Y, the interface width δ, the free energy change per atom for the formation of phase β from α: $g^{\beta\alpha}$, and the activation energy per atom Δg^*. It is formulated below:

$$Y = \delta\nu \exp\left(-\frac{\Delta g^*}{kT}\right)\left[1-\exp\left(-\frac{\Delta g^{\beta\alpha}}{kT}\right)\right] \qquad (14)$$

This expression can however be simplified by expanding the exponential term involving $\Delta g^{\beta\alpha}$ into a MacLaurin series and neglecting those terms of degree larger than 1, that is, if $\Delta g^{\beta\alpha}$ is small compared to k, which is satisfied in practice (7). We then get the following expression for the velocity of an interface:

$$Y = \frac{\delta\nu}{k}\frac{\Delta g^{\beta\alpha}}{T} \exp\left(-\frac{\Delta g^*}{kT}\right) \qquad (15)$$

In the two equations, k is Boltzman's constant, and ν a frequency factor described as kT/h by Eyring's theory, where h is Planck's constant. From equation (15), we see that the growth veolocity is proportional to the free energy difference between the two phases. Assuming a negligible entropy change in the expression $\Delta G = \Delta H - T\Delta S$, we can replace the activation energy term in equation (14) by the enthalpy

difference ΔH which was found to be of the order of ~ 4 kcals/mole (19, 49).

Rewriting equation (14) for a gram-atom we obtain

$$Y = \left(\frac{\delta kT}{h}\right) \left(\frac{\Delta H}{RT}\right) \quad \exp \left(-\frac{Q}{RT}\right) \qquad (16)$$

If we take ΔH to be $\sim 4 \times 10^3$ cals/mole, $\delta = 10\text{Å}$ and take Q = 116,000 cals per mole (the value obtained for the activation energy of the transformation), and substitute these values in equation (16) we obtain the veolcity of the interface. The values calculated for all temperatures are shown on Table VI.

TABLE VI

Interface Velocity Obtained
from Christian's Relationship

T°K	Y cm/sec
1298	1.24×10^{-13}
1323	2.97×10^{-13}
1348	5.47×10^{-13}
1373	1.27×10^{-12}
1393	2.57×10^{-12}
1413	4.40×10^{-12}
1423	6.36×10^{-12}
1433	8.36×10^{-11}
1443	1.12×10^{-11}
1453	1.46×10^{-11}
1463	1.90×10^{-11}
1473	2.50×10

The figures obtained are very small. They are smaller than those obtained from Cahn's empirical relationship by a factor of approximately 10^4 as we can see from Table VII:

TABLE VII

Comparison of Growth Rate Obtained from Cahn's Relationship and Christian's Interface Velocity Equation

T°K	G from Cahn cm/sec	Y from Christian cm/sec	G/Y
1298	1.18×10^{-9}	1.24×10^{-13}	9.52×10^{-3}
1323	2.65×10^{-9}	2.97×10^{-13}	8.95×10^{-3}
1348	5.00×10^{-9}	5.47×10^{-13}	9.14×10^{-3}
1373	9.09×10^{-9}	1.27×10^{-12}	7.22×10^{-3}
1393	1.75×10^{-8}	2.58×10^{-12}	6.83×10^{-3}
1413	4.40×10^{-8}	4.40×10^{-12}	1.002×10^{-4}
1423	6.92×10^{-8}	6.36×10^{-12}	1.096×10^{-4}
1433	8.33×10^{-8}	8.35×10^{-11}	1.002×10^{-4}
1443	8.33×10^{-8}	1.12×10^{-11}	7.41×10^{-3}
1453	1.11×10^{-7}	1.46×10^{-11}	7.60×10^{-3}
1463	1.66×10^{-7}	1.90×10^{-11}	8.75×10^{-3}
1473	2.22×10^{-7}	2.50×10^{-11}	8.90×10^{-3}

A possible interpretation for this discrepancy is that α-Al_2O_3 nucleates from about $\sim$10000 sites per grain of θ-Al_2O_3 and grows simultaneously from all these nuclei. There should in fact be more than 10000 nuclei per grain if one were to take the impingement effect of growing α-Al_2O_3 grains.

It is of interest to note in passing that five to six

catalytic sites have been reported to have catalytic properties for every 10,000$\mathring{A}^2$ (68) on γ-Al_2O_3. If one assumes a cubic particle size of 1μ edge ($10^4\mathring{A}$) it has a surface area of 6 x $10^8\mathring{A}^2$ or 6 x 10^4 x 10,000$\mathring{A}^2$; if the above statement is correct we should have approximately 10^4 sites per particle of metastable alumina, which is of the same order of magnitude as the G/Y ratio obtained on Table VII. While this coincidence may be merely fortuitous, it is nevertheless of interest since catalytic sites are of higher energy and likely to act as nuclei.

Assuming there is only one nucleus per grain, that the transformation front moves at the velocity calculated from Christian's relationship, and that it has to cross a grain of assumed cube-shape of 1μ edge, the time for the interface to sweep across the entire grain was calculated for each temperature (Table VIII).

If one now calculates the time for one of these grains to transform completely from the relationship $c = kt$, where $c = 1$ and k is the rate constant, one finds that at each temperature the time t for 100% transformation is given by the reciprocal of the rate constant.

TABLE VIII

Comparison of Interface Velocity from Christian's Relation and Time Calculated for Interface to Travel 1μ

T°K	Interface velocity Y (cm/min)	Time t for interface to travel 1μ (min)
1298	7.35×10^{-12}	1.36×10^{-7}
1323	1.78×10^{-11}	5.61×10^{-6}
1348	3.48×10^{-11}	2.87×10^{-6}
1373	7.50×10^{-11}	1.33×10^{-6}
1393	1.54×10^{-10}	6.50×10^{-5}
1413	2.63×10^{-10}	3.80×10^{-5}
1423	3.78×10^{-10}	2.64×10^{-5}
1433	4.98×10^{-10}	2.01×10^{-5}
1443	6.72×10^{-10}	1.49×10^{-5}
1453	8.76×10^{-10}	1.14×10^{-4}
1463	1.04×10^{-9}	9.62×10^{-4}
1473	1.50×10^{-9}	6.68×10^{-3}

TABLE IX

Estimation of No of Nuclei per Grain

T°K	Time for 100% transformation t (min)	Ratio $\frac{\tau}{t}$ No of nuclei
1298	3176	4.23×10^3
1323	1264	4.33×10^3
1348	616	4.66×10^3
1373	382	3.48×10^3
1393	218	2.98×10^3
1413	76	5.00×10^3
1423	48	5.50×10^3
1433	39	5.14×10^3
1443	40	3.75×10^3
1453	28	4.08×10^3
1463	20	5.00×10^3
1473	15	5.06×10^3

If we assign a cube shape of 1μ edge to each grain of θ-Al_2O_3 and assume the shape of the resulting α grain is unchanged, the ratio of the time τ required to travel a length of 1μ over t the time for 100% transformation may be used to get an approximate value of the number of nuclei originally present.

We get a value of approximately 4-5 x 10^3 nuclei per grain. This compares to about 10^4 nuclei/grain obtained by comparing Christian and Cahn's relationship in Table VII and to 10^4 active sites per grain of γ-Al_2O_3 which has been estimated by Peri (68).

Karlyn, Cahn and Cohen (69) postulated that in interface controlled processes, interface motion occurs by thermally activated jumps across the transformation boundary. Massalski (70) proposed that the atoms would move in the disordered boundary region with grain boundary characteristics and called such changes massive transformations. In such transformations, the parent structure transforms into a new one by noncooperative transfer of atoms across a relatively high energy interface. Since they do no involve any compositional changes,any polymorphic non-martensitic transformation can be regarded as massive. Massalski also advanced that massive transformations can occur between metastable and stable phases.

It is not possible at this stage to determine clearly

the exact mechanism behind the transformation. There seems to be an extensive surface rearrangement but no over-all change in particle size and distribution.

From the general observations the γ to α-Al_2O_3 transformation may also be considered to be of the massive (non-martensitic) type of phase transformations. These are characterized by the absence of a compositional change and an interface controlled thermally activated process starting at preexisting nuclei (69,70).

V. CONCLUSION FOR THE γ- To α-Al_2O_3 PHASE TRANSFORMATION WORK

In this first part the transformation kinetics of a commercially available high purity "gamma" alumina have been investigated. The transformation sequence was found to comprise an intermediate step which was identified as θ-Al_2O_3.

The following results were established from this investigation:

1 - The transformation is sluggish and appears to be of reconstructive nature.

2 - The transformation is a thermally activated process following zero order kinetics, ie. $c = kt$.

3 - The rate constant k can be described by the relationship

$$k = 10^{16} \exp\left[-\frac{116{,}000 \pm 5{,}000}{RT}\right]$$

4 - The value of the activation energy obtained is

significantly different from those obtained by other workers. It does not appear at this point that a universal value can be assigned to this transformation. Impurities play a significant part in hindering or promoting the transformation.

5 - Results from isothermal kinetics appear to indicate that the parent phase is saturated with nucleating sites. It is therefore believed the transformation is a discontinuous process starting at pre-existing nuclei.

6 - This polymorphic transformation can be considered as a special case of an interface controlled massive transformation.

VI. SYNERGETIC HOT-PRESSING

Introduction. In a second part of the present investigation, it was decided to utilize the previous findings to investigate whether hot-pressability could be improved by making use of the transformation. It has been definitely established that sintering temperatures can be considerably lowered if the process is assisted by mechanical energy (71). It has also been proposed that the process reactivity could be enhanced even further by the cooperative action of pressure and a phase transformation leading to a denser structure (72). Examples of such operations can be found in the literature. Among the most notable are the works of Chaklader (73) on fire clay products and non-stabilized monoclinic ZrO_2, and that of Gazza, et al. (74), involving the gamma to alpha alumina transformation.

In the case of zirconia, a tentative explanation based on super-plasticity was put forward. In the second case, it was proposed that the diffusional processes involved in the densification were accelerated either by changes in the particles' surface energy or by a high degree of strain induced by the application of pressure during the transformation. It, however, appeared in the

case of alumina that little benefit resulted from using γ-Al_2O_3 as a starting material (74), although other workers reported the possibility was worth investigating (75).

It was therefore decided to make use of the phase transformation work in the earlier part and establish with a maximum degree of certainty if any benefit might result in terms of densification behavior and/or mechanical properties from using γ instead of α-Al_2O_3 as a starting material.

Procedure. To compare the hot-pressing behavior of γ and α-Al_2O_3, samples of identical sizes were pressure-sintered in both the as-received and in the α-form as starting materials. The latter was obtained by isothermally annealing the as received γ-Al_2O_3 for ten hours at 1100°C, which was found to be more than sufficient for complete transformation. The relatively low temperature should ensure that no grain growth takes place.

A single pressure of 10,000 psi and two temperatures, 1300° and 1400°C, respectively, were chosen. The apparatus used for this experiment was identical to that used for an earlier work (76).

The alumina powder was loosely filled in the die cavity and allowed to outgas for approximately four hours

at 750°-800°C (some tests involving overnight outgassing around 500°-550°C showed no measurable difference in the end products) to remove adsorbed moisture and any other volatile impurity. A minimum of pressure was applied during this period so as to minimize the amount of entrapped gases. The next step was to apply the pressure gradually to the desired value and, once it was reached, to allow the die assembly to equilibrate thermally for ten minutes, at the end of which the temperature was raised as rapidly as possible to the desired level. The sequence was identical for both kinds of alumina. The outgassing temperature was well below that where the transformation starts in pressureless conditions. The pressure was first applied before the transformation occurred. The latter was allowed to take place during thefinal heating-up stage to the operating temperature. A fast heating rate of the order of 130°-150°C/minute was chosen so as to take advantage of the transformation.

Each sample consisted of five grams of powder which was contained in graphite sleeves of one inch inner diameter within the die body (Fig. 31). The plungers and the die were made from a Ti-Cb-Mo-C alloy (commercially known as TZM and manufactured by Amax Inc.). Graphite spacers were inserted between the powder and the plungers to avoid diffusion of metal atoms into the alumina. Finally, both

the sleeves and the spacers were coated with a boron nitride wash to ensure easy removal of the finished specimen and avoid contamination from the surrounding graphite. The temperature was continually recorded by Pt-Pt/10%Rh thermocouple and densification followed by measuring the ram movement at regular time intervals with a Starrett precision dial gauge that was attached to the ram. The final density was determined as the bulk density by the following procedure:

The dry specimen was immersed in a Toluene filled beaker and out-gassed in a vacuum bell jar. After cessation of bubbling, the beaker was removed from the bell jar. Since the outgassing operation caused endothermic evaporation of Toluene more liquid was added in the beaker until a temperature of 22°C was reached at which Toluene's density was 0.867 gr/cm^3 The bulk density of the sample was then obtained from the relation,

$$\text{bulk density} = \frac{Wd}{W_{sat} - W_s} \times 0.867 \qquad (16)$$

where

W_d = dry weight

W_{sat} = saturated weight

W_s = suspended weight

Fig. 31

Hot Pressing Die Assembly

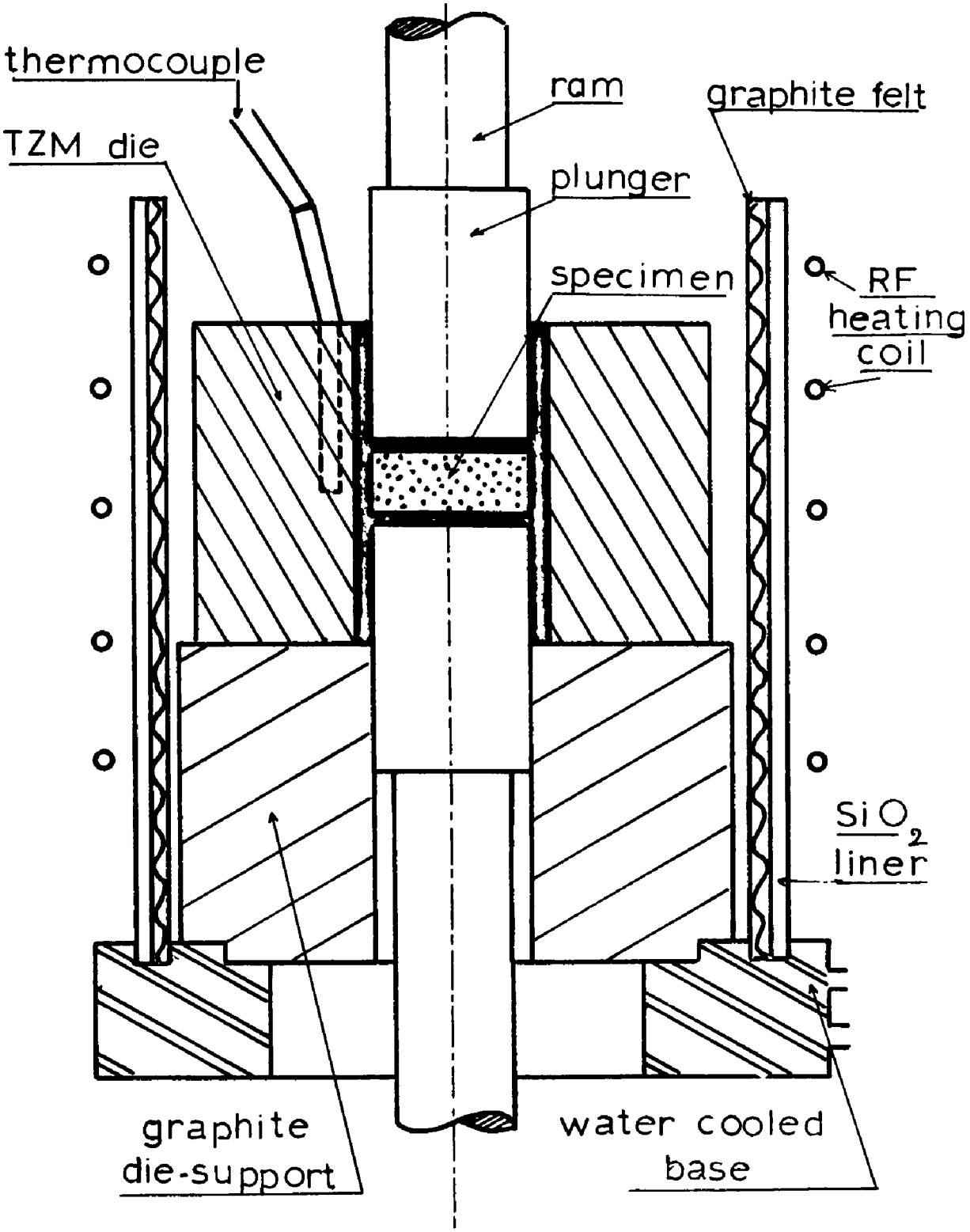
thermocouple
TZM die
ram
plunger
graphite felt
specimen
RF heating coil
SiO_2 liner
graphite die-support
water cooled base

TABLE X

Hot Pressing: Densification Results

Starting Material	Run N°	T°C	Final relative density	Average relative density
$\alpha - Al_2O_3$	4	1300	96.53%	91.78%
	5	1300	91.97%	
	12	1300	88.20%	
	14	1300	90.51%	
	20	1300	91.69%	
$\gamma - Al_2O_3$	2	1300	95.73%	94.53%
	3	1300	96.78%	
	13	1300	94.15%	
	15	1300	95.60%	
	19	1300	90.38%	
$\alpha - Al_2O_3$	6	1400	95.38%	95.55%
	7	1400	95.60%	
	11	1400	96.50%	
	16	1400	95.33%	
	21	1400	94.95%	
$\gamma - Al_2O_3$	8	1400	99.60%	99.11%
	9	1400	99.00%	
	10	1400	99.27%	
	17	1400	99.00%	
	18	1400	98.67%	

The estimated error in the relative density was estimated to be of the order of 0.05% (76).

Four sets of conditions were selected: γ-Al_2O_3 and α-Al_2O_3 as initial materials hot pressed at 1300° and 1400°C. In all, 20 runs were performed, the results of which are tabulated in Table X. The 1300°C runs were made to last 180 minutes and those at 1400°C, 120 minutes.

As we can see, if we take the average final relative density for five runs for each particular set of pressure and temperature conditions, we find the final density increases in the following manner: α-Al_2O_3 hot pressed at 1300°C, γ-Al_2O_3 at 1300°C, α-Al_2O_3 at 1400°C and γ-Al_2O_3 at 1400°C.

A density vs. time plot for a typical run in each group is illustrated in Figs. 32 and 33. They were chosen from those samples with a final relative density as close as possible to the average of that particular group.

A lower green density was observed in the case of γ-Al_2O_3, although the green compacts were made under identical conditions of pressure. This can be attributed to α-Al_2O_3's higher density. But it is of interest to note that Bruch (79) found that under identical conditions of pressure, different alumina powders produced different green densities, those with the highest specific area giving the least dense compacts.

Fig. 32

Typical Densification Curves

for γ- and α-Al_2O_3 at 1300°C

Fig. 33

Typical Densification Curves

for γ- and α-Al_2O_3 at 1400°C

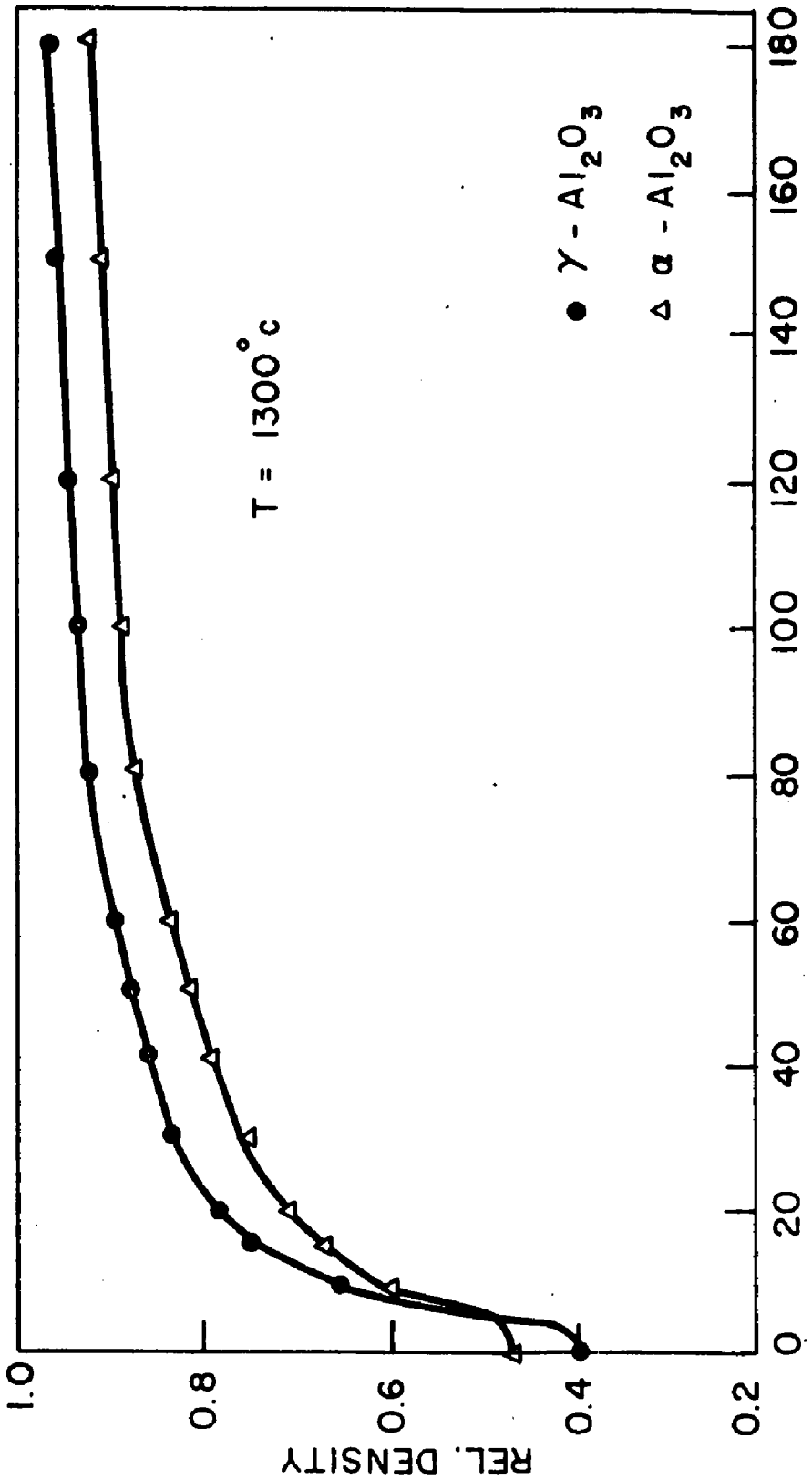
REL. DENSITY
1.0
0.8
0.6
0.4
0.2
0
20
40
60
80
100
120
140
160
180
TIME (minutes)
T = 1300°c
● γ - Al2O3
△ α - Al2O3

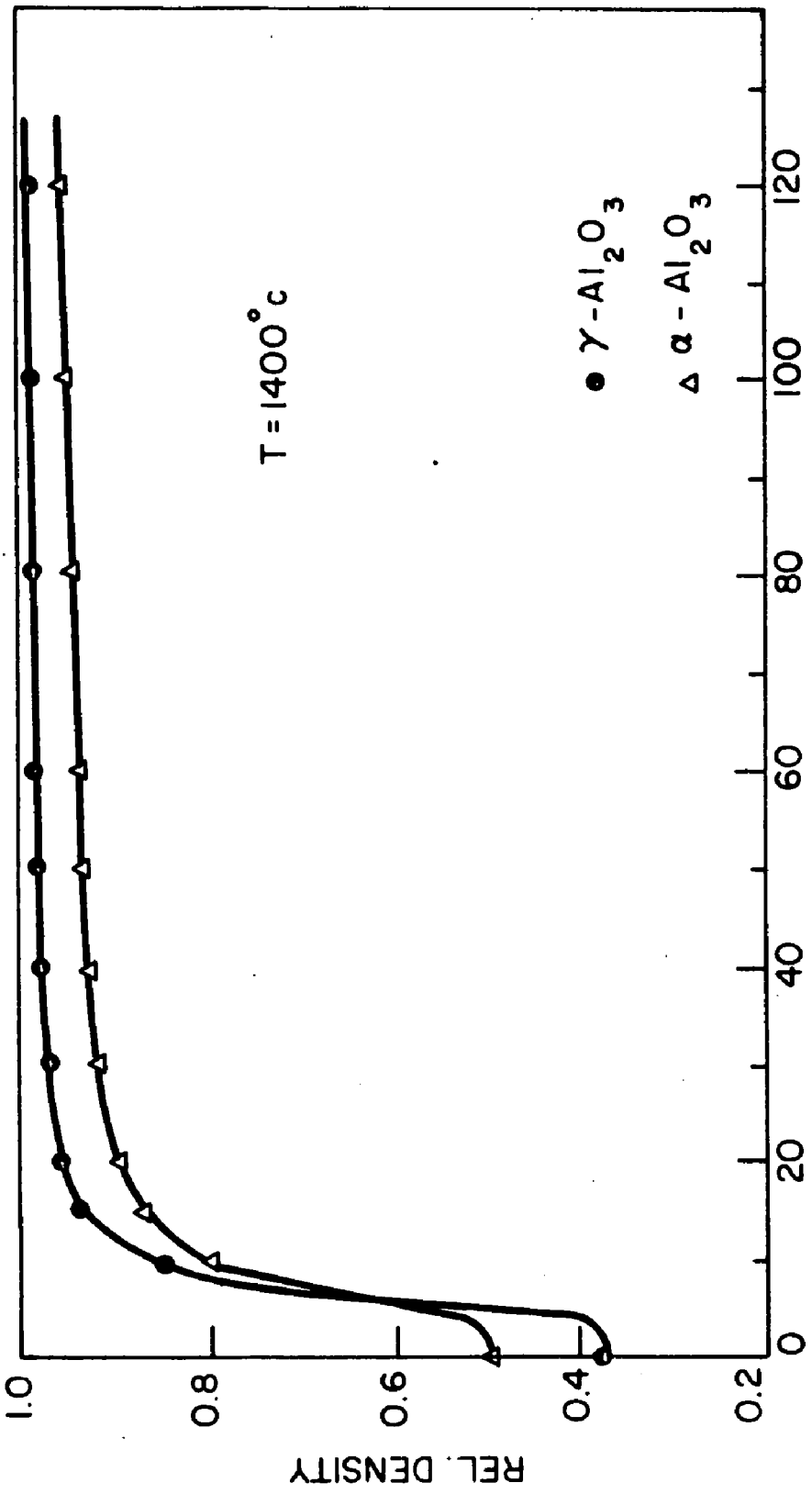
T = 1400°c
● γ-Al2O3
△ α-Al2O3
REL. DENSITY
1.0
0.8
0.6
0.4
0.2
0
20
40
60
80
100
120
TIME (minutes)

It is apparent from our results that for identical conditions of pressure, temperature and time, a higher final density will be obtained if γ-Al_2O_3 instead of α-Al_2O_3 is used as a starting material. These results are in contrast to those of Gazza and Barfield (74). However, they used slower heating rates of 10-15°C/min in their experiment and by the time they reached the operating temperature, their powder was long transformed into α-Al_2O_3.

A possible explanation is the formation of small α-Al_2O_3 grains when the larger θ-Al_2O_3 particles break up during the transformation. These very small α-Al_2O_3 grains would thus have a large grain boundary area and would be responsible for the higher final relative density; this is consistent with Spriggs and Vasilos' observations on a wide variety of materials (78).

The heating rates in the present experiment were ten times higher than Gazza's. It is believed the operating temperature was reached before most of the transformation took place. During the transformation, sintering of the α-Al_2O_3 grains would then be enhanced by a Hedvall-type phenomenon which could account for the marked densification increase in the early part of each run when γ-Al_2O_3 is used as starting material.

Strength measurements. The specimens were then cut

into bars approximately 0.080 inches thick for flexural strength measurements with a diamond impregnated saw. The cutting stresses were subsequently relieved by annealing the bars in air for 15 hours at 1150°C and prior to mechanical testing. Two to six bars were obtained from each hot pressed sample.

The flexural strength was measured at room temperature with an Instron testing machine at a cross-head speed of 0.1"/minute in three point loading with two rolling supports and a span of 0.500" as also used by Kirchner (79). This was rendered necessary by the samples' small size. The flexural strength of the bars with rectangular cross-sections was calculated from the following formula:

$$\sigma = \frac{1.5PL}{bd^2} \qquad (17)$$

in which

σ is the tensile stress in the outermost material;

P is the total load at the breaking point;

L is the total span: 0.502: in this case;

b is the specimen width;

d is the specimen height.

The results of the mechanical testing are tabulated in Table XI. They are also plotted as a function of porosity in Figs. 34 and 35. These figures show strength vs.

TABLE XI

Hot-pressed Material: α-Al_2O_3 at 1300°C

Relative density %	88.20	90.51	91.70	91.97	96.53
Flexural Strength (psi)	75,400 58,900 76,500 78,800	66,500 55,900 63,900 84,300 57,500	71,500 76,150 70,200 67,000 76,400	78,700 77,700	79,000 41,400 84,800 34,800 75,300 64,600
Average	62,400	65,200	72,250	78,200	63,800

Hot-pressed Material: γ-Al_2O_3 at 1300°C

Relative density %	90.38	94.15	95,60	95.73	96.78
Flexural Strength (psi)	81,900 83,300	84,900 65,600	76,200 93,500 67,000 70,000	62,400 82,200 91,800 73,600	74,300 62,800 58,800 57,500
Average(psi)	82,600	75,200	76,700	77,500	63,400

Hot-pressed Material: α-Al_2O_3 at 1400°C

Relative density %	94.95	95.33	95.38	95.60	96.50
Flexural Strength (psi)	59,700 64,900 42,100 64,200 69,200	107,800 70,500	95,300 87,700 71,700	58,600 72,250 56,350 70,600 49,500	48,000 77,100 75,000 77,100 21,100 48,300
Average(psi)	60,000	89,150	84,800	61,500	57,800

Hot-pressed Material: γ-Al_2O_3 at 1400°C

Relative density	98.67	99.00	00.00	99.27	99.60
Flexural Strength (psi)	69,000 73,800 99,000 93,300 55,600	80,300 72,850 64,100 73,800 87,100 65,800	91,900 85,600 93,100	82,700 69,300 88,000 62,400 77,700	63,400 62,300 62,400 58,550 55,800
Average(psi)	78,150	74,100	90,200	76,000	60,400

Fig. 34

Flexural Strength vs. Porosity

for Specimens Made at 1300°C

Fig. 35

Flexural Strength vs. Porosity

for Specimens Made at 1400°C

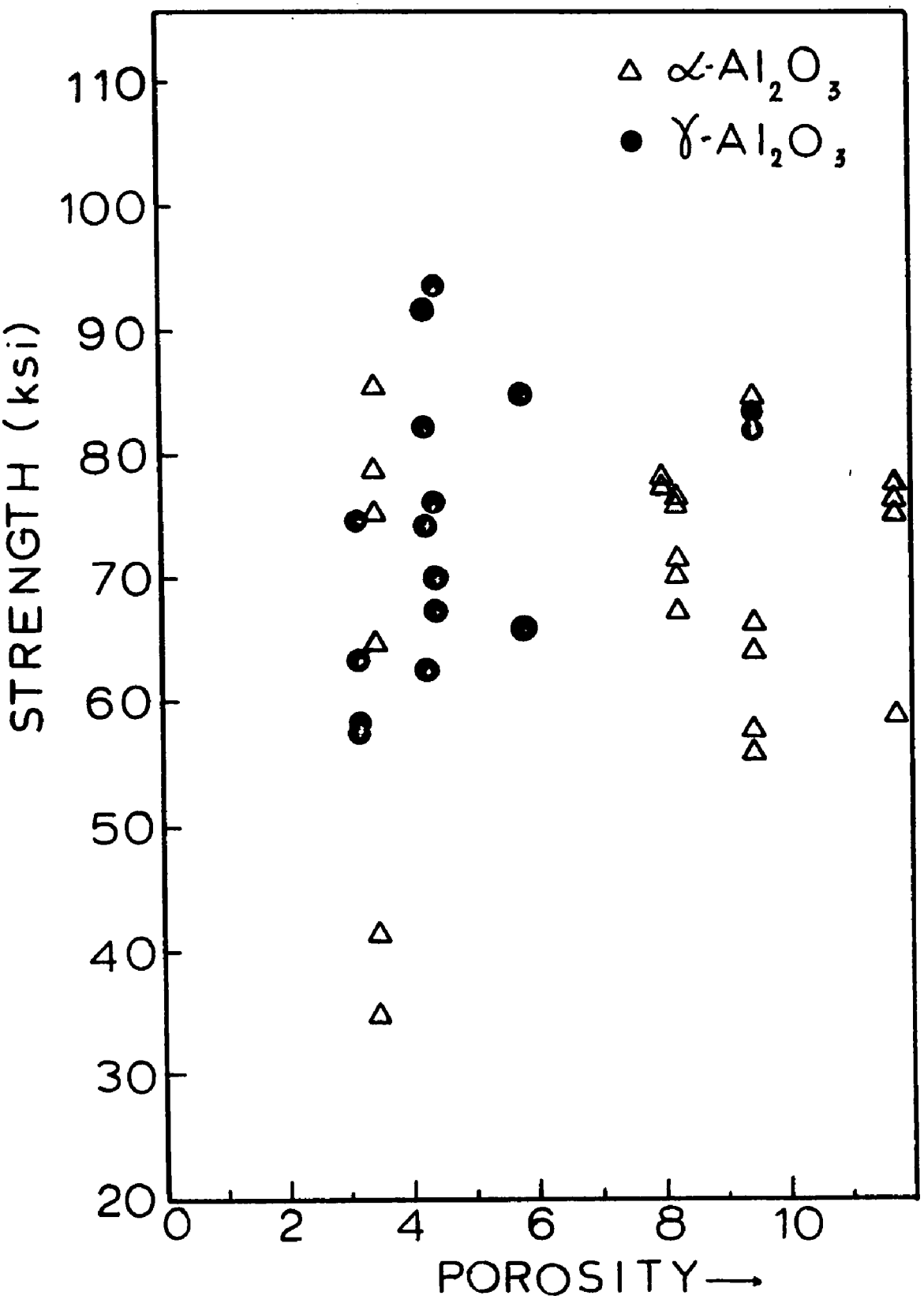
△ α-Al2O3
● γ-Al2O3
STRENGTH (ksi)
110
100
90
80
70
60
50
40
30
20
0
2
4
6
8
10
POROSITY →

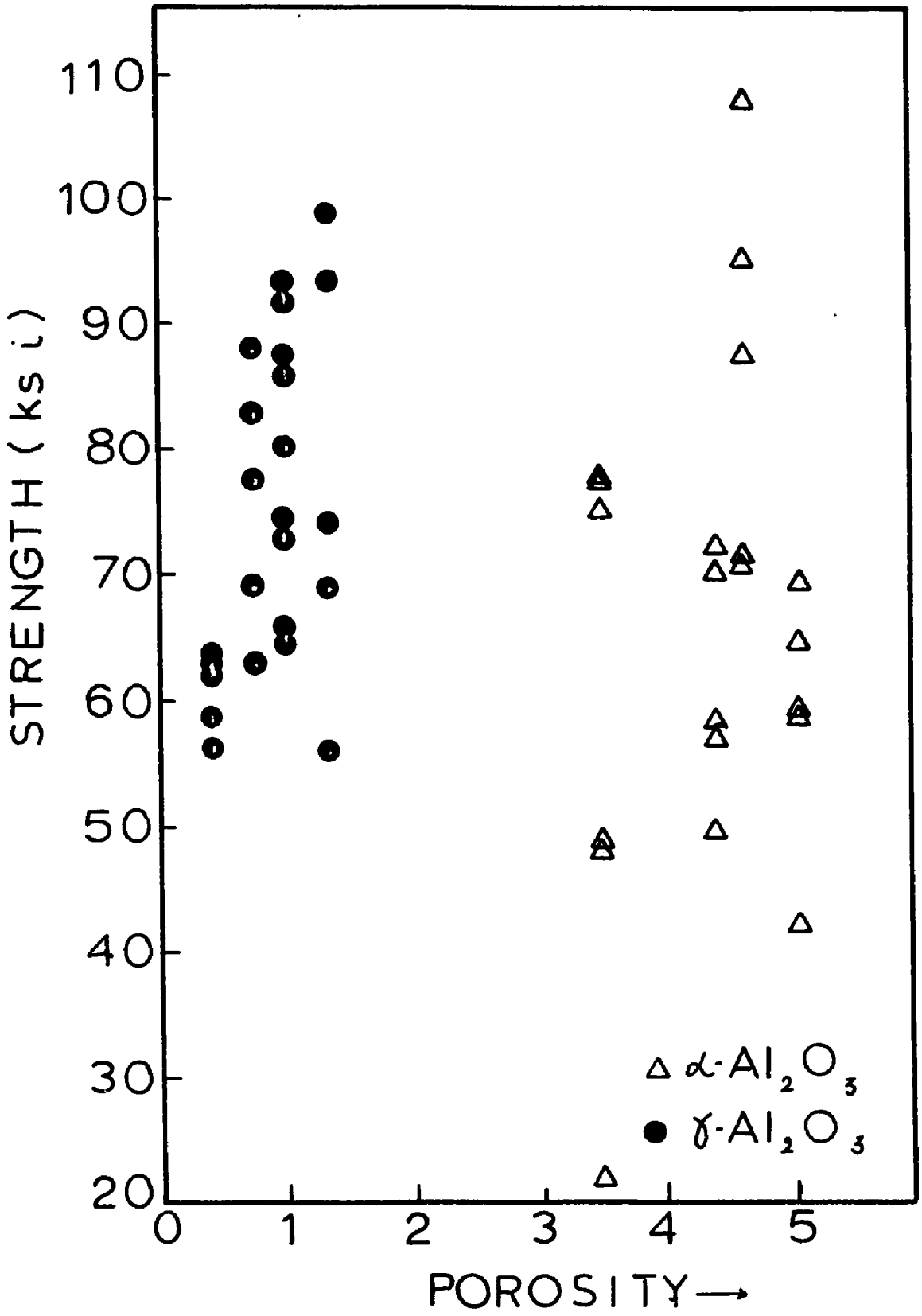
STRENGTH (ksi)
110
100
90
80
70
60
50
40
30
20
0
1
2
3
4
5
POROSITY →
△ α-Al2O3
● γ-Al2O3

porosity data for samples made at 1300° and 1400°C, respectively.

As we can see in Fig. 34, porosity appears to have little influence on strength, most values lying between 55,000 and 85,000 psi in the case of samples made initially from α-Al_2O_3 with an average value of 65,000 psi and between 60,000 and 95,000 psi with an average value of 75,000 psi for those made initially from γ-Al_2O_3. The scatter is also less pronounced in the latter case. The standard deviation for the specimens made from α-Al_2O_3 is 12,900 psi or 19.8% of the average value, while it is only 11,000 psi, or only 14.6% of the average value for those samples made from γ-Al_2O_3. There does not appear to be any strong conclusive evidence of higher strength for lower porosity, but only a slight tendency.

When α-Al_2O_3 was hot pressed at 1400°C, the strength values were mostly found to vary between 50,000 and 95,000 psi with an average of 67,000 psi and one value reaching 107,000 psi; however, a large scatter was unfortunately present, as visible on Fig. 35. Besides markedly higher final densities, higher strength values with an average of 79,000 psi were obtained when γ-Al_2O_3 was hot pressed, together with a lesser degree of scatter than when α-Al_2O_3 was used. Four samples exceeded 90,000 psi and five more 80,000 psi. The standard deviation for these two groups of tests was

18,700 psi or 26% in samples made from α-Al_2O_3 but only 13,400 psi or 17% for those made from γ-Al_2O_3.

It is therefore possible at this point to affirm that the phase transformation enables us to produce specimens with:

1 - higher final relative densities,

2 - a higher strength with some decrease in scatter.

Electron microscopical observations were carried out on a limited number of specimens. They were examined chiefly for morphological appearances and grain size, to seek a possible explanation for the different results obtained.

The fracture surfaces were first shadowed with carbon and then with platinum to improve contrast.

The procedure adopted for grain size measurement was the planimetric procedure recommended by ASTM (80), which is best suited for specimens consisting of equiaxed grains. This method is acceptable for fractured samples since it has been established that fracture grain sizes agree well with correspondingly measured grain sizes obtained from conventionally polished and etched samples (81).

In this method, the number of grains included completely within a given area plus one-half the number of grains intersected by the perimeter of a square of 5000 mm^2 gave the number of equivalent whole grains measured at the magnification used within the area. A square perimeter was

selected because some workers feel it produces a lower error of measurement than a circle as a limiting line (82).

The total area divided by the number of grains thus counted gave the average grain area $\bar{A}$. The square root of this value is denoted as the "grain size" (83). Three fields of 5000 mm^2 were counted to assure a reasonable average.

The grain size in all specimens appeared to fall in a narrow range. The smallest one reported was 0.5μ for a hot-pressed γ-Al_2O_3 of high strength.† As our original material's particle size is of the order of 0.5μ it appears that no grain growth has taken place. We can conclude that grain size differences do not account for the observed variations in strength. It does however appear that cleavage steps are more frequent on low strength specimens as shown on Fig. 36 which is taken from a α-Al_2O_3 sample hot-pressed at 1300°C.

Fig. 37 shows the microstructure of the specimen with the highest strength in this study. It is made from α-Al_2O_3 hot pressed at 1400°C. The failure is mostly intergranular with some round-shaped pores left within the grains.

Figs. 38 and 39 respectively show fracture surfaces from a specimen made by hot pressing γ-Al_2O_3 at 1400°C. In

---

†while the largest one was 0.71 in a hot-pressed α-Al_2O_3 also of high strength.

Fig. 36

Electron Fractograph of a Sample

from Hot Pressed α-Al_2O_3 at 1300°C (16,100x)

Fig. 37

Electron Fractograph of a Sample

from Hot Pressed α-Al_2O_3 at 1400°C (16,100x)

Fig. 38

Electron Fractograph of a Sample

from Hot Pressed γ-Al_2O_3 at 1400°C (16,100x)

Fig. 39

Electron Fractograph of a Sample

from Hot Pressed γ-Al_2O_3 at 1400°C (16,100x)

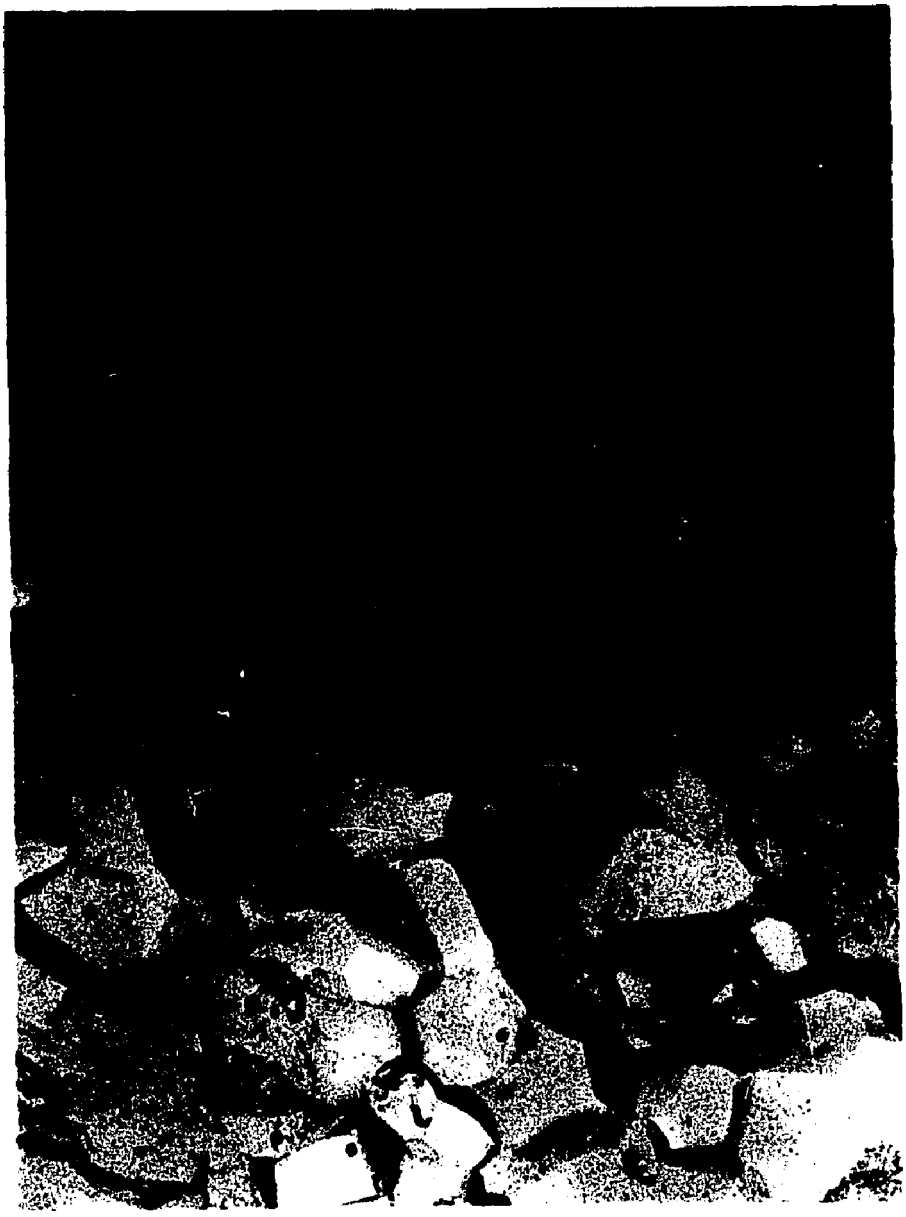

both the fractures appear to be predominantly intergranular. It would also appear that the porosity distribution is an influential factor in controlling the flexural strength, but that within limits the actual amount of porosity is not all that important since we got many high strength results from higher porosity specimens. Coble (84) has shown that strength and mechanical properties in ceramics with a pore phase reached their maximum values in structures where the solid phase was continuous and contained isolated spherical pores.

The apparent lack of correlation between strength and grain size confirms previous work by Spriggs et al. (85) who also suggested that small round shaped pores would cause blunting of Griffith's crack tips. However, the very small pore size as seen on the micrographs suggests, especially when they are uniformly distributed throughout the grains, that their effect on strength will be quite small (86).

VII. CONCLUSION FOR THE HOT-PRESSING WORK

To summarize the second part of our experiment, the use of γ-Al_2O_3 as initial material for the hot-pressing of alumina was investigated and found to be beneficial on the following accounts when it is assisted by high heating rates:

1 - The densification kinetics are markedly accelerated in the initial stage

2 - A higher final relative density is obtained for a given time

3 - Although the trend towards higher strengths together with less scatter is noticeable there is as yet not enough statistical evidence to make this conclusion significant

BIBLIOGRAPHY

1. W. D. Kingery, *"Introduction to Ceramics,"* John Wiley, New York (1960).

2. A. H. Cottrell, *"An Introduction to Metallury,"* 1st ed., Arnold, London (1967).

3. W. R. Moore, *"An Introduction to Polymer Chemistry,"* Aldine Publishing, Chicago (1963).

4. M. J. Buerger, "The Role of Temperature in Mineralogy," Am. Min., 33, (3-4), 101-121 (1948).

5. M. J. Buerger, "The General Role of Composition in Polymorphism," Proc. Natl. Acad. Sc. 22, 685-689 (1936).

6. J. H. Westbrook, "Impurity Effects at Grain Boundaries in Ceramics," *Science of Ceramics*, vol III, 263-284, Academic Press, New York (1967).

7. J. W. Christian, *"The Theory of Transformations in Metals and Alloys,"* 1st ed., Pergamon, Oxford (1965).

8. B. C. Weber, "Bibliography of Research on the Structural and Physical Properties of Zirconia," ARL-605, The Aerospace Research Labs WPAFB, November 1964.

9. R. W. Cahn, *"Physical Metallurgy,"* 1st ed., North Holland, Amsterdam (1965).

10. A. G. Verduch, "Kinetics of Cristoballite Formation from Silicic Acid," J. Am. Ceram. Soc., 41, 427-432 (1958).

11. M. J. Buerger, "Crystallographic Aspects of Phase Transformations," *Phase Transformations in Solids*, Symposium, Cornell University, 1948, John Wiley, New York (1951).

12. M. J. Buerger, "The Temperature-Structure-Composition Behavior of Certain Crystals," Proc. Nat. Acad. Sc., 20, 444-453 (1934).

13. C. Oftedahl, Norsk Geol Tids, 24, 75 (1936).

14. M. J. Buerger, "Derivative Crystal Structures," J. Chem. Phys. 15, 1-16 (1947).

15. J. H. Cannon and J. White, "Some Rate Processes in Ceramics," Trans. Brit. Ceram. Soc., 55, 82-111 (1956).

16. S. Benson, *"Fundamental of Chemical Kinetics,"* 2nd ed., McGraw-Hill, New York (1960).

17. W. Gomes, "Definition of Rate Constant and Activation Energy in Solid State Reactions," Nature, 192, 865-866 (1961).

18. *"Engineering Properties of Selected Ceramic Materials,"* compiled by Batelle Memorial Institute, Columbus, Ohio, pub. by the American Ceramic Society, Columbus, Ohio (1966).

19. B. A. Scott and W. H. Horseman, "Structural Changes During the Production of Corundum by Calcination of Gibbsite and Their Influence on Fabrication," Trans. Brit. Ceram. Soc., 69, 36-43 (1970).

20. E. Ryschkewitch, *"Oxide Ceramics,"* Academic Press, New York (1960).

21. H. Saalfeld, "Strukturen des Hydrargillits und der Zwischenstufen beim Entwaessern," N. Jahrb. f. Min. Ab., 95, 1-88 (1960).

22. R. Tertian and D. Papee, "Thermal and Hydrothermal Transformations in Alumina," J. Chem. Phys. 55, 341-353 (1958).

23. J. H. deBoer, "Steady State Processes Involving Lattice Rearrangement," Farad. Soc. Discuss. 23, 171-182 (1957).

24. L. Pauling and S. B. Hendricks, "Crystal Structure of Hematite and Corundum," J. Am. Chem. Soc., 47, 785-790 (1925).

25. R. E. Newnham and Y. M. deHaan, "Refinement of the α-Al_2O_3, Cr_2O_3, Ti_2O_3 and V_2O_3 Structures," Z. f. Krist. 117, 235-237 (1962).

26. W. Biltz and A. Lemke, "Ueber γ-Tonerde und Spinelle," Z. Anorg. Chem. 186, 373-386 (1930).

27. H. C. Stumpf, A. S. Russell, J. W. Newsome and C. M. Tucker, "Thermal Transformations of Alumina and Aluminum Hydrates," Ind. Eng. Chem. 42, 1398-1403 (1950).

28. M. Prettre, L. Blanchin and B. Imelik, "Etudes Aux Rayons χ des Produits de Deshydratation d'une Hydrargillite Crystallisée," C. R., 236, 1025-1028 (1953).

29. H. Jagodzinski and H. Saalfeld, "Kationenverteilung und Strukturbeziehungen in Mg-Al Spinellen," Z. fuer. Krist, 110, 197-218 (1958).

30. J. H. Cowley, "Stacking Faults in γ-Alumina," Act. Cryst., 6, 53-54 (1953).

31. M. H. Jellinek and I. Fankuchen, "X-Ray Diffraction Examination of Gamma-Alumina," Ind. Eng. Chem, 37, 158-163 (1945).

32. B. Frisch and K. Krieger, "Untersuchungen and Aluminiumoxydgrenzflachen," Ber. Deu. Keram. Ges., 46, 403-408 (1969).

33. R. Tertian, "Constitution et Structure de l'Alumine Activée," C. R., 230, 1677-1679 (1950).

34. G. Yamaguchi and W. C. Chiu, "Delta and Theta-Al_2O_3 under Hydrothermal Conditions," Bull Chem. Soc. Jap., 41, 741-744 (1968).

35. P. H. Rooksby, *"The X-Ray Identification and Structure of Clay Minerals,"* The Mineralogical Society, London (1951).

36. M. Day and V. J. Hill, "Thermal Transformations of the Alumina and their Hydrates," J. Phys. Chem., 57, 946-950 (1953).

37. W. Gitzen, *"Alumina as a Ceramic Material,"* The American Ceramic Society, Columbus, Ohio, (1970).

38. A. M. Kalinina, "Polymorphism and Thermal Conversions of Aluminum Oxide," Russ. Jnl. of Inorg. Chem., 4, 568-573 (1959).

39. D. J. Stirland, A. G. Thomas and N. C. Moore, "Observations on Thermal Transformations in Alumina," Trans. Brit. Ceram. Soc., 57, 69-84 (1958).

40. W. H. Hüttig and H. Ginsberg, "Einfluss des Ausgangsmaterials aufden Verlauf des Alterns der γ-Hydroxyd," Z. Anorg. Chem., 293, 204-213 (1957).

41. R. L. Coble and J. E. Burke, *"Progress in Ceramic Science,"* Vol 3, 197-252, MacMillan, New York (1963).

42. R. K. Iler, "Fibrillar Colloidal Boehmite, Progressive Conversion to Gamma, Theta and Alpha-Alumina," J. Am. Ceram. Soc., 44, 618-624 (1961).

43. A. C. D. Chaklader and A. L. Roberts, "Transformation of Quartz to Cristoballite," J. Am. Ceram. Soc., 44, 35-41 (1961).

44. G. Fink, "Roentgenographische Verfolgung der Umwandlung von Nichtkristallinem Al_2O_3 in Korund," J. Inorg. Nucl. Chem., 30, 59-61 (1968).

45. P. W. Clark and J. White, "Some Aspects of Sintering," Trans. Brit. Ceram. Soc., 49, 305-333 (1950).

46. Yangjuo-Ching and Yentungsheng, "Kinetics of Phase Transformations in Alumina," Kwei. Suan. Hsueh. Pao, 5, 1-11 (1966).

47. J. H. deBoer, J. M. Fortuin and J. M. Steggerda, "The Dehydration of Alumina Hydrates I + II," Prod. Kon. Nederl. Akad. Wetensch.,B57, 170-180 and 434-443 (1954).

48. H. Yanagida, G. Yamaguchi and J. Kubota, "The Role of Water Vapor in Formation of Alpha-Alumina from Transient Alumina," J. of Ceram. Assoc. of Japan, 74, 371-377 (1966).

49. O. J. Kleppa and T. Yokokawa, "A Calorimetric Study of the Transformation of Some Metastable Modification of Alumina to α-Alumina," J. Phys. Chem., 68, 3246-3249 (1964).

50. H. P. Klug and L. E. Alexander, *"X-Ray Diffraction Procedures,"* John Wiley, New York (1954).

51. C. M. R. Rao, S. R. Yoganasimhan and P. Faeth, "Studies on the Brookite-Rutile Transformation," Trans. Farad. Soc., 57, 504-510 (1961).

52. R. K. Iler, "Effect of Silica on Transformation of Fibrillar Colloi dal Boehmite and Gamma Alumina," J. Am. Ceram. Soc., 47, 339-341 (1964).

53. Catalyst, U. S. Patent 2,487,564, November 8 (1949).

54. C. G. Durdaller, W. R. Robinson and G. M. Pound, "Nucleation Rates in the α to β Transformation in Tin," Trans. AIME, 230, 193-200 (1964).

55. Crystal Structure Transformation, Discuss. Farad. Soc., 32, 1579-1585 (1962).

56. R. Roberts, *"Kinetics of High Temperature Process,"* ed. by W. D. Kingery, Technology Press and John Wiley, New York (1959).

57. C. N. Rao, A. Turner and M. J. Hüttig, "Some Effects of Impurities on the Anatase-Rutile Transition," Phys. Chem. of Solids, 11, 173-174 (1959).

58. S. Carniglia, "Grain Boundary and Surface Influence on Mechanical Behavior of Refractory Oxides — Experimental and Deductive Evidence," *Material Science Research*, Vol 3, 425-472, Plenum Press, New York (1966).

59. F. C. Tompkins, "Influence of Structure on Solid State Reactions," Pure and Appl. Chem., 9, 397-407 (1954).

60. W. G. Burgers and L. G. Groen, "Mechanism and Kinetics of the Allotropic Transformation of Tin," Discuss. Farad. Soc., 23, 183-194 (1957).

61a. M. Avrami, "Kinetics of Phase Change I," J. Chem. Phys., 7, 1103-1112 (1939).

61b. "Kinetics of Phase Change II," ibid., 8, 212-214 (1940).

62. F. Slattery and M. M. Heberlin, *"The Mechanism of Phase Transformation in Crystalline Solids,"* Symposium held in Manchester 1968, The Institute of Metals (1969).

63. S. W. Freiman and L. L. Hench, "Kinetics of Crystallization in Li_2O-SiO_2 Glasses," J. Am. Ceram. Soc., 51, 382-387.

64. Y. Wakao and J. Hibino, "Effects of Metallic Oxides on the Transformation to α-Al_2O_3," Nagoya. Kogyo, Gijutsu. Shikenko.Hahoku, 11, 588-595 (1962).

65. G. Fink, "Reaction of Vanadium Pentoxide with Metastable Alumina," Ber. Deu. Keram. Ges., 41, 627-631 (1964).

66. G. Beghi and E. Cazzaniga, "Examination of the Alumina Phases in SAP after Irradiation," En. Nucleare, 15, 142-144 (1968).

67. J. W. Cahn, "The Kinetics of Grain Boundary Nucleated Reactions," Acta. Met., 4, 449-459 (1956).

68. J. B. Peri, "A Model for the Surface of γ-Alumina," J. Chem. Phys., 69, (1), 220-230 (1965).

69. Karlyn, J. W. Cahn and M. Cohen, "The Massive Transformation in Copper-Zinc Alloys," Trans. AIME, 245, 197-207 (1969).

70. T. B. Massalski, "Massive Transformations," ASM Seminar on Phase Transformations, Metals Park, October 1968, ed. ASM (1970).

71. R. M. Spriggs and T. Vasilos, "Progress in Ceramic Science," Vol 4, 95-132, MacMillan, New York (1965).

72. R. M. Spriggs, R. B. Runk and L. Aatteras, "Thermomechanical and Thermochemical Adaptations to Pressure-Sintering of Ceramics," Proceeding 12, British Ceramic Society, Second Meeting on Fabrication Science, Leeds 1967, ed. by The British Ceramic Society (1969).

73. A. C. D. Chaklader, "Reactive Hot-Pressing, Fabrication and Densification of Non Stabilized ZrO_2," Am. Ceram. Soc. Bull., 44, 606-610 (1969).

74. G. E. Gazza, J. R. Barfield and D. L. Preas, "Reactive Hot-Pressing to Alumina with Additives," Amer. Ceram. Soc. Bull., 48, 606-610 (1969).

75. W. H. Rhodes, D. J. Sellers, R. M. Cannon, A. H. Heuer, W. R. Mitchell and P. Burnet, Summary Report, Contract N00019-67-C0336, 25 April 1967 - 24 May 1968.

76. W. J. MacDonough, Ph.D. Diss., Lehigh University (1970).

77. C. A. Bruch, "Sintering Kinetics of the High Density Alumina Process," Am. Ceram. Soc. Bull., 41, 799-802 (1962).

78. T. Vasilos and R. M. Spriggs, "Pressure Sintering Mechanism and Microstructures," J. Am. Ceram. Soc., 46, 493-496 (1963).

79. H. P. Kirchner, "Chemical Strengthening of Ceramic Materials," 6th December 1970 Summary Report, U. S. Navy Contract N000 19-70-60-0418.

80. ASTM Designation E 112-60T, part 31 (1969).

81. B. F. Sheppard, "Inherent Hardenability of Tool Steels," Trans. Am. Soc. for Metals, 17, 90-110 (1930).

82. S. A. Saltykov, *"Streometric Metallography,"* 2nd ed., Metallurgizdat, Moscow, USSR (1958).

83. R. T. deHoff and F. Rhines, *"Quantitative Microscopy,"* McGraw-Hill, New York (1968).

84. R. L. Coble, "Effect of Microstructure on the Mechanical Properties of Ceramic Materials," *Ceramic Engineering Processes*, MIT Press, Boston (1959).

85. R. M. Spriggs, T. Vasilos and E. M. Passmore, "Strength-Grain Size-Porosity Relation in Alumina," J. Am. Ceram. Soc., 48, 1-7 (1965).

86. D. P. H. Hasselman, "Griffith Flow and the Effect of Porosity on Tensile Strength of Brittle Ceramics," J. Am. Ceram. Soc., 52, 457 (1969).

VITA

Charles J-P. Steiner was born in October 1938 to Drs. A. J-P. and M. Steiner in Paris (France). His early education was obtained in France and England. He graduated from the French Lycee system with the National Baccalaureate Examination (science option) in 1958.

He entered the College of Advanced Technology (now the University of Aston) in Birmingham (England) in 1959, was called up in the French Army in 1962-63 and returned to Birmingham from which he graduated with honors in 1965 with a B.Sc. in Metallurgy.

As part of his undergraduate studies he held student traineeships in both Britain and France.

He entered Lehigh University in the fall of 1966 and received an M.S. in Metallurgy in 1968 and subsequently embarked on a Ph.D. program in the Physical Ceramics Laboratory of the above department.

The author is a member of the American Ceramic Society, The Metallurgical Society of AIME and The British Ceramic Society.